# Locus Coeruleus Optogenetic Stimulation and the Estrous Cycle Manipulate Sleep Characteristics and Memory Consolidation

by

Kevin M. Swift

A dissertation submitted in partial fulfillment
of the requirements for the degree of
Doctor of Philosophy
(Molecular and Integrative Physiology)
in the University of Michigan
2019

Doctoral Committee:

Professor Sue Moenter, Co-Chair
Professor Gina R. Poe, Co-Chair, University of California Los Angeles
Assistant Professor Sara Aton
Associate Professor Jimo Borjigin
Associate Professor Michael Sutton

Kevin M. Swift

swiftke@umich.edu

ORCID iD: 0000-0002-5527-5904

## ACKNOWLEDGMENTS

Funding for this research was provided by National Institute of Mental Health R01 60670, Rackham Merit Fellowship, Rackham Pre-candidate and Post-candidate Research Grant, and NIH Systems and Integrative Biology T32. Additionally, I would like to thank Rackham Graduate School as well as the Molecular and Integrative Physiology Department for five years of consecutive travel awards which allowed me to attend numerous domestic and international conferences.

I would also like to thank the Integrative Biology and Physiology graduate program at the University of California Los Angeles and its chair, Mark Frye, for allowing me to be a visiting graduate student in their department for two years.

Finally, this research was made possible through the sacrifice of the lives of numerous laboratory animals, specifically rats. Thank you for your commitment to science.

## TABLE OF CONTENTS

## LIST OF FIGURES

Chapter 1 Figures



Chapter 2 Figures

Chapter 3 Figures

## LIST OF ABBREVIATIONS

EEG—electroencephalogram

REM (sleep)—rapid eye movement (sleep)

NREM—non rapid eye movement (sleep)

EMG—electromyograph

TRN—thalamic reticular nucleus

IS—intermediate sleep

β-AR—beta adrenergic receptor

PKA—protein kinase A

PP1—protein phosphatase 1

LTP—long term potentiation

NMDAR—N-methyl-D-aspartate receptors

$\alpha^1$-AR—alpha 1 adrenergic receptor

$\alpha^2$-AR—alpha 2 adrenergic receptor

LC—locus coeruleus

OVX—ovariectomized

FFT—fast Fourier transform

RMS—root mean square

mPFC—medial prefrontal cortex

V2—secondary visual cortex

ZT—Zeitgeber time

SWA—slow wave activity

PTSD—post-traumatic stress disorder

NE—norepinephrine

## ABSTRACT

Sleep and is critical for proper memory consolidation. The locus coeruleus (LC) releases norepinephrine throughout the brain except when the LC falls silent throughout rapid eye movement (REM) sleep and prior to each non-REM (NREM) sleep spindle. We hypothesize that these transient LC silences allow the synaptic plasticity necessary to incorporate new information into preexisting memory circuits. We found that spontaneous LC activity within sleep spindles triggers a decrease in sleep spindle power. By optogenetically stimulating norepinephrine-containing LC neurons at 2 Hz during sleep, we reduced sleep spindle occurrence as well as NREM delta power and REM theta power, without causing arousals or changing sleep amounts. Stimulating the LC during sleep following a hippocampus-dependent food location learning task interfered with consolidation of newly learned locations, and reconsolidation of previous locations, disrupting next-day place cell activity. The LC stimulation-induced reduction in NREM sleep spindles, delta, and REM theta, and reduced ripple-spindle coupling all correlated with decreased hippocampus-dependent performance on the task. Thus, periods of LC silence during sleep following learning are essential for normal spindle generation, delta and theta power, and consolidation of spatial memories.

Sleep quantity and quality also impact many physiological and neural processes. Sleep is affected by the menstrual cycle; however, few studies have examined the effects of the estrous cycle on sleep in rodents. Thus, studies of disease mechanisms in females lack critical information regarding estrous cycle influences on relevant sleep characteristics. We recorded electroencephalographic (EEG) activity from multiple brain regions to assess sleep states as well as sleep traits such as spectral power and interregional spectral coherence in males and freely cycling females across the estrous cycle. Our findings show that the high hormone phase of proestrus decreases the amount of non-rapid eye movement (NREM) sleep and rapid eye movement (REM) sleep and increases the amount of time spent awake compared with males and other

estrous phases. This spontaneous sleep deprivation of proestrus was followed by a sleep rebound in estrus with increased NREM and REM sleep and rebound-like sleep architecture. Spectral power increased in the delta 0.5-4 Hz) and the gamma (30-60 Hz) ranges during NREM sleep of proestrus, and in the theta range (5-9 Hz) during REM sleep of both proestrus and estrus. Slow wave activity and cortical sleep spindle density also increased in NREM sleep of proestrus. Finally, interregional NREM and REM spectral coherence increased during proestrus. This work demonstrates that the estrous cycle affects more facets of sleep than previously thought and reveals further sex differences in feature of the sleep-wake cycle, which are relevant to a myriad of physiological processes influenced by sleep.

# CHAPTER I

## Introduction: Sleep, Neural Rhythms, and Memory Consolidation

*A note to the reader: this introduction is a review of the state of the field near the onset of the following research in 2016. Few references will be included following that time unless deemed necessary.*

*"I love sleep. My life has the tendency to fall apart when I'm awake, you know?"*
*-attributed to Ernest Hemmingway*

### 1.1 Sleep as an evolutionary quandary

Sleep is an essential facet of life: from sea sponges lacking a nervous system[1], to complex vertebrates with billions of synapses. All these organisms experience cyclical periods of activity and inactivity, i.e. waking and sleep. While the manifestation of waking and sleep varies wildly across species—from fluctuations of water filtration in sponges[1], and pulsatile movements in jellyfish[2] to the canonical examples of sleep in terrestrial mammals such as inactivity, decreased response to stimuli, and changes in brain activity—sleep as a behavior remains remarkably evolutionarily conserved[3].

Despite the conservation of sleep, the function of sleep evolutionarily is not overtly evident. While asleep, species are at a distinct disadvantage: they are unable to locate food, are not aware of environmental dangers such as predators, and cannot mate to pass along their genetic code[3]. Further, during sleep, thermoregulation is impaired[4], and metabolically, sleep provides only marginally less energy expenditure than simple inactivity[5]. Moreover, sleep occupies an inordinate amount of time: from approximately 33% of the human lifespan to approximately ~85% of the life of *Macrotus calfornicus,* the California leaf-nosed bat[6]. In relation to both fitness and self-preservation, sleep creates an evolutionary quandary so much so that seminal sleep researcher Allan Rechtschaffen who conducted the foundational work in insomnia and narcolepsy is quoted as saying *"If*

*sleep doesn't serve an absolutely vital function, it is the greatest mistake evolution ever made.*[7]*"*

### 1.2 Sleep is necessary for normal physiology

While the evolutionary function of sleep is not immediately evident, the effects of sleep deprivation are stark. Early work in the late 19th century provided initial evidence that sleep deprivation can cause death. In 1894, Russian physician Marie de Manaceine deprived puppies of sleep by keeping them constantly active and found that it was 100% fatal within a few days[8]. Later in 1898, Italian physiologists Lamberto Diddi and Giulio Tarozzi kept adult dogs awake with constant activity and found it was 100% fatal within 17 days[8]. While macabre and poorly controlled, these experiments established that sleep was necessary for life. Work in the mid-late 20th century by Allen Rechtschaffen found that total sleep deprivation was fatal to rodents in 11-32 days[9,10]. In humans, fatal sleep deprivation is rare, however disease states with fatal insomnia have been recorded as early as the 18th century. Fatal Familial Insomnia, an extremely rare and uncurable prion disease, presents with patients who become increasingly unable to fully initiate or maintain sleep[11]. Following manifestation of sleep issues, FFI is fatal within one year, and within weeks once the total insomnia phase is initiated. While the necessity of sleep for life has not been systematically examined across all species, there is overwhelming evidence that life is not sustainable without sleep.

Short of lethality, Rechtshaffen's early studies on sleep deprivation in rodents found numerous systemic effects on the body including, but not limited to, weight loss, increased food intake, decrease in body temperature, decreased immune function, and cognitive impairment[10]. One region that is particularly affected by sleep deprivation is the nervous system. In the aforementioned studies in dogs by Manaceine, and by Daddi and Tarozzi, both groups found lesions within the brains of the animals post-mortem[8]. In humans, studies have shown that reduced sleep was associated with reduced brain volume and greater brain atrophy[12,13]. Chronic sleep disruption from conditions such as sleep apnea led to higher levels of micro infarcts throughout the brain[13]. Patients with chronic insomnia are more likely to develop dementia and exacerbate the progression of neurodegenerative disorders such as Alzheimer's and Parkinson's disease[14,15]. While

sleep provided a refuge from *"a tendency to fall apart"* for Hemmingway, systemically, sleep is necessary part of life for maintaining health and normal physiologic function.

### 1.3 Neural rhythms as a method of classifying sleep

Observationally, sleep is defined as a behavioral state characterized by inactivity, reversible loss of consciousness, and decreased response to stimuli[16]. It was not until 1887 when Richard Canton, an English physician and pioneer in electrophysiology first recorded electrical activity from the brain of a sleeping animal[8,17]. He noted that recorded electrical currents increased during sleep compared to waking. Later in 1924, German physician Hans Berger was the first person to record electrical signals from the brains of humans and coined the term electroencephalogram (EEG) to describe this activity[8]. Work in the 1950's by Eugene Aserinsky and Nathaniel Kleitman characterized a unique stage of sleep with eye movements, called rapid eye movement (REM) sleep[18]. Due to the similarities in EEG traces between REM sleep and waking, REM sleep is also called paradoxical sleep as EEG traces from both states display lower amplitude and faster frequency. REM sleep also presents with skeletal muscle atonia which further distinguishes the state from NREM sleep

In modern clinical and basic research, the use of EEG and electromyographical (muscle activity, abbreviated as EMG) recordings allows sleep-waking behavior to be divided into unique states. In humans, sleep is divided into waking, NREM stage 1, NREM stage 2, NREM stage 3, and REM sleep[19]. In animals, sleep is most commonly divided into waking, NREM sleep, and REM sleep. However, rodent sleep, particularly rats, can be further divided to include quiet waking at sleep onset, and intermediate sleep (IS) which will be discussed later[20].

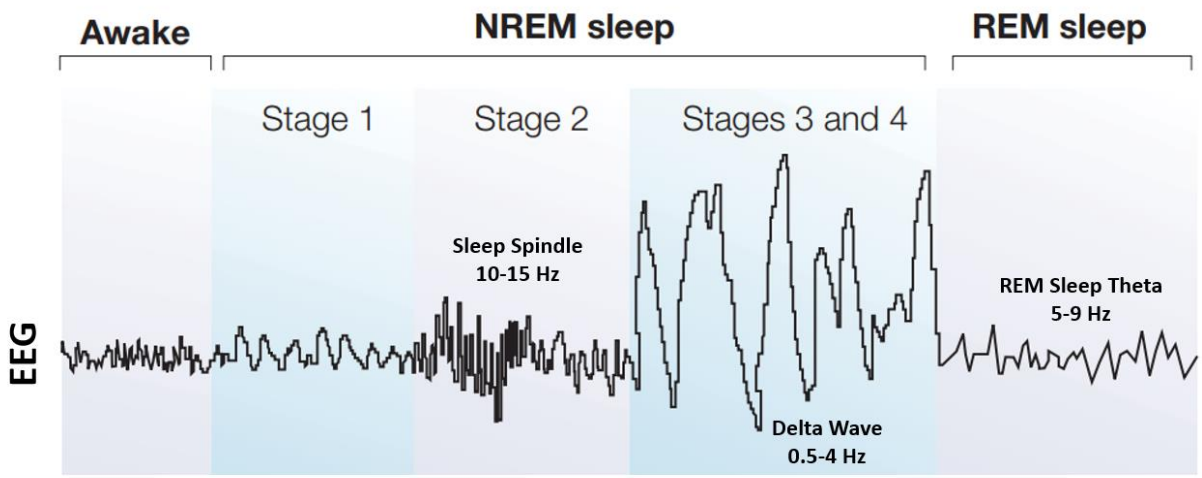


Figure 1.1 Example EEG traces and waveforms of human sleep stages. Adapted from Bryant PA, et al. 2004. *Nature Reviews Immunology.* 4(6):457-67.[21]

Waking is characterized by a dynamic and high amplitude EMG, with lower amplitude EEG showing primary activity in the alpha (8-11 Hz) and gamma frequencies in humans, and in the theta (5-9 Hz) and gamma range (30-60 Hz) in the cortex of rodents[19,20]. In humans and rodents, the onset of sleep is characterized by a reduction in EMG amplitude as muscle activity decreases. In humans, EEG frequency slows as theta waves (4-7 Hz) become the prominent frequency in stage 1 sleep[19]. Stage 1 sleep is not commonly identified within animals, although some parallels have been drawn between stage 1 and what is referred to as quiet waking or drowsiness.

In stage 2 sleep, EEG activity continues to increase in amplitude and decrease in frequency. Most notably there is the appearance of two unique waveforms: the sleep spindle and the K-complex[19]. The sleep spindle is canonically a cortical NREM sleep waveform of 11-15 Hz, lasting 0.5-1 second in length which waxes and wanes in amplitude. This unique waveform is the result of a complex interplay between the inhibitory thalamic reticular nucleus (TRN), and excitatory thalamocortical projections from medial thalamic nuclei. During NREM sleep, inhibitory GABAergic neurons from the TRN (which project to medial nuclei), change their firing from tonic spiking to rhythmic bursting activity[22]. This burst of inhibitory input increasingly hyperpolarizes thalamocortical neurons until the hyperpolarization-activated cation current, $I_h$, generates

a low-threshold $Ca^{2+}$ spike[22–24]. As thalamocortical neurons have excitatory inputs to both the cortex and back to the TRN, this $Ca^{2+}$ spike is seen in the thalamus and the cortex, but more importantly releases excitatory post-synaptic potentials back on to TRN neurons. This excitation of inhibitory TRN neurons results in further inhibitory activity from the TRN to the thalamocortical nuclei and the cycle of inhibition-activation repeats, with growing amplitude, until the loop is terminated. Although the exact mechanism of this termination is not known, feedback from cortical neurons as well as noradrenergic input has been hypothesized to desynchronize thalamocortical neuron activity leading to termination[25,26]. The result of this complex interplay is the canonical waxing and waning spindle activity seen in the cortical EEG.

The K-complex is defined as a short, high-voltage negative deflection followed by a slower high-voltage positive deflection resulting in the highest amplitude waveform of any EEG signature[27,28]. These high amplitude K-complexes result from periods of cortical "down-states" in which there is a pronounced neural silence followed by subsequent pronounced "up-states" of highly synchronous neural activity[27]. Unlike the sleep spindle, the mechanism and neural circuitry for K-complex generation is not well known, although previous research has implicated both the thalamus and the cortex. Patients with uni-hemispheric thalamic lesions do not display K-complexes in the cortical EEG in the hemisphere ipsilateral to the lesion[29]. Meanwhile recordings from cats have suggested that cortical slow oscillations (<1 Hz) during sleep and anesthesia underlie the generation of K-complexes[30]; although no specific region of the cortex has been directly implicated in K-complex generation[31].

Within rodents, intermediate sleep (IS) is a similar, but not analogous state to stage 2 sleep in humans[20,32–34]. Like human stage 2, IS in animals precedes NREM slow wave sleep (stage 3 in humans) and is characterized by the decrease in frequency and increase in amplitude of EEG activity. Further, like stage 2, animals display prominent sleep spindles during IS[20]. However, unlike humans, K-complexes are not always characteristic of IS sleep and IS sleep in rodents makes up less of the overall sleep (20%) compared to stage 2 sleep (50%) in humans. Also sleep spindles in humans are isolated to stage 2 sleep (i.e. they are not characteristic of stage 3 sleep), whereas in rodents, sleep spindles can be identified throughout NREM slow wave sleep. Finally, IS may also comprise a

period of time known as transition to REM sleep[20,35]. Transition to REM sleep precedes REM sleep and is characterized as a spindle rich period, with the loss of slow wave amplitude and increase in frequency of EEG as the brain transitions to REM sleep[36]. This transitionary state is not commonly identified in humans, leading to further differences between stage 2 and IS.

Stage 3 (formerly known as stage 3 and stage 4) sleep in humans and NREM slow wave sleep in animals is characterized by the dominance of high-amplitude slow waves or delta waves (0.75-4 Hz). Similar to K-complexes, these slow waves are the result of periods of cortical down-states and up-states, but unlike K-complexes which appear as isolated waveforms, delta waves comprise the vast majority of this state. Further, these slow waves are highly synchronous, in that they are generated by the activity of large populations of neurons, and further travel anterior to posterior throughout the brain[37].

REM sleep in humans and rodents is characterized by the lowest levels of activity in EMG due to complete muscle atonia[38], and a faster low-voltage theta rhythm, 4-7 Hz in humans and 5-9 Hz in rodents, particularly in the hippocampus. This characteristic theta rhythm is driven by inhibitory parvalbumin interneuron projections and cholinergic projections from the medial septum to the hippocampus[39–41]. Inhibition of these inputs has been directly shown to decrease REM sleep theta amplitude[40]. Finally, while the theta rhythm is seen throughout the brain during REM sleep, unlike NREM slow waves, REM sleep theta is highly asynchronous across brain regions[16,42]. Evidence for this derives from seizure propagation in sleep. NREM sleep synchrony better allows the propagation of electrical seizure activity across the brain, while REM sleep does not allow such propagation; this results in the vast majority of sleep-related seizures occurring in NREM as opposed to REM sleep[42,43].

### 1.4 Sleep and memory consolidation

While sleep is necessary for several facets of normal physiology, sleep's role in proper memory consolidation remains one of its most enigmatic functions. Memory consolidation refers to the neural processes by which newly encoded information is stored in memory circuits for future use[44,45]. Historically, the hypothesis that sleep is involved in memory consolidation is not new; early work in 1924 by Jenkins and Dallenbach

demonstrated the effects of sleep on memory consolidation[46]. In their study, participants were taught nonsense syllables, and then were allowed to sleep, or were kept awake. Participants that slept remembered significantly more syllables. Since then numerous studies have demonstrated that sleep has beneficial effects on memory formation[16,35,44,47,48]. The timing of sleep in relation to learning is also important; sleep after learning, within 4-6 hours of initial learning is most advantageous to memory consolidation[49,50]. Additionally, the benefits of sleep for memory do not require a full night of sleep; recent work has found that naps following learning were sufficient to improve memory as much as a full night of sleep[51].

While the mechanism for how sleep facilitates memory consolidation remains unknown, there is evidence across the board in humans and in rodents that all sleep stages play a role in the consolidation process[16,52–54]. Work in recent years in both basic science and clinical research has begun to highlight the role of different sleep states' neural oscillations in the formation of memories. The most prominent of these oscillations are NREM sleep slow waves or delta waves (0.5-4 Hz), sleep spindles (10-15 Hz), hippocampal ripples (100-250 Hz), and REM sleep theta (5-9 Hz). While this list is not exhaustive (K-complexes and PGO waves will not be discussed further in this thesis), slow waves, spindles, ripples, and theta have amassed the greatest evidence for their role in memory consolidation[35].

NREM sleep slow waves represent perhaps the most thoroughly investigated and manipulatable oscillation in both humans and rodents. In humans, slow waves in sleep following learning increased in amplitude within cortical regions directly associated with the learning task (e.g., motor task and motor cortex)[55]. Using transcranial stimulation to enhance slow waves improved memory performance on a declarative pair-words memory task[56]. Further, auditory enhancement of slow waves improved performance on similar paired-word memory task[57]; similar results were seen in a study using older adults, a population with reduced slow wave amplitude[58]. Conversely, interfering with slow waves solely within the motor cortex following a motor learning task interfered with the ability to learn the task[59]. In rats, optogenetic activation across the cortex during NREM in the slow wave frequency improved performance in a tactile-perception variation of the novel object task[60]. Also, enhancement of NREM slow waves in rats improved performance on working

memory task[61]. In nonhuman primates, surface electrical stimulation to induce slow waves improved performance in a neuroprosthetic task[62]. Finally, artificially enhancing slow wave and spindle coupling increased memory in a novel object placement task and in a paired associated learning task in rats and humans respectively[57,63].

Whereas slow waves are an easy target for manipulation, sleep spindles, due to the complex interplay necessary for their generation, cannot be as simply manipulated. However, sleep spindles possess two strong associations with learning and memory. The first association, sleep spindle density increases following learning[64–72]. Although the exact mechanism remains unknown, learning increases pressure for spindle generation. In humans, the increase in spindle generation has been isolated to regions of the cortex associated with the previous learning; e.g. a motor learning task will increase spindles in the motor cortex in subsequent sleep[73]. While spindles were previously thought to be a global cortical phenomenon, these studies provide evidence that spindles are localized events within the cortex. Furthermore, it provided evidence that spindles can be upregulated within regions of the brain where there is a distinct need for memory consolidation.

The second association between sleep spindles and memory consolidation is a series of findings that changes in spindle density after learning predict memory performance[67,73–77]. Like changes in spindles density, correlation of spindle density with performance is highly conserved within mammals[65,78]. Independent of learning, studies in humans have linked innate spindle density to intelligence and to cognitive flexibly for learning[79,80].

Additional evidence for the role of spindles in learning and memory comes from the coupling of spindles with other neural oscillations during sleep that are thought to support memory consolidation. As previously mentioned, the coupling of slow-waves and spindles within the cortex has been shown to enhance memory; however, spindles also couple to ripples, 100 msec long 100-250 Hz oscillations, within the hippocampus in both rodents and humans[81–84]. Ripple-spindle coupling is unique as it represents the rhythmic coupling of two very distinct regions of the brain. The coupling of these two rhythms has been proposed to be one mechanism that drives the transfer of newly encoded

information in the hippocampus to less densely distributed circuits in the cortex where it can be stored long term and fully consolidated[35,44].

Beyond simple memory storage, spindles have also been implicated in more nuanced forms of offline memory processing. In particular, spindles have been associated with the integration of new information in existing knowledge[85,86]—or functionally, the updating of previously formed memory circuits with newly encoded information. Corroborating work in rodents has shown that interfering with spindles prevents the integration of newly-learned information[65]. Spindles have also been associated with directed remembering and forgetting. In a seminal study, subjects were directed to remember or ignore specific word-image associations and then instructed to nap or stay awake[87]. The nap group had improved recall of associations compared to the awake group. Within the nap group the spindle density strongly correlated with recall of the associations that subjects were directed to remember, and further, the forgetting of the forgetting of associations that subjects were instructed to ignore. More work is necessary to parse out other facets of offline processing that may be directed by sleep spindles.

Finally, recent work in both humans and animals has attempted to manipulate spindles in order to manipulate memory. Optogenetic stimulation of TRN neurons to artificially generate spindles with in relation to slow oscillations, enhanced consolidation of both spatial and fear memory in mice[88]. In the same study, optogenetic inhibition of TRN neurons to inhibit spindle generation prevented the consolidation of fear memory. In humans, enhancement of spindle activity utilizing transcranial alternating-current stimulation improved performance on a motor task[89]. While limited, these studies provide preliminary evidence that artificial enhancement of spindles may improve memory consolidation. Moreover, in diseases such as schizophrenia and Alzheimer's', in which both memory and spindles are impaired, enhancing spindles could mitigate memory deficits[90,91].

Ripples are transient (100 msec) periods of 100-250 Hz high frequency oscillatory activity that result from the activation of hippocampal pyramidal neurons during NREM sleep (ripples also occur during periods of inactive quiet wake, but that will not be covered here)[35,92,93]. Ripples occur predominantly at the upstate of slow oscillations during sleep but represent unique on-periods of highly synchronous neural activation. Whereas slow

waves represent global activation of neurons, ripples can convey highly precise information. Hippocampal pyramidal cells which encodes sequential spatial information during waking, reactivate these sequential neural ensembles during ripples, i.e. memory replay[92,94]. Direct electrical stimulation to the hippocampus to interfere with ripples in NREM sleep in rats prevents both the consolidation and replay of spatial information[95]. Optogenetic inhibition of the pyramidal neurons during ripples destabilizes spatial mapping information and reduces ripple power[93]. Further, decoupling of the ripples from spindles also interferes with memory consolidation[96]. In humans, due to the invasiveness necessary for hippocampal recordings, our knowledge of ripples comes exclusively from seizure patients implanted with focal electrodes. Humans show similar ripples and ripple-spindle coupling compared to other mammals, although ripple manipulations in humans are not experimentally possible[84].

While NREM sleep has several distinct neural oscillations that contribute to memory formation, theta is the chief rhythm of REM sleep[35]. REM sleep theta is generated in, and emanates from, the hippocampus and is often sawtooth in appearance within the hippocampus and adjacent cortices[97]. As REM sleep is chiefly comprised of theta oscillations, separating the role of the state from the rhythm in memory consolidation is difficult. REM sleep theta amplitude increased in rodents following avoidance tasks and fear conditioning and further that fear memory consolidation was correlated with REM sleep theta power[70,98,99]; although a different study found a decrease in REM sleep theta amplitude following fear conditioning[100]. Another study found that consolidation of fear memory was correlated with REM sleep theta coherence among the amygdala, hippocampus, and prefrontal cortex (a circuit associated with fear consolidation)[101]. In humans, REM sleep theta power in the prefrontal cortex correlated with consolidation of emotional memory in an association task[102]. Interestingly, REM sleep theta activity is higher in patients resilient to developing post-traumatic stress disorder (PTSD) compared to similarly traumatized patients that later develop PTSD[103].

There is also evidence that REM sleep theta plays a role in non-fear driven tasks. Work in rats has found that hippocampal spatial information is active at different theta phases in the waking performance and is reactivated during REM sleep at different phases of the theta rhythm[104]. While novel information is activated at the peaks of theta,

familiar previously consolidated information is activated at theta troughs which is hypothesized to strengthen or weaken circuits respectively. Additionally, REM sleep theta was also shown to reactivate hippocampal spatial neural ensembles on a similar time scale to which they occurred in waking theta[105]. In humans, one study found that REM sleep theta amplitude increased following a paired words task[70].

A recent noteworthy study provided what may be the most mechanistic evidence for REM sleep theta in memory consolidation[40]. By optogenetically inhibiting medial septal neurons that project to the hippocampus which generate REM sleep theta, Boyce et al.,[40] was effectively able to inhibit the theta rhythm independent of the state. Inhibition of REM sleep theta had detrimental effects on hippocampal learning tasks—contextual fear conditioning and novel object place recognition—but had no effect on non-hippocampal cued fear conditioning. These results together with previous hippocampal spatial reactivation studies point to REM sleep theta having a distinct function in hippocampal memory.

There is ample evidence for the role of neural oscillatory activity during sleep in memory consolidation. What should not be overlooked is that the process of memory consolidation requires the combination of all oscillations, rather than a single oscillation in isolation. The phase locking of slow waves, spindles and ripples in NREM sleep provides a unique orchestra of interregional communication throughout the brain that is not permissive in any other state. While REM sleep theta lacks the intracortical synchrony of other rhythms, this relative interregional isolation combined with state-specific neuromodulator tone (high acetylcholine levels and decreased norepinephrine and serotonin levels[41]) provides a unique neurophysiological state different from waking and from NREM sleep for offline processing. While NREM and REM represent two distinct facets of a single phenomenon clear and convincing evidence has been published indicating they are both necessary for normal memory function.

### 1.5 The role of the noradrenergic system in memory consolidation

The consolidation of memories is also supported by neuromodulatory systems such as the noradrenergic system. The noradrenergic system is comprised of the locus coeruleus (LC) and its projections throughout the forebrain[106]. LC neurons are the primary

supplier of norepinephrine (NE) to the central nervous system. NE acts at α- and β-adrenergic receptors to promote arousal, attention, and alter mood[107]. LC neurons are most active during waking to promote vigilance but decrease in firing during sleep to allow somnolence. During REM sleep, LC neuronal activity ceases entirely[108,109]. Within waking, LC neurons are tonically active, but also phasically increase their firing rate in response to startling stimuli, or novelty[108,110]. Finally, decreased NE within the brain can cause depression whereas increased NE in response to different stressors and time courses can cause anxiety[111,112].

NE also plays an essential role in maintaining synaptic strength. The presence of NE at synapses both blocks synaptic depotentiation or weakening, and enhances synaptic strength[113,114]. Following activation of the β-adrenergic receptor (β-AR), protein kinase A (PKA) phosphorylates inhibitor-1, which binds to and suppresses the activity of protein phosphatase-1 (PP1)[114]. Suppression of PP1 promotes a host of downstream effects that are necessary for the induction of long-term potentiation (LTP), or the strengthening of synapses. First, it facilitates the activation of protein kinases necessary for LTP such as CAMKII[115]. Additionally, PKA phosphorylates N-methyl-D-aspartate receptors (NMDAR) and AMPA receptors leading to increase $Ca^{+2}$ permeability in NMDARs and increases the open probability of both NMDARs and AMPA receptors[114,116,117]. Activation of the β-AR also promotes trafficking of AMPA receptors to the synaptic membrane, and expression of further β-ARs[114]. Together these mechanisms both prevent the weakening of synapses through depotentiation and strengthen synaptic connections.

NE's ability to manipulate synaptic connections plays a pivotal role in memory consolidation[118]. Blocking the activation of β-ARs following encoding with propranolol, a β-AR antagonist, following encoding, interferes with the consolidation of memories in both rodents and humans[119–124]. In contrast, application of NE or isoproterenol, a β-AR agonist directly following learning enhances the memory consolidation[125,126]. Increasing noradrenergic tone by inhibiting negative feedback from alpha-2 adrenergic autoreceptors (α2-AR) via yohimbine following learning similarly enhances memory conslidation[121,123].

While noradrenergic tone can alter initial memory consolidation, it can also alter the reconsolidation of memories following recall. During recall, previously stored memory circuits become activated and labile. Reconsolidation is the process by which this reactivated labile memory must be re-stored for future use. This lability allows noradrenergic mechanisms to alter synaptic strength upon reconsolidation. Application of propranolol just after memory recall interferes with subsequent reconsolidation in both humans and rodents[127–130]. Activation of β-ARs or inactivation of α2-ARs enhances memory reconsolidation[123,131].

Alpha-1 adrenergic receptors (α1-AR) play a unique role in memory consolidation and reconsolidation. Inactivation of α1-ARs with antagonists such as prazosin have no effect on initial memory consolidation; when given simultaneously with yohimbine, propranolol, but not prazosin, interfered with memory consolidation[123]. However, application of prazosin during memory reactivation interferes with reconsolidation, and further counteracts the effects of yohimbine on reconsolidation[123,132]. The specific role α1-ARs in consolidation vs reconsolidation is likely due to their expression within the brain[132]. Whereas β-ARs are widely expressed throughout the brain, α1-ARs are expressed largely in the cortex. As reconsolidation involves the storage of previously consolidated cortical circuits, due to their greater density in the cortex, α1-ARs likely have a greater role in reconsolidation rather than consolidation.

### 1.6 The effect of LC activity and the estrous cycle on sleep

While there is ample evidence that sleep and noradrenergic activation both promote memory consolidation, the relationship between the LC, memory, and sleep is not well parsed out. While high noradrenergic tone may promote memory, it prevents sleep. LC neurons decrease their firing during sleep, but activation of these neurons is necessary for consolidation—creating a paradoxical relationship with memory.

During sleep, endogenous LC activation is not simply tonic or random. LC neurons cease firing prior to sleep spindles and resume firing during the spindles[133]. Additionally, subsets of LC neurons are phase-locked to the up-states of cortical slow waves[134]. Finally, the silence of LC neurons during REM sleep suggests that LC activity during sleep is highly regulated, rather than being simply decreased to promote somnolence.

Moreover, this silence may play a critical role in the unique function of REM sleep for learning and memory. The relationship between LC activity and neural oscillations, particularly sleep spindles, suggests a function for LC silence as well as timed activity in learning and memory. Chapter 2 explores the relationship between LC sleep activity, neural rhythms during sleep, and the consolidation and reconsolidation of memories.

In order to delineate the complex relationship between sleep and memory, it is first necessary to possess a fundamental understanding of how sleep and neural rhythms are affected by systemic physiology. Research pertaining to how the estrous cycle affects sleep in female animals used in preclinical models of sleep is particularly lacking.

In rodents the estrous cycle is comprised of four recurring phases: metestrus, diestrus, proestrus, and estrus. The cyclical reoccurrence of these phases is driven by the hypothalamic-anterior pituitary-gonadal (HPG) axis which controls reproductive hormone release. Ovarian hormones estradiol and progesterone alter sleep-waking behavior endogenously or if administered exogenously to ovariectomized (OVX) rats. However, beyond simple amounts of sleep, little is known about how estrous cycle alters other facets of sleep such as sleep architecture and neural rhythms. Chapter 3 investigates the role of the estrous cycle on sleep spindles, as well as spectral power and interregional coherence. Additionally, sleep at each phase of the estrous cycle is compared to males to examine if the estrous cycle produces sex differences in sleep-wake behavior.

# CHAPTER II

# Abnormal Locus Coeruleus activity alters Sleep Signatures of Memory Consolidation and Impairs Place Cell Stability and Memory

## 2.1 Introduction and methods

### Introduction

Much work has focused on the interplay between the hippocampus and neocortex during sleep to promote memory[81,82,135,136]. However, the neuromodulatory systems necessary for memory formation during waking are relatively unexamined during sleep. The noradrenergic system and its source for the forebrain, the locus coeruleus (LC), is active during waking to promote vigilance, and is responsive to novel information, enabling rapid learning by boosting long term potentiation (LTP) mechanisms[107,114]. During sleep, decreased LC neuronal activity was thought to simply promote somnolence[137].

However, the decrease in LC firing is not uniform across all phases of sleep in rats and higher mammals[134,138,139]. The LC is active throughout the slow wave sleep stage of NREM sleep, but LC neurons fall silent prior to the onset of each sleep spindle (10-15 Hz, high-amplitude, 0.3-3 s long oscillations in electrographic signals) in NREM sleep[139]. During rapid eye movement (REM) sleep, LC neurons also fall silent while cholinergic activity increases[139] and 5-9 Hz theta frequency activity dominates in the electrographic signals. Both REM sleep theta and sleep spindles have been shown to be important for memory consolidation[40,54,73,74], but the physiological relevance of these LC silences for the function of sleep for memory has not been evaluated. We hypothesize that, because norepinephrine supports strengthening of neuronal synapses (LTP) in memory circuits, these transient LC silences uniquely allow depotentiation (resetting strengthened synapses to baseline efficacy) that is necessary for certain types of learning[140,141].

We tested whether normal, transient decreases in LC firing are necessary for the generation of normal REM sleep theta and NREM sleep spindles as well as for memory consolidation and next day memory neural encoding. Using optogenetics to maintain

waking LC activity levels during NREM and REM sleep, combined with simultaneous tetrode recordings of hippocampal place cells during place learning, we tested the effect of increased LC activity during sleep on a sleep-dependent hippocampal place memory learning task[142]. Although the stability and duration of sleep states were not changed, the learning-related signatures of NREM and REM sleep were impaired. Results showed that LC silences are necessary for normal NREM sleep delta power, REM sleep theta power, sleep spindle generation and the coupling of sleep spindles to hippocampal ripples — drops in all of which correlated with decreases in different facets of task performance. Furthermore, while overall place cell firing rates were unchanged during sleep or wakefulness, sustained LC activity during sleep also led to decreased next day encoding stability of maze locations during the tasks.

## Methods

### Experimental models and subject details

A total of twenty-six male Long-Evans rats (Charles River), age 4-5 months and weighing approximately 350-400g were individually housed in cages (45.7 x 24.1 x 20.3 cm) with shaved cellulose bedding, climate controlled (23 ± 3°C and 40 ± 10% humidity) and with 12:12 hour light/dark cycle. Food and water were available *ad libitum* prior to food restriction during behavioral training. All animal procedures were carried out in accordance with the National Institutes of Health Guide for the Care and Use of Laboratory Animals and in accordance with the University of Michigan Committee on the Use and Care of Laboratory Animals.

### Viral Injection

Animals were orally administered (20 mg/kg) ciprofloxacin and liquid acetaminophen (orally 30ml/150 ml water) 24 hours prior to surgery. Rats were anesthetized with isoflurane vapor (4% induction, 1-2% maintenance) and placed in a stereotaxic frame. All stereotaxic measurements were from bregma. A vector expressing a light sensitive channelrhodopsin-2 (ChR2) under the control of PRSx8 (synthetic dopamine beta hydroxylase promoter), lenti-PRSx8-ChR2-mCherry or CAV2-PRS-ChR2-mCherry (Li et al., 2016), or a control vector, AAV-PRSx8-mCherry, was bilaterally injected (1.2 µl) into

the locus coeruleus (AP -12.1 mm; ML ±1.3mm; DV 6.1 mm at 20°) through 30-gauge injection cannula at a rate of 0.2 ml $min^{-1}$ for 6 minutes. Post-injection, needles were left in tissue for 10 minutes prior to removal.

Electrode Implantation

LC and CA1 single cell recordings were collected with dual eight independently movable tetrodes (groups of four twisted microwires) microdrives. The anterior microdrive contained two bilateral cannulas containing four tetrodes each targeting the hippocampus (from bregma: -4.0 mm AP; ± 2.5 mm ML; - 2.0–2.5 mm DV). The posterior microdrive contained two bilateral cannulas containing four tetrodes each targeting the LC (from bregma: AP -12.1 mm; mediolateral ML ±1.2mm; DV -6.1 mm at 20° to avoid the transverse sinus). A screw electrode (Plastics One) was implanted over the prefrontal cortex (from bregma: +2.0 mm AP; ± 2.0 mm ML) to be used as a ground. Two nuchal electromyographic (EMG) electrodes were implanted into the dorsal neck muscles. All implanted tetrodes were used to measure local field potential (LFP) and detect single unit activity. Anchor screws and dental cement were used to adhere implants to the skull.

Behavioral Training and Motivation

Rats were trained on an octagonal version of an eight-box spatial learning task originally developed in our lab[143]. Eight boxes were positioned with one at each corner of an elevated octagonal track. Each box consisted of a reward reservoir that is hidden behind a hinged door that must be opened to reach the food reward (Ensure® Abbott Labs, Columbus, OH). Each reservoir was fed by a plastic tube coupled to a syringe allowing the observer to fill reservoirs without interacting with the maze. Below each box, an inaccessible compartment was baited with Ensure so that all boxes smelled as though they contain a reward to prevent use of olfaction to locate the reward.

Rats were food restricted to >85% of their free feeding weight and trained daily at ZT 0.5 (30 minutes into the light phase) in 30-minute sessions. Rats were trained to run clockwise on the track and locate the three of eight boxes that contained a food reward (0.5 mL Ensure) using static visual cues in the room. A training session consisted of three 5-lap

trials (totaling 15 laps). Following a trial of five complete laps, the animal was removed from the maze and placed in a towel lined box for two minutes to encourage animals to use hippocampal-dependent learning and not working memory. During these two minutes, reservoirs were cleaned of food residue, and the maze was rotated (minimum 45 degrees, max 180 degrees). In all trials, reward boxes were located at the same allocentric locations with respect to visual cues of the room. At the beginning of each trial, rats were reintroduced to the maze at different locations to prevent learning reward location relative to initial placement on the maze.

Rats were trained on this familiar layout until they reached the defined performance threshold criterion of averaging less than one error per lap (16.1 ± 1.2 days). Errors consisted of skipping a reward box and checking a non-reward box. Animals were then implanted as described above in *Electrode Implantation,* above. Following 10 days of surgical recovery in their home cages, animals were reintroduced to the maze with the familiar layout, now tethered for electrophysiological recording, and retrained until they met the performance criterion threshold again.

Behavioral Protocol and Rectangular Maze

The experimental protocol consisted of rats running 15 laps on the familiar layout, followed by a 20-minute break from the maze in a towel lined box. Light intensity in the room was kept low during running to minimize animal anxiety and optimize video tracking of the animal through headstage-mounted LEDs. Light was increased during the break between mazes as a cue for maze change. After the break, the lights were returned to low intensity and rats were run 15 laps in three trials on the reversal maze where two of the three previous locations of the food were changed. In addition to counting total errors per lap, error type was also characterized. As two box positions changed between familiar and reversal mazes, there are four potential errors that could be made at those four boxes and they were termed “maze choice” errors. Four potential “static errors” could be made at the four box positions that were never changed between mazes. Thus, the probability of either error type being made at random on either the familiar or reversal mazes is 0.5. Errors occurring at positions that remained static between mazes indicate an impaired

hippocampal-dependent memory or perhaps abandonment of the hippocampal spatial strategy, whereas errors at baited positions that alternated between familiar and reversal mazes indicate confusion between familiar and reversal maze maps. This 15-lap familiar, 20-minute break, 15-lap reversal was run days 1-5.

Rats were given a break from running on days 6 and 7 and fed their normal restrictive diet. On days 8-10, animals were run on a rectangular maze with eight boxes, three of which contained food, similar to the days 1-5 exercise, only in a different room with different visual cues[143]. Animals were run for three days to determine their ability to learn a new maze to the same criterion of less than one error per lap.

Electrophysiological Recording

Electrode data were recorded at a sampling rate of 32 kHz using Neuralynx Digital Lynx system (Neuralynx, Bozeman, MT). Hippocampal CA1 spikes were detected in real-time from 600 Hz to 6 kHz filtered continuously sampled tetrode data using amplitude threshold crossing. LC spikes were detected in the same manner, but with a 300 Hz to 6 kHz filter.

Tetrode placement in CA1 of the hippocampus was confirmed by moveable tetrode depth, as well as by waveform shape, frequency and audio-converted sound of pyramidal neural spikes. Tetrode placement in the LC was confirmed using calculated moveable tetrode depth, LC firing frequency i.e. relatively low firing during waking and silent during REM sleep quiescence [10], responsiveness to acoustic and/or tactile stimuli (Sara and Segal, 1991), and broad action potential waveform shape.

LC Optical Stimulation

All photostimulation experiments were conducted bilaterally. Two high powered blue LEDs (470 nm Luxeon) were coupled to optical fibers (200 mm core diameter, ThorLabs) using clear optical-grade epoxy (EPOTECH spectral transparency >99% 380-980nm) and implanted targeting the LC (same coordinates as tetrodes). Light pulses from LEDs were generated using a waveform generator (Agilent 3320A arbitrary waveform generator). Generated light pulses were 15 msec in duration and had a consistent 5-10 mW intensity

at the fiber tip prior to implantation. *In vivo* confirmation of light evoked potentials from ChR2 expressing LC cells was confirmed with LC tetrode recordings (Figure 2.3B).

LC stimulation and Arousal Experiments

Frequencies 4 Hz and above of LC optogenetic stimulation during NREM sleep decreased the animal's latency to arousal. Figure 2.3C shows example LFP spectral heatmaps and EMG traces in response to light stimulation during NREM sleep in ChR2- and a ChR2+ rats. Only ChR2+ rats arose from NREM sleep, and the effect only occurred in response to light stimulation at 4 Hz frequencies or greater, which was confirmed by increased EMG activity and a power spectral density shift from slow wave delta power (0.4-4 Hz) to waking theta power (5-9 Hz) in the hippocampal CA1 LFP (Figure 2.3C middle). Light pulses at any frequency were insufficient to produced arousal in ChR2- rats. 1-3 Hz LC stimulation was incapable of awakening the ChR2+ rats from NREM sleep (Figure 2.3D). We therefore chose a 2 Hz LC stimulation frequency in order to maintain sleep continuity and avoid inducing arousals in ChR2 rats, a sub-arousal threshold frequency that we used in all subsequent experiments. As spontaneous LC firing rates vary from 0-20 Hz, our evoked <2 Hz activity rate was well within physiological parameters and similar to previous work[137].

Histology

Rats were anesthetized with 1.0 mL sodium pentobarbital (intraperitoneal injection), then transcardially perfused through the left ventricle with 150 mL phosphate buffered saline (1X PBS) followed by 150 mL 10%formalin. The brain was removed and placed in 10% formalin for 24 hours, and then in 1x PBS solution containing 30% sucrose for 48-72 hours. Brains were sectioned into 50 μm coronal sections on a cryostat and then washed for 10 min in 1x PBS three times. The sections were blocked for 30 min in a solution containing 0.5% Triton, followed by 30 min in 5% normal goat serum. Primary antibodies for tyrosine hydroxylase (TH), 1:500 mouse-anti-TH (Immunostar), and mCherry (1:500, rabbit anti-mCherry; Biovision) were applied for 24 hours at 4 $^{o}$C, followed by 1 hour at room temperature (~23 $^{o}$C). After three 10-min washes with 1X PBS, secondary antibodies (1:1000, Goat anti-Rabbit AlexaFluor-594 and 1:1000, Goat anti-Mouse

AlexaFluor-488, Fisher) for were applied for 24 hours at 4 $^{o}$C. After three 10-min washes with 1X PBS, sections were mounted to slides (Fisher Superfrost Plus) with the ProLong Gold Antifade mounting medium (Invitrogen). Images of antibody stained sections were acquired with an Olympus BX-51 fluorescence microscope using wide-field mode.

Quantification and Statistical Analysis

All statistical tests were conducted in Prism 7 analytical software (GraphPad). All data sets were first tested for normality using Shapiro-Wilk normality test as recommended[144]. Data set normality was calculated without performing any transform (e.g. log10, or z-score) on the data set. Outliers were removed using ROUTs outlier test in Prism 7 with Q=1%. Statistical tests including ANOVA, Pearson correlations, t-tests, and their non-parametric equivalents were performed in a similar matter to previous research. Post-hoc analysis to adjust for multiple comparisons was used in accordance with Prism 7 statistical guide. Alpha was set to 0.05 for all analyses and was always calculated in a two-tail manner. Graphical representations of data were created using Graphpad Prism 7 and MATLAB.

Behavioral Task Performance

Animals' total errors on the familiar and altered task divided by 15 laps to show the average number of errors per lap and analyzed using repeated measures two-way ANOVA (Sidak post-hoc) for performance within a group across days and two-way ANOVA (Tukey post-hoc) for comparing between groups. For the difference between map errors and procedural errors the total number of each type of error was analyzed rather than error per lap. A repeated measures two-way ANOVA (Tukey post-hoc) was used to analyze within each error type and a two-way ANOVA (Sidak post-hoc) was used to compare both types of errors.

Sleep State Analysis

Sleep/waking states were scored manually using CA1 LFP and EMG recordings in the same manner as Emrick et al., 2016[36]. As the present study focuses on hippocampal learning and sleep, and previous work from our lab showed that the cortex and the

hippocampus can be in two different sleep states simultaneously (Emrick et al., 2016), CA1 LFP recordings were used instead of cortical EEG for sleep scoring and spindle identification. LFP and EMG recordings were down-sampled to 1000 Hz Epochs (10 s) were assigned a state of active waking, slow-wave sleep (SWS), Intermediate Sleep (which is a non-REM sleep state with high spindle power and occurrence equivalent to Stage 2 non-REM sleep in humans), or REM sleep using a sleep scoring program developed in our lab (Gross et al., 2009). The percentage of time spent in sleep across days within each group and between groups was analyzed using a two-way ANOVA (Sidak post-hoc).

Power Spectral Band Analysis

Down-sampled raw LFP from intervals of each scored state were entered into Neuroexplorer 5 software (Nex Technologies, Madison, AL). LFP data underwent a Fast-Fourier transform (FFT) using a window with a Hann taper. Change from baseline was identified using raw spectral power normalized to baseline across bands and expressed as a percent change from baseline by: ((day 1 – Baseline/Baseline) * 100%). The percent change from baseline to day 1 sleep in the full power spectra and the specific bands was analyzed using a two-way ANOVA (Sidak post hoc). The percent change from baseline to day 1 in REM sleep theta power was analyzed further in Figure 2.9 was analyzed via Mann-Whitney test.

Sleep Spindle and Ripple Identification

Sleep spindles were identified automatically from the entire sleep record. Automatic spindle identification was performed according to Eschenko et al 2006 [64]. Briefly, the sigma frequency (10-15 Hz) was filtered in the CA1 LFP data down-sampled to 200 Hz, taking the root-means-square (RMS) over a 100 msec window, then smoothing it with a moving average. Spindles were counted from periods at least 0.3 s in length where the RMS exceeded three times the standard deviation of the RMS mean of all NREM sleep intervals. Reduction in NREM sleep spindle occurrence from baseline to 2 Hz stimulation was analyzed via paired t-test in Figure 2.2. The percent change in spindle occurrence between baseline and day 1 was analyzed via Mann Whitney Test in Figure 2.9.

Ripples were automatically identified similar to the methodology described in Girardeau et al 2009[95] using a custom script written in MATLAB. Using the RMS of the 100-200 Hz bandpass filtered LFP, ripples were identified when the RMS crossed an upper threshold of five times the standard deviation of the average RMS for NREM and IS sleep. Ripple edges were detected when the RMS fell below a second threshold of two times the RMS standard deviation. Ripples were considered only in segments corresponding to NREM sleep states. Ripple occurrence and ripple length between groups and days was analyzed with a two-way ANOVA (Sidak post hoc) whereas percent change in ripple length and occurrence from baseline was analyzed via Mann Whitney Test.

Ripple-Spindle Coupling

Spindles and ripples were automatically identified (see previous section). Using custom MATLAB scripts, peri-event time histograms (PETHs) were generated using the start time of ripples as the event, and the start time of the spindles as the as the corresponding response. A range of 2500 msec prior to and following ripple onset was used, and bins were 50 msec in width. The number of spindle start times per bin was then divided by the total number of events (ripple start times) to convert to normalized probability. To test that this ripple-spindle coupling was non-random, shuffled ripple start time data (n=15 per animal per day) was generated using a Monte Carlo method similar to Siapas 1998[81] (we note this is a method of shuffle can be liberal). Shuffling was performed only during periods of NREM sleep to prevent an artificial reduction in the shuffled correlations. Spindle probability between ChR2- and ChR2+ rats, as well as either group vs shuffled data was analyzed using via two-way ANOVA (Sidak post hoc).

Single Unit Isolation

Spike data were sorted into individual neurons using Offline Sorter x64 V3 (Plexon). For each tetrode recording of spikes, the data was manually sorted into single units using spike features of each of the four channels of the tetrode (e.g. principle component analysis or peak amplitude of each channel). LC and CA1 pyramidal cell firing rate by state was analyzed using a repeated measures two-way ANOVA with Sidak post hoc.

Place Cell Identification and Analysis

Following unit isolation, CA1 units were first separated into pyramidal cells and fast spiking interneurons based upon firing rate while the animal was running on the maze, as well as by spike width (pyramidal cells having a wider spike than fast-spiking interneurons). Interneuron data was then discarded from future analysis. Position tracking data from the rats running on the octagonal tract was separated into laps for the familiar and altered task. The track was then broken into 3 cm bins and linearized. Pyramidal cell spiking data was then used to generate raw rate maps and occupancy maps. Periods of less than 5 cm/s velocity were removed. Information content was calculated as in Skaggs et al. 1993[145]. Cells with less than an information content of 0.15 were removed similar to Fuhs et al[146] and all cells that were not active a minimum of five laps on a maze were also discarded. A Gaussian smoothing filter (SD=4) was then applied to the firing rate data. Cells were determined to be place cells if their smoothed firing rate crossed threshold (1 Hz) for 3 or more consecutive 3 cm bins, in addition to meeting the above criteria. Place cell stability or lap to lap correlation (r), was computed per cell via a bin-by-bin Pearson's correlation between firing rate maps for all laps that the cell was active similar to[93]. Place cell average lap to lap correlation cumulative probability was analyzed using K-S test, and average day 2 place field lap to lap correlation were analyzed via Mann-Whitney test. Place field absolute shift and size were analyzed using a Kruskal Wallis (Dunn post hoc) and place field center of mass shift from original position was analyzed using a two-way ANOVA (Dunnett post hoc).

## 2.2 Endogenous locus coeruleus activity decreases during spindle-rich intermediate sleep and terminates NREM spindle when occurring simultaneous

Tetrode recording of endogenous LC neural activity across sleep and wakefulness showed highest LC activity during waking and significant reductions in activity during all stages of sleep: NREM-slow wave sleep, NREM-intermediate sleep, and REM sleep. (Figure 2.1). Within NREM sleep, LC neuron activity during spindle-rich intermediate sleep (IS)[20] was similar to REM sleep, when LC activity reached its lowest point. Thus,

both REM sleep and spindle rich IS sleep are periods of greatly reduced LC neuronal activity.

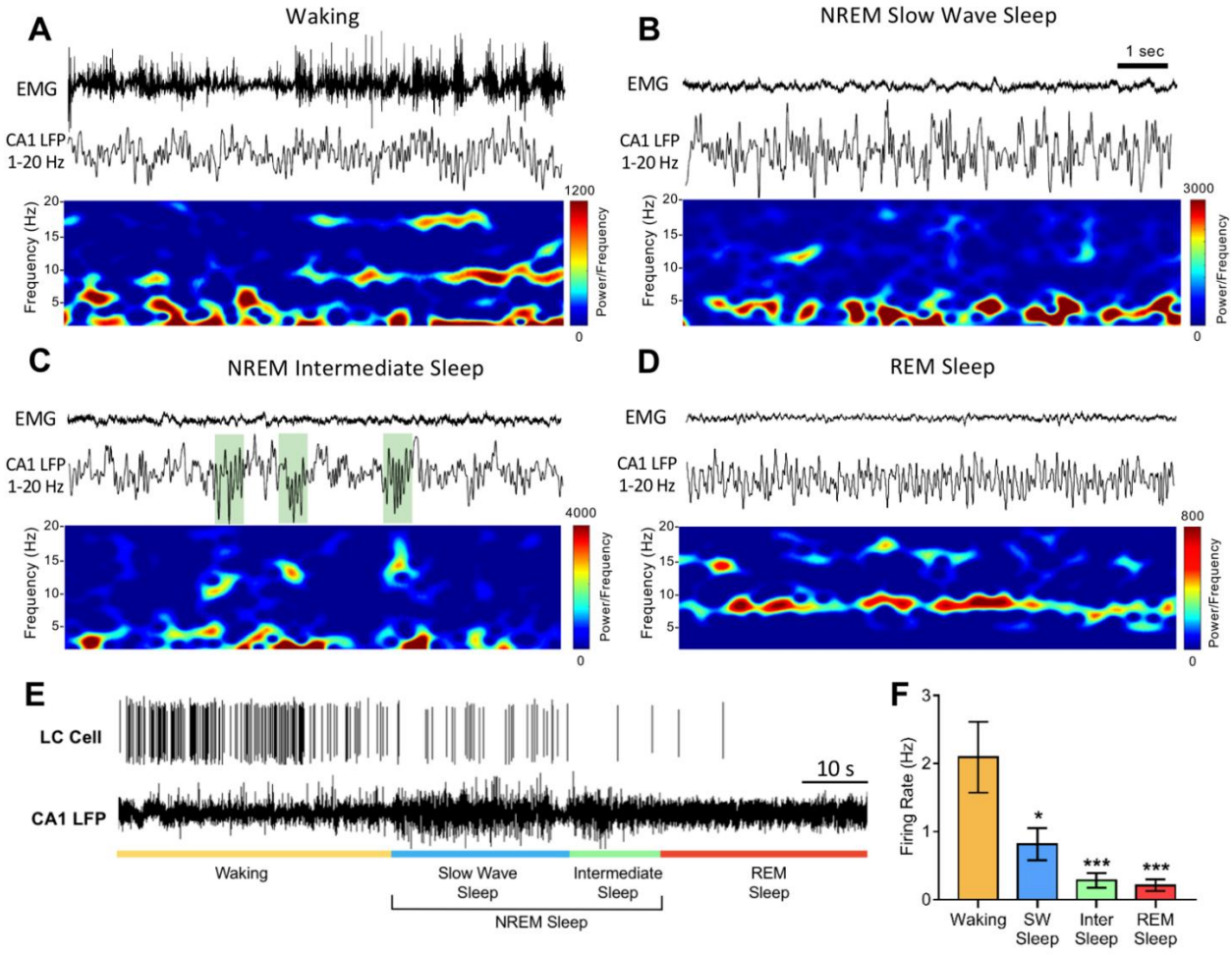


Figure 2.1 10 second epochs of each scored state of sleep with neck EMG and CA1 LFP (0-20 Hz) and LC spiking activity.
(A) Waking with high EMG activity and CA1 theta (5-9 Hz) activity.
(B) NREM slow wave sleep with low EMG activity and characteristic slow waves (0.4-4 Hz).
(C) NREM intermediate sleep that also has low EMG activity, and slow waves but also contains a high occurrence of sleep spindles highlighted in green (spindles can also occur in NREM slow wave sleep).
(D) REM sleep with the lowest EMG activity and characteristic high-power theta activity and the absence of slower frequency activity that pervades NREM sleep.
(E) Representative example of LC cell spiking activity across different states of waking and sleep as identified by CA1 LFP.
(F) Quantified LC firing rate across different states of sleep compared to waking (in wild type rats). Bar colors match designated state colors in part A. n=12 cells from five rats; comparison of each state versus waking. One-way ANOVA, Tukey post hoc: waking versus SW (slow wave) sleep p=0.019; waking versus inter (intermediate) sleep p=0.0004; waking versus REM sleep p=0.0003. *p<0.05, ***p<0.0005.

Aston-Jones and Bloom[133] demonstrated that LC neurons fire with a specific temporal relationship to sleep spindles, falling silent one second prior to the onset of each sleep spindle. In the latter half of the sleep spindle, LC neurons resume firing (see example in

Figure 2.2A). We posit that this resumption of LC activity mid-spindle leads to spindle termination, possibly through the depolarizing action of norepinephrine on thalamocortical neurons; norepinephrine repolarizes thalamocortical neuronal membranes and terminates the voltage-gated Ca++ spikes that generate sleep spindles[22,24]. We found that LC spikes within sleep spindles occurred when the spindles reached maximal power in the 10-15 Hz sigma band. These within-spindle LC spikes were followed by an immediate and rapid reduction of sigma power (Figure 2.2B, C), supporting the idea that LC activity leads to spindle termination. This phenomenon was spindle-specific as LC spikes occurring outside of sleep spindles (during NREM sleep) had no effect on sigma power.

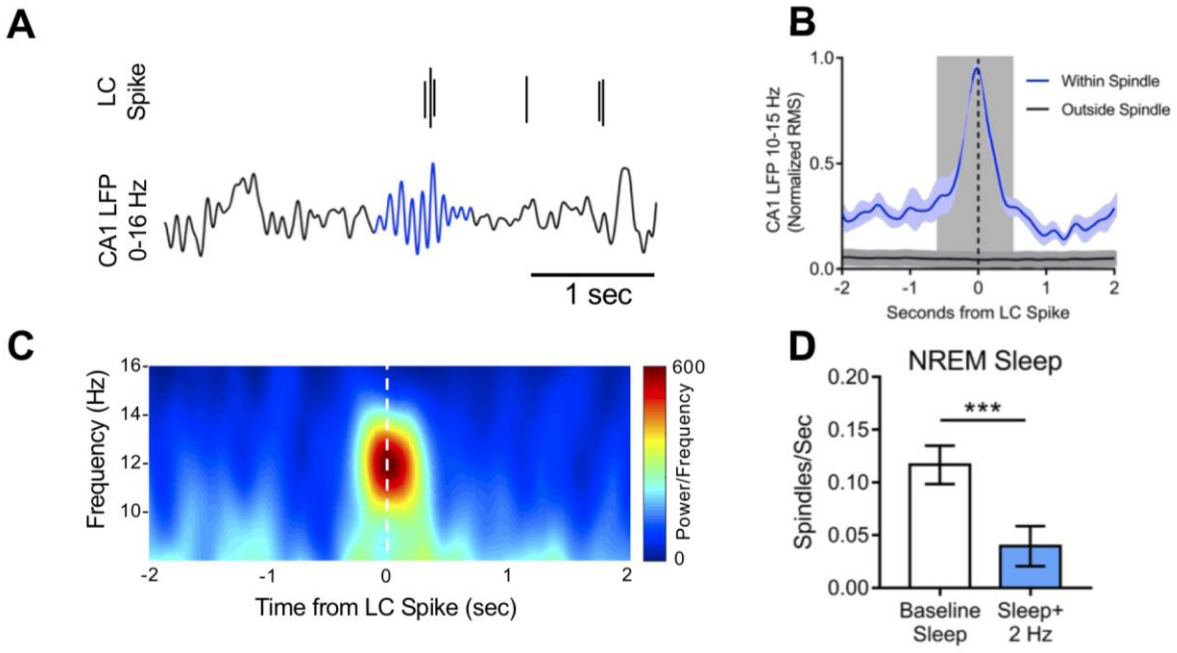


Figure 2.2 LC spikes sync to peak spindle power and LC optogenetic stimulation decreases spindle occurrence.
(A) Example of LC timing in relation to spindles. LC activity ceases prior to spindle onset, and during the spindle (in blue) LC activity returns, leading to a decrease in spindle power.
(B) Normalized root mean square of spindle power (10-15 Hz) during sleep spindles centered on LC spikes. The blue line represents the mean (± sem) effect of LC spikes on spindle power when spikes occur within identified spindles, whereas the dark grey line represents the effect of LC spikes on mean spindle power (± sem) outside of identified spindle (n=3 rats). The light grey area indicates values with significant differences between the two with significance from $p<0.05$ to $p<0.0001$ from t=-0.67 to t=0.54 seconds.
(C) Example heat map displaying rise and fall of spindle power (color bar in $\mu V^2/Hz$) centered on LC spikes occurring within the spindles (n=561 spindles from three animals).
(D) Two Hz LC stimulation during sleep decreases CA1 spindle occurrence rate in ChR2+ rats, n=4. Paired t-test ***p=0.0003. Displayed as mean ± sem.

## 2.3 Locus coeruleus optogenetics stimulation during sleep decreases spindle occurrence

Due to the precise timing of LC neuronal spikes during spindles, along with previous work showing that norepinephrine infusions into thalamic nuclei *in vitro* abolishes spindle generation[24], we hypothesized that optogenetically enhanced LC activity during sleep could be used to reduce spindle occurrence during NREM sleep. To test this, we expressed channelrhodopsin (ChR2) in LC cells under the control of PRSx8, a synthetic dopamine-beta hydroxylase promoter[147] (Figure 2.3A). Extracellular recordings of ChR2 expressing LC cells *in vivo,* showed light-evoked action potentials in response to 473 nm light pulses (Figure 2.3B).

We conducted a series of experiments to determine what frequency of LC stimulation was permissible to maintain sleep without evoking arousals (see methods and Figure 2.3C-E). We found 2 Hz LC stimulation did not generate arousals and, further, was within the normal physiological activity range. In addition, a previous study in performing LC optogenetic stimulation in mice found that 3 Hz over the course of 6 hours did not significantly change sleep architecture[137]. Therefore, 2 Hz was used throughout the remainder of the studies.

As predicted, stimulating noradrenergic LC neurons of ChR2+ rats at 2 Hz during sleep resulted in a significant decrease in NREM sleep spindle occurrence compared to baseline sleep lacking stimulation in the same animals (Figure 2.2D).

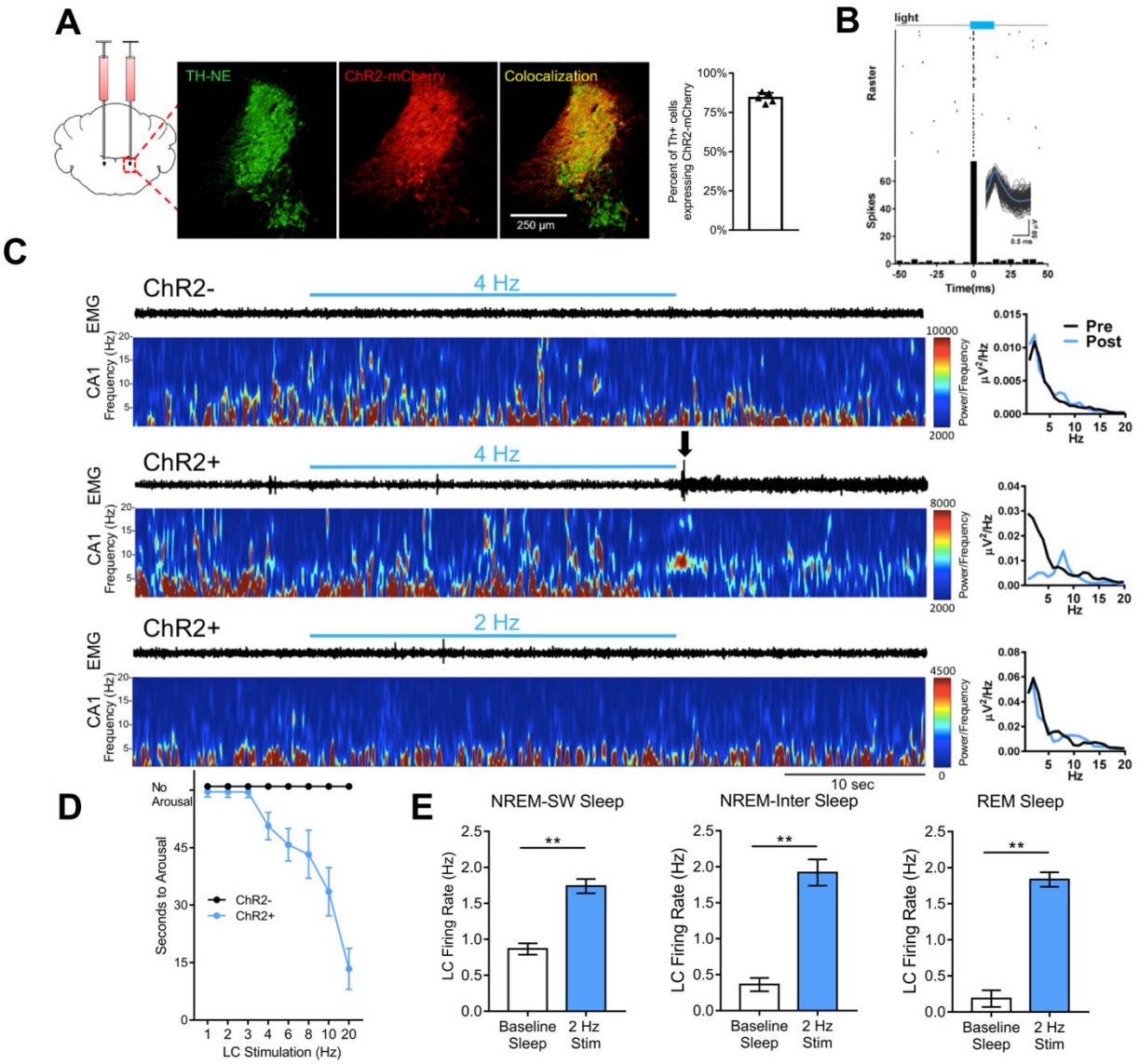


Figure 2.3 LC stimulation at low frequencies does not generate arousals.
(A) Immunostaining of TH-expressing (TH+) LC cells (green), cells expressing ChR2-mCherry (red), and colocalization of TH and mCherry expressing cells (yellow). Quantification of ChR2-mCherry expression in Th+ cells (n=5 rats).
(B) Perievent raster and spike histogram of LC cells firing in response to 470 nm light stimulation during NREM sleep (75 trials). Subplot of LC spontaneous non-evoked LC waveforms overlaid in grey and the mean of light-evoked LC waveforms shown in blue.
(C) LFP and EMG traces showing LC optogenetic stimulation effects. The blue bar represents light stimulation with the frequency labeled above. The entire trace length is one minute in length. Top left: 4 Hz stimulation in a ChR2- rat showing no arousal. Middle left: 4 Hz stimulation in a ChR2+ rat, black arrow shows point of arousal from NREM sleep. Bottom left: 2 Hz stimulation in a ChR2+ rat, showing no arousal. The LFP spectral power from the 10 sec pre- and 10 sec post-stimulation are shown to the right of each trace. Arousal following LC stimulation shows clear shift from delta to theta band.
(D) Increasing frequencies of LC stimulation decreases latency to arousal from NREM sleep in ChR2+ rats; ChR2- n=5, ChR2+ n=8.
(E) The change in LC firing rate between baseline and 2 Hz optogenetic stimulation across slow wave sleep, intermediate sleep, REM sleep. Baseline sleep n=5; 2 Hz stim n=8. NREM-SW Sleep baseline versus 2 Hz Mann-Whitney p=0.0016; NREM-Inter sleep baseline versus 2 Hz Mann-Whitney p=0.0016; REM sleep baseline versus 2 Hz Mann-Whitney p=0.0016. **p<0.005; bars represent mean ± SEM.

## 2.4 Locus Coeruleus stimulation during sleep impaired subsequent hippocampal spatial encoding

Sleep spindles are strongly implicated in memory consolidation and in the integration of new information into existing knowledge[74,85]. Previous work from our lab showed that pharmacologically enhancing noradrenergic activity across the post-training sleep period (using the selective noradrenergic reuptake inhibitor Desipramine) impaired hippocampal learning[142]. We tested whether enhancing noradrenergic activity selectively during only post-training sleep was sufficient to impair hippocampal spatial encoding. Rats in a separate cohort from those shown in Figure 2.2 were pretrained on a hippocampus-dependent spatial learning task[143] that presented food rewards at three familiar positions on an elevated octagonal track (Figure 2.4A). Once the rats reached behavioral criteria (< 1 error per lap) during the training period, they ran the track daily with food at the familiar task locations, and then ran the track for an additional 15 laps with two of the three food reward locations shifted to altered positions (the altered task) that remained in the same altered place for the last 15 laps each day. The function of the task was to evaluate whether rats could remember both reward location maps: the three previously consolidated, familiar locations and the new, altered locations. Following the familiar and altered track running sessions, we monitored rats' sleep-wake behavior via neck EMG and CA1 LFP activity, and optogenetically stimulated the LC at 2 Hz whenever the rat was asleep (both NREM and REM) in the 5-hour post learning period. This 5-hour post-learning window has been shown to be a critical period for hippocampal sleep-dependent memory consolidation (see for review[50]). Stimulation occurred on the first two days as, by day 3, REM sleep signs of memory consolidation are already apparent[104,148].

We first examined the effect of LC stimulation on hippocampal place cell spatial encoding. Stimulating the LC during sleep after day 1 exposure to the familiar and altered tasks resulted in reduced lap-to-lap spatial stability of place fields during both familiar and altered tasks on day 2 in ChR2+ rats (Figure 2.4B, E). Figure 2.4C and 2.4F show representative heat maps of place field locations across laps with each field's associated stability metric (i.e., the Pearson correlation of the field firing maps across laps – higher r values represent higher spatial stability). The decrease in place field stability in ChR2+

rats went hand-in-hand with a significant increase in lap-to-lap shifts in place field location on both tasks (Figure 2.4D, G).

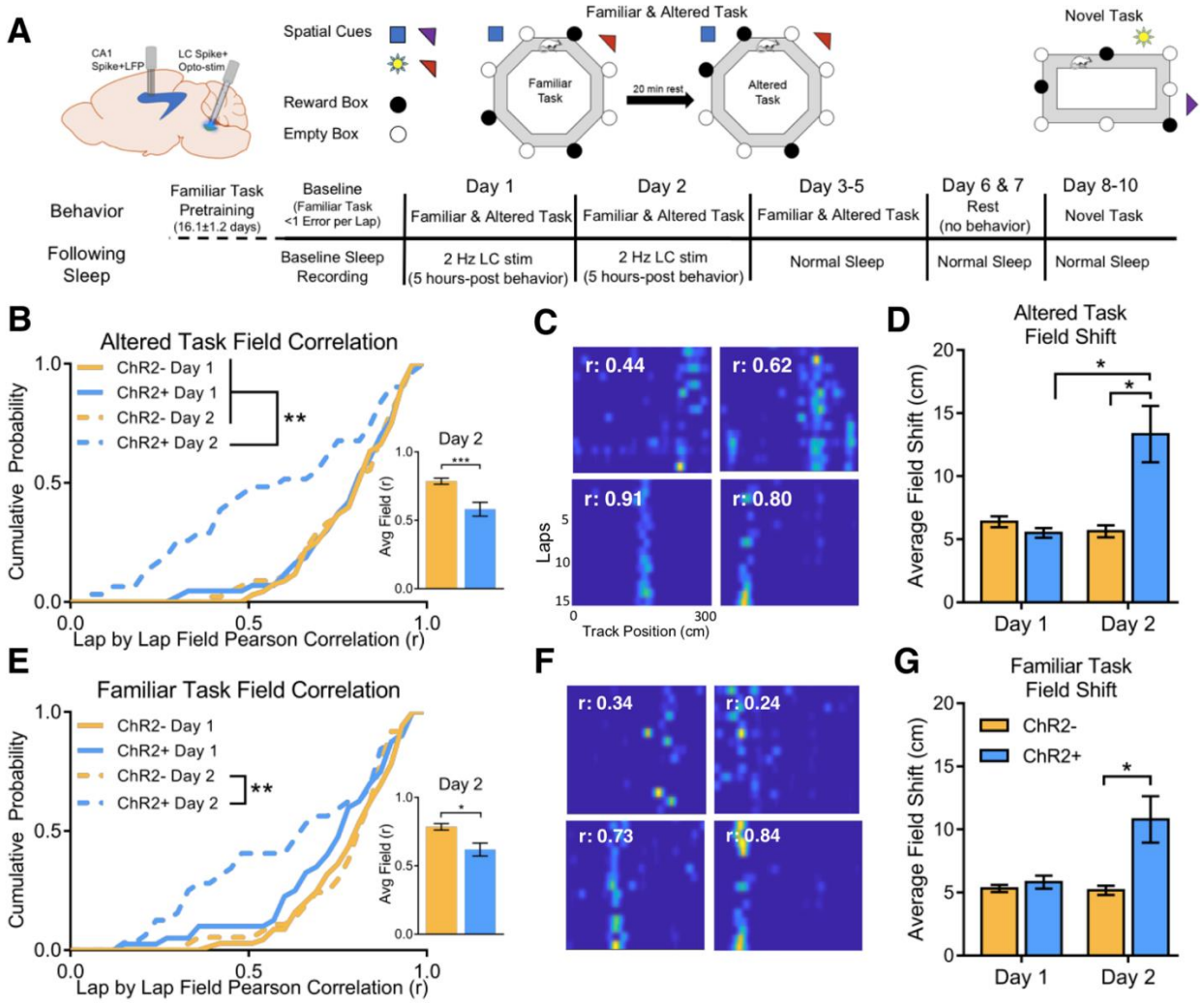


Figure 2.4 LC stimulation during sleep impairs next day place field encoding.
(A) Illustrations of recording electrode placements in the rat brain, task layout, and experimental timeline.
(B) The cumulative probability of the lap-to-lap place field Pearson correlation on altered task. Fields with high spatial stability have a higher correlation. On Day 2 ChR2+ rats show a shift towards more fields having lower correlation values. Kolmogorov-Smirnov Test **p<0.01. Subplot bar graph displays the overall average Day 2 field correlation. Mann-Whitney ***p=0.003.
(C) Representative heat maps of place field spatial encoding with warmer colors displaying where CA1 pyramidal spikes were located along the track (horizontally), and where firing occurred across multiple laps (vertically). The top two represent lower correlation fields from ChR2+ Day 2. The bottom two represent higher correlation fields from ChR2- Day 2.
(D) Average place field shift per lap on the altered task on Day 1 and Day 2. As shifts can be in positive or negative direction, the absolute value of the shifts are used to calculate the averages in part B and D. Part A and C: ChR2- Day 1 n=61, ChR2+ Day 1 n=43, ChR2- Day 2 n=45, ChR2+ Day 2 n=31 (outlier removed from Control Day 1 and Control Day 2). Kruskal-Wallis, Dunn post hoc: ChR2+ day 1 vs ChR2+ Day 2 p=0.040, ChR2- Day 2 vs ChR2+ Day 2 *p=0.013.

(E) The average lap-to-lap place field correlation on familiar task with ChR2+ Day 2 rats showing decreased field correlation. Kolmogorov-Smirnov Test **p<0.01. Subplot bar graph displaying the overall average Day 2 field correlation. Mann-Whitney *p=0.023.
(F) Representative heat maps of place field spatial encoding on the familiar task. Top two represent lower correlation fields from ChR2 Day 2. Bottom two represent higher correlation fields from Control Day 2.
(G) Average place field shift per lap on the familiar task on Day 1 and Day 2. Part D and G: ChR2- Day 1 n=66, ChR2+ Day 1 n=40, ChR2- Day 2 n=37, ChR2+ n=32 (one outlier removed from ChR2- Day 2). Kruskal-Wallis, Dunn post hoc: ChR2- Day 2 vs ChR2+ Day 2 *p=0.046. Bar graphs displayed as mean ± sem.

Next, we examined place field expansion. While performing a lap-based task, the center of mass (COM) of a place field (i.e., the region within the place field where the place cell has the highest activity) shows a net shift backwards across multiple laps, expanding the overall field size as the place cell begins to fire slightly earlier on the track. This phenomenon is better known as place field backward expansion[149,150]. Place field backward expansion is an NMDA-dependent plasticity effect[151]. As place fields do not grow across days[152] and remain relatively stable in position, the field size and center of mass must reset between days and running sessions. We have previously posited that this reset function is accomplished by depotentiation that is allowed by the absence of LC activity during REM sleep[104,148]. The abnormal presence of LC activity during REM sleep would prevent this resetting of place field size and center of mass. We found that while place field backward expansion occurred normally on day 1 (before intervention) on both tasks, on day 2 in ChR2+ rats, the familiar place fields did not again expand backwards during the maze session, but rather, shifted abnormally forward (Figure 2.5B). There was also a significant increase in familiar task place field size on day 2 selectively in ChR2+ rats (Figure 2.5D). These abnormal expansion and forward shifts were not seen on the altered task (Figure 2.5A, C), suggesting a specific effect on previously consolidated, familiar spatial information.

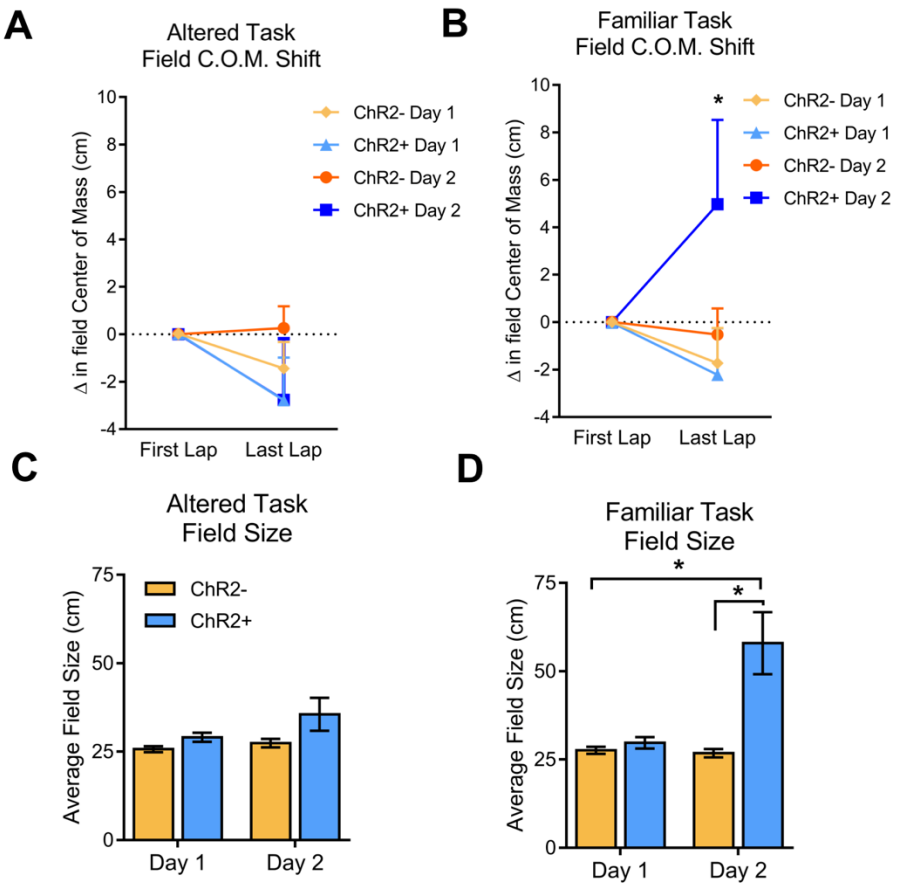


Figure 2.5 LC stimulation during sleep leads to abnormal place field expansion on the familiar task during next day task performance.
(A) Place field center of mass shift from the original position on the first lap to the last lap of the altered task. Both groups expand backwards as previously shown on day 1 and there was no difference between groups on day 2.
(B) Place field center of mass shift from original position on the first lap to the last lap of the familiar task. Both groups expand backwards as previously shown on day 1, however on day 2, ChR2+ rats' center of mass significantly shifts forward. Two-way ANOVA, Dunnett post hoc: ChR2- day 1 versus ChR2+ day 2 p=0.0032; ChR2+ day 1 versus ChR2+ day 2 p=0.0033; ChR2- day 2 versus ChR2+ day 2 p=0.039. *p<0.05.
(C) Average place field size on the altered task.
(D) Average place field size on the familiar task. Kruskal-Wallis, Dunn post hoc: ChR2- day 1 versus ChR2+ day 2 p=0.045, ChR2- day 2 versus ChR2+ day 2 p=0.027. Data displayed as mean ± SEM.

Both spatial mapping abnormalities of place field stability and abnormal place field backward expansion indicates that LC stimulation during sleep following learning on day 1 caused abnormal CA1 place field consolidation of the altered task and abnormal reconsolidation of the familiar task. Interestingly, these effects occurred independent of any changes in CA1 pyramidal cell firing rate during NREM, REM sleep, or waking (Two-way ANOVA, Sidak post hoc p=0.92, 0.66, and 0.98, respectively).

## 2.5 Locus coeruleus stimulation during post-learning sleep impaired spatial learning and memory performance

Just as place encoding was impaired on both the altered and familiar task by enhanced LC activity during sleep, behavioral performance was similarly impaired on both tasks. On the altered task, ChR2+ rats showed no day-to-day improvement, whereas ChR2- rats improved significantly from day 1 to day 5 and performed significantly better than ChR2+ rats on day 4 and 5 (Figure 2.6A). Not surprisingly, given the place field encoding deficits, ChR2+ rats also performed significantly worse on the familiar task than ChR2- rats, showing a significant decline in performance between days 1 and 5, and performing worse than controls by day 4 and 5 (Figure 2.6B). To ensure that LC stimulation during sleep had no lasting effect on learning once the stimulation protocol ceased, the following week both groups were run on a completely novel hippocampal task with new novel spatial cues and reward locations, followed by normal sleep. Both groups learned the novel task at similar rates and showed significant improvement in performance within two days (Figure 2.6C).

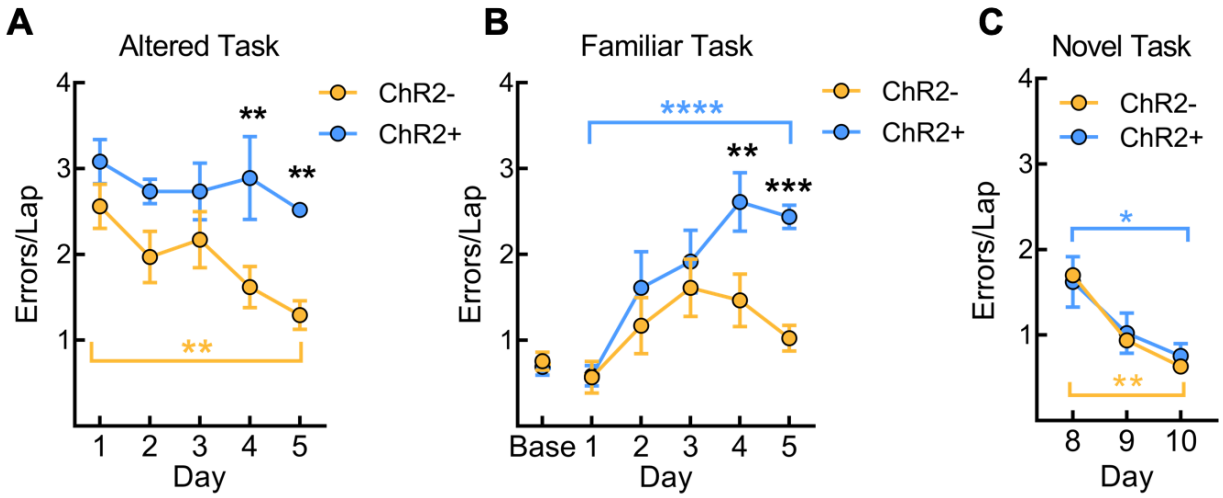


Figure 2.6 LC stimulation during sleep impairs learning and memory.
(A) The average errors per lap by day for the ChR2- and the ChR2+ groups on the altered task. Two-way ANOVA, Sidak post hoc (in black): ChR2- vs ChR2+ Day 4 p=0.0012, Day 5 p=0.0017. Two-way ANOVA, Tukey post hoc (in yellow): ChR2- Day 1 vs Day 5 p=0.002. **p<0.005.
(B) The average errors per lap for ChR2- and stimulated ChR2+ groups on the familiar task. Two-way ANOVA, Sidak post hoc (in black): ChR2- vs ChR2+ Day 4 **p=0.0032, Day 5 ***p=0.0004. Two-way ANOVA, Tukey post hoc (in blue): ChR2+ Day 1 vs Day 5 ****p<0.0001.
(C) The average errors per lap for ChR2- and ChR2+ groups on the novel task with both groups meeting criteria of less than one error per lap after three days of maze running. Two-way ANOVA, Tukey post hoc: ChR2- Day 8 vs Day 10 (in yellow) **p=0.0019, ChR2+ Day 8 vs ChR2+ Day 10 (in blue) *p=0.0084.
Five rats for each group for panels A and B; three rats for each group in panel C. Data displayed as mean ± sem. *p<0.05 **p<0.005, ***p<0.0005, ****p<0.0001.

## 2.6 Locus coeruleus stimulation during sleep altered task-solving strategies

In addition to the error count, we were curious to see whether rats utilized hippocampal strategies to solve the task or instead reverted to a random search strategy[153]. We termed errors “map errors” if they were errors committed at the reward locations that differed between the tasks, and “procedural errors” if the error was at a location where the reward contingency remained static (i.e. checking any of the three box positions that were not rewarded on either the familiar or altered tasks, or skipping the one box position that was rewarded on both mazes) (Figure 2.7A). For the altered task, as expected, ChR2- rats consistently committed significantly more map errors than procedural errors, checking for food in previously rewarded positions (Figure 2.7B). In contrast, in LC stimulated rats there was no difference in the number of map errors compared to procedural errors by day 2, and each day the average number of procedural errors climbed until they were on par with the number of map errors (Figure 2.7C)—suggesting adoption of a random search strategy. On the familiar task (after the first exposure to the altered maze on day 1), ChR2- rats committed significantly fewer procedural errors than map errors and showed an overall downward trend in procedural errors across days, whereas ChR2+ rats committed a similar number of procedural and map errors across days with an overall trend to increasing errors of both types across days (Figure 2.7D, E).

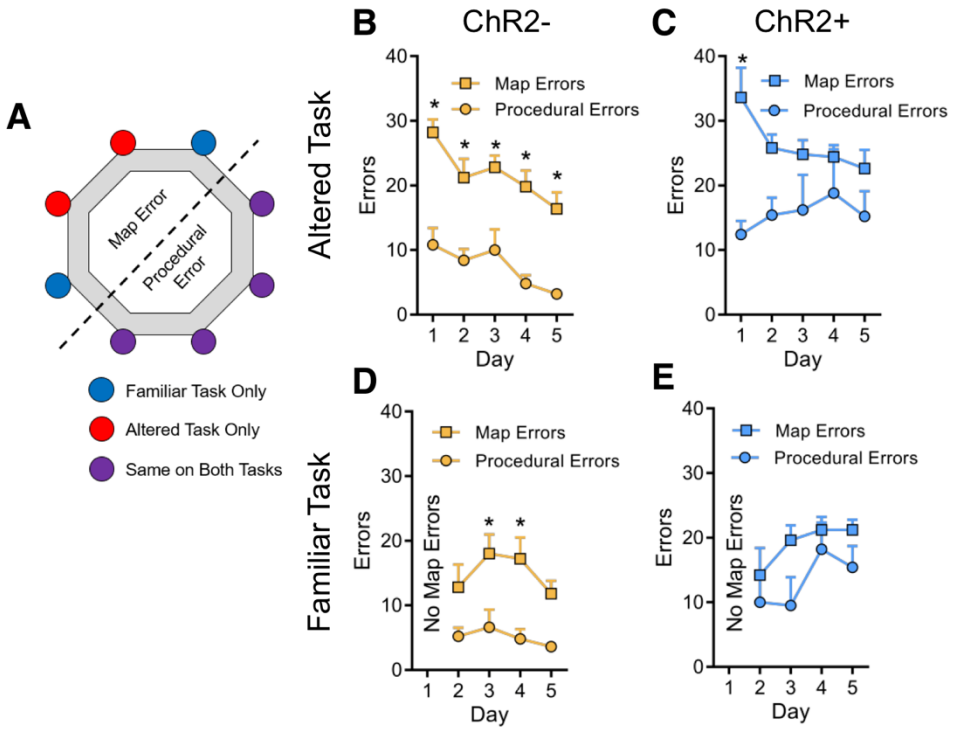


Figure 2.7 LC stimulation during sleep alters maze solving strategies.
(A) Schematic showing difference between procedural errors and map errors. Red dots would be map errors on the familiar task as they are only baited during the altered task, and blue dots represent map errors on the altered task as those boxes are only baited on the familiar task. Purple dots are boxes that are consistent (whether baited or non-baited) between the familiar and the altered task.
(B) ChR2- group performance on the altered task, broken down by error type. Two-way ANOVA, Sidak post hoc: map vs procedural errors Day 1 $p<0.0001$, Day 2 $p=0.0012$, Day 3 $p=0.0012$, Day 4 $p=0.0001$, Day 5 $p=0.0009$. *$p<0.005$.
(C) ChR2+ group performance on the altered task broken down by error type. Two-way ANOVA, Sidak post hoc: map vs procedural errors: Day 1 $p=0.0016$. *$p<0.005$.
(D) ChR2- group performance on the familiar task broken down by error type. Two-way ANOVA, Sidak post hoc: map vs procedural errors Day 3 $p=0.01$, Day 4 $p=0.0047$. *$p<0.05$
(E) ChR2+ performance on the familiar task broken down by error type.
Five rats in each group for panels B-E. Symbols and error bars represent day mean ± sem.

## 2.7 Locus coeruleus stimulation during sleep altered spectral frequency bands, but not sleep architecture

We next examined whether LC sleep stimulation caused any change in sleep characteristics. Looking first at waking, there was no difference in the percent of the total time spent awake between ChR2- and ChR2+ rats, i.e., LC stimulation did not prevent sleep (Figure 2.8A). Within sleep, there was no difference in the percent of time spent in any state between groups (Figure 2.8B) and there was no difference in the number of transitions from either NREM sleep or REM sleep to waking (Figure 2.8C). That is, there was no increase in the number of arousals with LC stimulation. Finally, there was no

rebound in sleep or change in percent spent in any sleep state on day 3 when no LC stimulation occurred.

However, LC sleep stimulation did cause decreases in CA1 spectral band power at several frequencies during specific sleep stages (Figure 2.8D, E). No change was seen in any band power during waking, although that is to be expected as LC stimulation was turned off once signs of waking were observed. There was no LC-stimulation associated change in higher frequency bands such as slow gamma (30-50 Hz) or fast gamma (61-100 Hz) during any sleep state. However, both NREM slow wave sleep and NREM intermediate sleep showed a selective decrease in delta (1-4 Hz) band power during LC stimulation periods. The decrease in NREM-SWS delta power correlated with Day 5 procedural errors on both the familiar and altered tasks (Table 2.1). Intermediate sleep also decreased band power in the frequency range associated with sleep spindles: sigma (10-15 Hz). During REM sleep, LC stimulation selectively decreased theta power (5-9 Hz) (Figure 2.8D, Figure 2.9A) and the percent drop in theta power correlated with overall day 5 performance. Theta power suppression accompanied day 5 procedural errors (i.e. errors at boxes that did not change between mazes) on both familiar and altered maze tasks but did not correlate with map errors (Table 2.1). Thus, NREM delta and REM sleep theta impairments corresponded with performance errors specifically in those areas of the maze that never changed their reward contingency. These types of errors can be associated with a general search pattern rather than reliance on a trusted map.

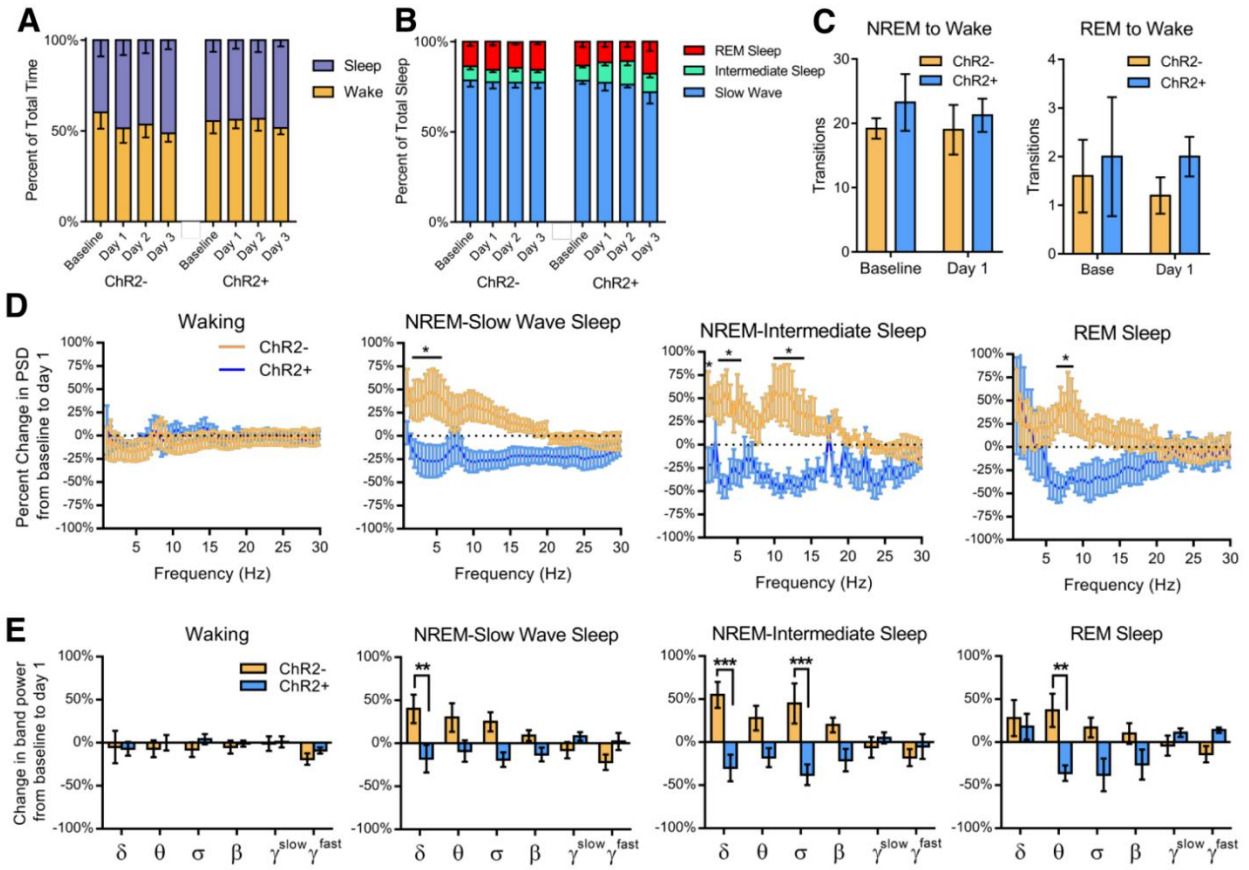


Figure 2.8 LC stimulation does not produce changes in sleep architecture but does alter spectral power.
(A) Mean (± sem) percent time spent awake and sleeping compared to total time.
(B) Mean (± sem) percent of total sleep spent in slow wave sleep, in intermediate sleep, and in REM sleep.
(C) The mean (± sem) number of transitions from NREM sleep to wake and from REM sleep to wake within the first hour of sleep.
(D) Percent change from baseline to Day 1 in CA1 LFP spectral power during waking, slow wave sleep, intermediate sleep, REM sleep. Five ChR2-, four ChR2+ rats for panels A-D. Two-way ANOVA, Sidak post hoc. Bars represent mean ± sem.
(E) Percent change in band power from baseline to Day 1 sleep. $\delta$ 1-4 Hz, θ 5-9 Hz, σ 10-15 Hz, β 16-20 Hz, $\gamma^{slow}$ 30-50, $\gamma^{fast}$ 61-100 Hz for all states. Two-way ANOVA, Sidak post hoc: Slow Wave Sleep delta p=0.0067; Intermediate Sleep delta p=0.0007, sigma p=0.0009; REM sleep theta p=0.005. *p<0.05, **p<0.01, ***p<0.005.

## 2.8 Locus coeruleus stimulation during sleep decreased sleep spindle occurrence and interfered with ripple-spindle coupling

In addition to frequency changes, we tested whether LC stimulation altered the rate of spindle occurrence during sleep following learning. While there was no difference in baseline spindle occurrence between groups (ChR2- 0.045±0.002 spindles/sec, ChR2+ 0.055±0.004 spindles/sec), the percent change from baseline to day 1 sleep was significant between groups: ChR2+ rats experienced a decrease in spindle occurrence and ChR2- animals saw an increase (Figure 2.9B). LC stimulation reduced spindle

occurrence in rats performing our learning task as well as in rats without a learning task. However, the absence of a learning task significantly increased this reduction in spindle occurrence caused by LC stimulation (Figure 2.10). However, in both cohorts, when LC optogenetic stimulation occurred within a spindle we found that spindle power decreased ~90 msec following light onset (Figure 2.9C). This 90 msec timeframe is consistent with the conduction of LC action potentials through unmyelinated axons to their terminals[154,155]. We found that the occurrence of spindles whose length exceeded our inter-stimulus interval, i.e. spindles ≥0.6 seconds in length, were disproportionately reduced, whereas shorter spindles were unaffected (Figure 2.9D). This change in spindle occurrence from baseline to day 1 correlated with overall day 5 performance on the altered and familiar tasks. The change in spindle occurrence specifically correlated with day 5 map errors on the familiar task (i.e. box positions that changed between mazes), but not with procedural errors (Table 2.1). That is, the rate of spindle occurrence was associated with disambiguating reward locations between the two tasks. As only long spindles were reduced, their reduction likely contributed to the confusion between familiar and altered reward locations.

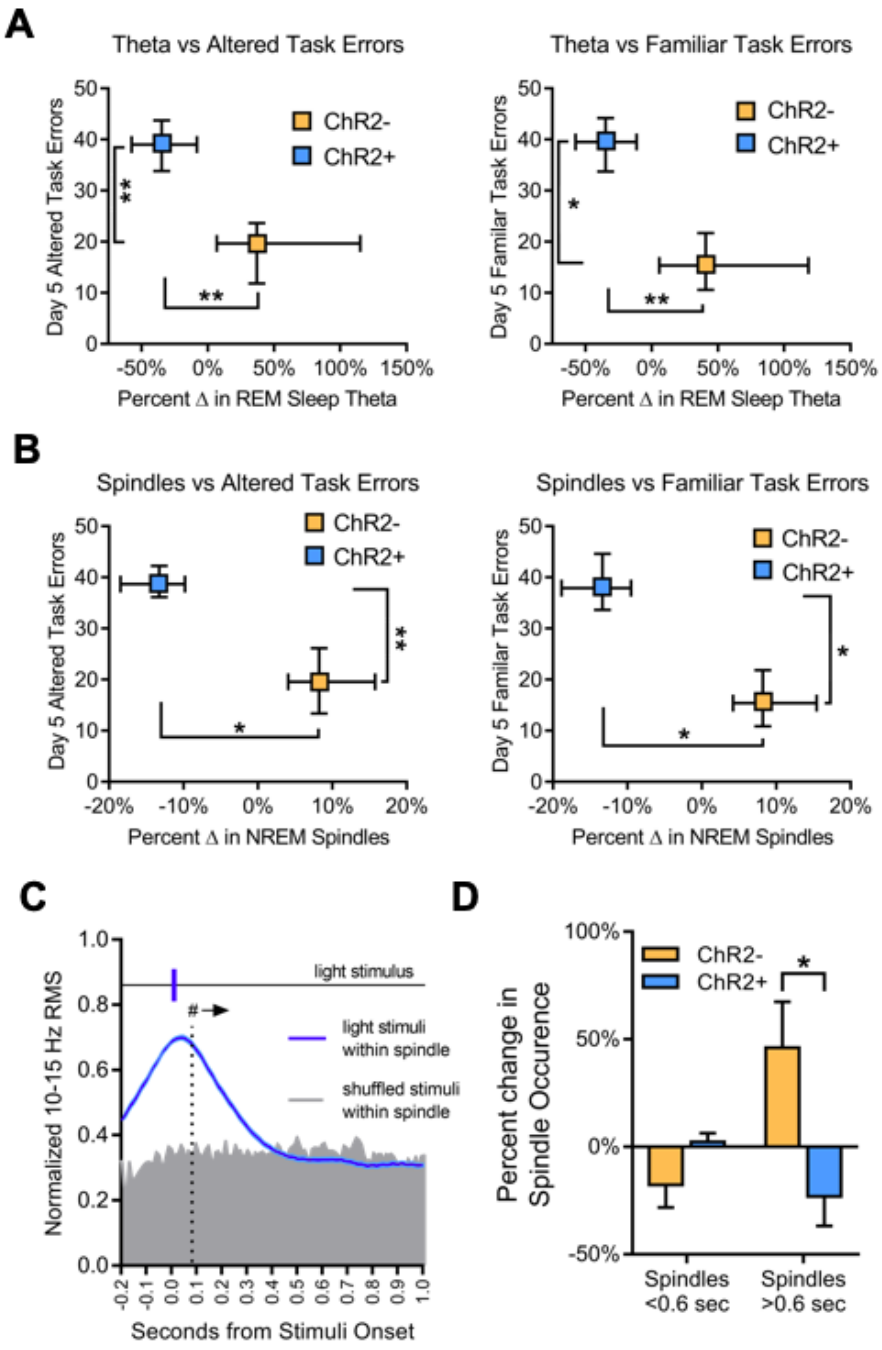


Figure 2.9 Changes in REM sleep theta power and NREM spindle occurrence from baseline sleep to day 1 sleep with LC stimulation.
(A) The percent change from baseline to Day 1 in REM sleep theta power vs Day 5 altered task total errors (left) and Day 5 familiar task total errors. ChR2+ vs ChR2- change in REM theta (x axis comparison) Mann-Whitney p=0.0079. ChR2+ vs ChR2- altered task errors (y axis comparison) Mann-Whitney p=0.008. ChR2+ vs ChR2- familiar task errors (y axis comparison) Mann-Whitney p=0.016.
(B) The percent change from baseline to Day 1 in CA1 spindle occurrence during NREM sleep vs Day 5 altered task total errors (left) and Day 5 familiar task total errors. ChR2+ vs ChR2- change in spindle rate (x axis comparison) Mann-Whitney p=0.016. ChR2+ vs ChR2- altered task errors (y axis comparison) Mann-Whitney p=0.008. ChR2+ vs ChR2- familiar task errors (y axis comparison) Mann-Whitney p=0.016.
Error bars represent the minimum and maximum within a data set; vertical and horizontal lines cross at the mean from each group, marked with symbols for both panels A and B.

(C) The effect of LC stimulation on mean (± sem) CA1 sigma power within spindles. Normalized CA1 sigma power is shown in relation to light stimulation events within spindles (n=700). Events were then shuffled within spindles to preserve spindle specificity for ten shuffled data sets of 700 shuffled events each. A two-way ANOVA, Sidak post hoc was calculated for the real data (n=700 events) vs. each shuffled set individually (n=700 per set), and then against the average of all ten shuffles. The effect of light stimuli was nonrandom ($p<0.05$ from shuffled) for t= -0.04 to 0.18 for all individual ANOVAS and the combined two-way ANOVAs. Light stimulation significantly reduced sigma RMS; two-way ANOVA, Dunnett post hoc light onset t=0 vs t>0. #$p<0.05$ at t=0.088 seconds (dashed line) and onward.
(D) The percent change in occurrence of spindles greater or less than 0.6 seconds in length. Two-way ANOVA, Sidak post hoc ChR2- vs ChR2+ p=0.013. Data displayed as mean ± sem. *$p<0.05$, **$p<0.01$.

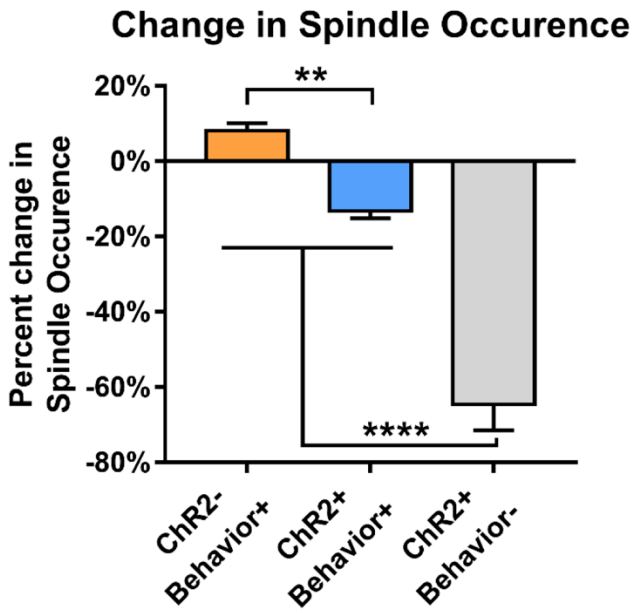


Figure 2.10 Training mitigates the detrimental effects of LC stimulation on spindle occurrence.
The effect of LC stimulation on spindle occurrence in rats performing the behavioral task (Behavior+) vs rats undergoing stimulation in the absence of behavior (Behavior-). Training on a spatial maze task reduces the effect of LC stimulation on spindle occurrence reduction. One-way ANOVA, Tukey post hoc: ChR2-Behavior+ versus ChR2+Behavior+ $p=0.008$; ChR2-Behavior+ versus ChR2+Behavior- $p<0.0001$; ChR2+Behavior+ versus ChR2+Behavior- $p<0.0001$. **$p<0.01$, ****$p<0.0001$. ChR2-Behavior+ n=5, ChR2+Behavior+ n=4, ChR2+Behavior- n=4. Data displayed as mean ± SEM.

Previous work has posited that the coupling of ripples to spindles is important for learning and memory consolidation[81,82]. Therefore, we examined whether LC stimulation had any effect on ripple-spindle coupling. During baseline sleep there was no difference between groups in ripple-spindle coupling, and coupling was significantly non-random in both groups when tested against shuffled data (Figure 2.11A). However, during day 1 sleep with LC stimulation, ChR2+ rats had significantly decreased ripple-spindle coupling compared to ChR2- rats, although coupling was still nonrandom for both groups (Figure 2.11B). To ensure that this difference in coupling was not due to

changes in CA1 ripple occurrence rate, we analyzed ripples and found that there was no change in ripple occurrence or the average length of ripples between groups or across days (Figure 2.12B-E), nor did ripples correlate with behavioral performance (Table 2.1). Moreover, ripple probability in relation to spindle onset was not different between groups on either day (Figure 2.12F). Therefore, this change in ripple-spindle coupling was likely due to the changes seen in spindles rather than ripples. Finally, the changes in coupling correlated with overall day 5 performance on both the altered and familiar tasks and were associated with both map errors and procedural errors on the familiar task and with procedural errors on the altered task (Table 2.1).

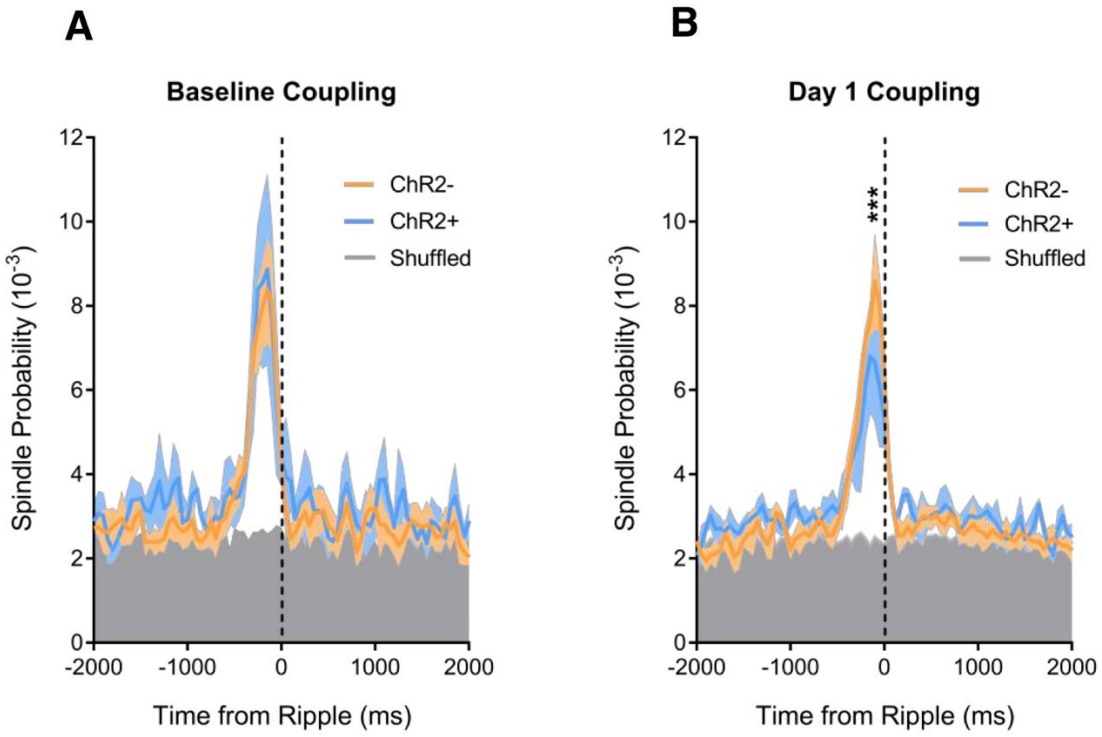


Figure 2.11 LC stimulation during sleep interferes with ripple-spindle coupling.
(A) Spindle onset mean (± sem) probability displayed with respect to ripple onset at t=0 during baseline sleep (no LC stimulation in either group). Ripple onset timestamps were shuffled within NREM sleep periods with no repeating timestamps within trials and were shuffled for a total of 15 trials to ensure coupling was non-random. Two-way ANOVA, Sidak post hoc; ChR2+ vs ChR2+ shuffled $p<0.0001$; ChR2- vs ChR2- shuffled $p<0.0001$. There was no difference between the shuffled values for ChR2+ and ChR2- groups ($p=0.997$), therefore only ChR2+ shuffled values (in gray region) are displayed for visual purposes. Any value within the gray region represents random probability for both ChR2+ and ChR2-.
(B) Spindle onset probability displayed with respect to ripple onset at t=0 during Day 1 sleep with 2 Hz LC stimulation. Two-way ANOVA, Sidak post hoc; ChR2+ vs ChR2+ -shuffled $p<0.0001$; ChR2- vs ChR2--shuffled $p<0.0001$. ChR2- vs ChR2+ significant difference from t=-50 to -250 msec $p<0.0001$. ChR2- n=4, ChR2+ n=5 ***$p<0.0001$. As there was no difference between either groups' shuffled data ($p=0.958$), within part B the gray region represents both ChR2+ and ChR2- shuffled data.
Displayed as mean (colored line) ± sem (same-colored shaded region).

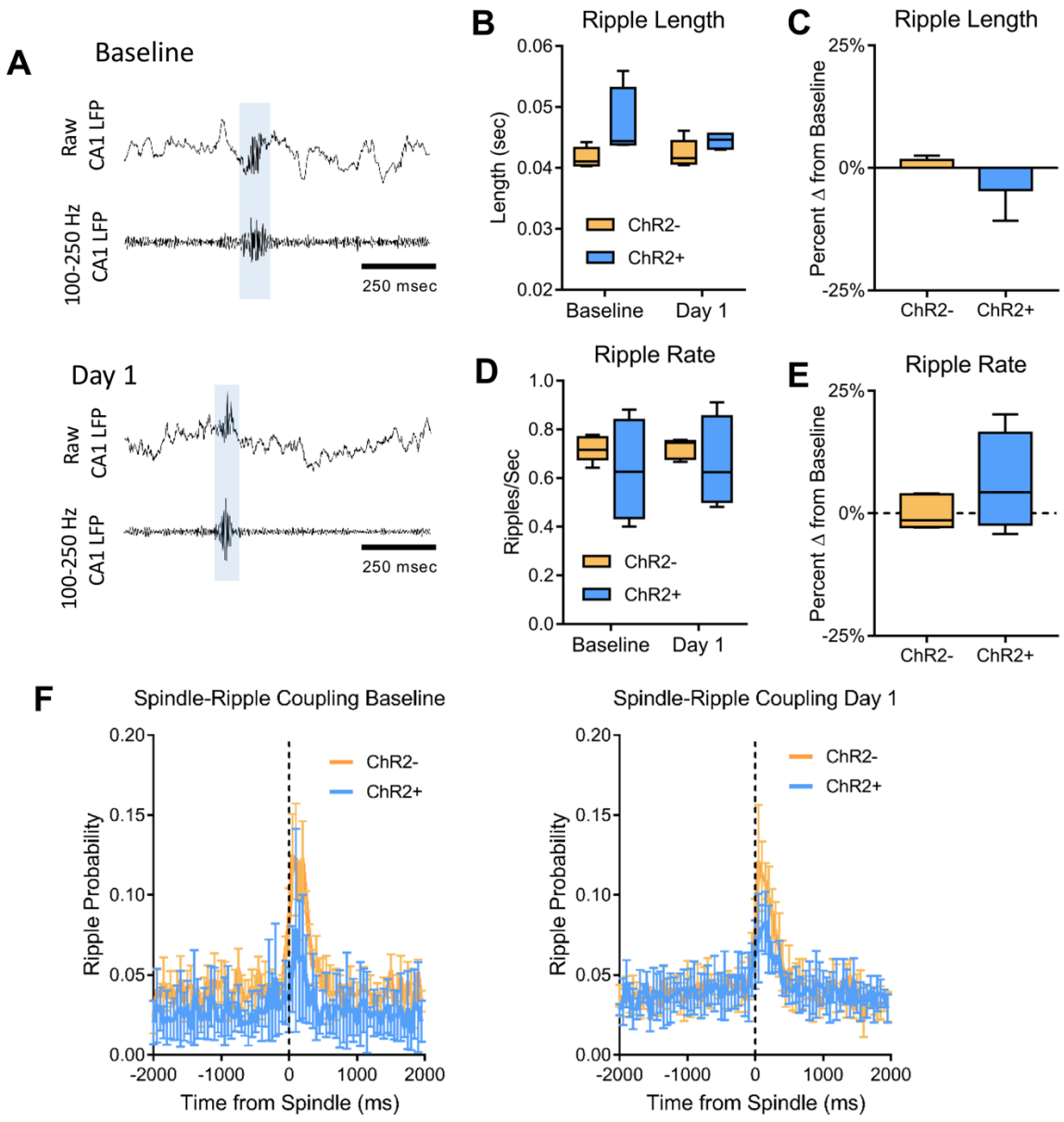


Figure 2.12 LC stimulation during sleep has no effect on ripple occurrence or length.
(A) Representative automatically identified ripple during baseline NREM sleep, and during day 1 NREM sleep with LC stimulation from ChR2+ rat.
(B) NREM sleep ripple occurrence rate during baseline and day 1 sleep.
(C) Percent change in NREM sleep ripple occurrence rate between baseline sleep and day 1 sleep with LC stimulation.
(D) NREM sleep ripple occurrence rate between baseline and day 1 sleep.
(E) Percent change in NREM sleep ripple rate between baseline sleep and day 1 sleep with LC stimulation.
Box and whisker plots: box displays first and third quartile with median, whiskers display maximum and minimum values. Five ChR2- rats, four ChR2+ rats for part B-E. Bar graph displays mean ± SEM.
(F) The probability of a ripple occurring in relation to the onset of a spindle during baseline sleep (left) and during day 1 sleep (right). Displayed as mean probability ± SEM.

| | | Spindle Occurrence Percent Change | | REM theta power Percent Change | | Spindle-Ripple Coupling Change | | Ripple Occurrence Percent Change | | NREM-SWS Delta Power Percent Change | |
|---|---|---|---|---|---|---|---|---|---|---|---|
| | n | rho | p value | rho | p value | rho | p value | rho | p value | rho | p value |
| Familiar Task | 9 | -0.8 | **0.014*** | -0.67 | 0.055 | -0.79 | **0.014*** | 0.24 | 0.53 | -0.30 | 0.43 |
| Familiar Task ChR2- Only | 5 | -0.15 | 0.83 | 0.2 | 0.91 | -0.67 | 0.26 | 0.10 | 0.90 | 0.10 | 0.90 |
| Familiar Task ChR2+ Only | 4 | -0.2 | 0.92 | 0.41 | 0.50 | 0.8 | 0.33 | 0.01 | 0.99 | 0.4 | 0.75 |
| Altered Task | 9 | -0.72 | **0.032*** | -0.72 | **0.034*** | -0.83 | **0.008*** | 0.23 | 0.54 | -0.35 | 0.35 |
| Altered Task ChR2- Only | 5 | -0.05 | 0.99 | -0.4 | 0.75 | -0.67 | 0.27 | 0.36 | 0.57 | 0.01 | 0.99 |
| Altered Task ChR2+ Only | 4 | 0.40 | 0.75 | 0.41 | 0.50 | 0.4 | 0.75 | -0.40 | 0.75 | 0.21 | 0.73 |
| Familiar Task P-Errors | 9 | -0.57 | 0.11 | -0.88 | **0.0032**** | -0.75 | **0.023*** | 0.18 | 0.65 | -0.73 | **0.032*** |
| Familiar Task P-Errors ChR2- Only | 5 | 0.72 | 0.17 | -0.56 | 0.43 | -0.10 | 0.90 | -0.36 | 0.63 | -0.82 | 0.133 |
| Familiar Task P-Errors ChR2+ Only | 4 | 0.80 | 0.33 | -0.40 | 0.75 | 0.20 | 0.92 | -0.20 | 0.92 | -0.6 | 0.42 |
| Familiar Task M- Errors | 9 | -0.84 | **0.0078*** | -0.41 | 0.27 | -0.8 | **0.013*** | 0.16 | 0.67 | 0.034 | 0.94 |
| Familiar Task M-Errors ChR2- Only | 5 | -0.36 | 0.63 | 0.67 | 0.27 | -0.56 | 0.37 | 0.46 | 0.43 | 0.74 | 0.33 |
| Familiar Task M-Errors ChR2+ Only | 4 | -0.74 | 0.33 | 0.63 | 0.50 | -0.32 | 0.67 | -0.11 | 0.99 | 0.41 | 0.50 |
| Altered Task P-Errors | 9 | -0.63 | 0.08 | -0.84 | **0.0057**** | -0.7 | **0.042*** | 0.14 | 0.71 | -0.75 | **0.025*** |
| Altered Task P-Errors ChR2- Only | 5 | 0.37 | 0.53 | -0.37 | 0.53 | 0.26 | 0.67 | -0.53 | 0.47 | -0.95 | 0.07 |
| Altered Task P-Errors ChR2+ Only | 4 | 0.80 | 0.33 | -0.40 | 0.75 | 0.20 | 0.92 | -0.20 | 0.92 | -0.6 | 0.42 |
| Altered Task M-Errors | 9 | -0.64 | 0.07 | -0.23 | -0.21 | -0.59 | 0.13 | 0.24 | 0.53 | 0.15 | 0.70 |
| Altered Task M-Errors ChR2- Only | 5 | -0.2 | 0.78 | 0.60 | 0.5 | 0.45 | 0.23 | 0.10 | 0.90 | 0.3 | 0.68 |
| Altered Task M-Errors ChR2+ Only | 4 | -0.95 | 0.17 | 0.21 | 0.83 | 0.11 | 0.99 | 0.01 | 0.99 | 0.74 | 0.33 |

**Table 2.1 Correlation Table of day 5 behavioral vs. changes from baseline sleep to day 1 sleep.**
Correlations of day 5 task performance with changes in spindle occurrence, REM theta, spindle-ripple coupling, and ripple occurrence, and NREM sleep delta power. All correlations were performed using Spearman's rho which is displayed above with its associated p-value. Significant correlations are in bold: *p<0.05, **p<0.005. M-Errors = Map Errors, P-Errors = Procedural Errors

## 2.9 Discussion

Our present findings demonstrate that LC activity normally decreases to near zero firing rate during spindle-rich NREM-intermediate sleep as well as REM sleep. We found that endogenous LC activity during a sleep spindle leads to spindle termination, and optogenetically enhanced LC activity during sleep reduces the rate of spindle occurrence, particularly longer spindles, as well as power in the theta band during REM sleep and in the delta band during NREM sleep, while leaving sleep as a behavioral state intact. Further, LC stimulation during sleep following learning decreases the fidelity of

hippocampal place encoding, while leaving hippocampal ripples and pyramidal cell activity rates unchanged. As a result, consolidation of spatial memory was also hampered, which led to rats utilizing non-hippocampal procedural strategies to solve the task. These alterations in learning strategies directly correlated with drops in sleep spindle occurrence and in REM sleep theta and NREM delta power, which were the result of LC stimulation during sleep. We believe the normal drop in LC activity prior to each sleep spindle and during REM sleep—while not required to maintain somnolence—is important for normal NREM sleep spindle generation and NREM delta and REM sleep theta power, and, by extension, hippocampal memory consolidation[40,74].

Previous work has shown that the pressure for sleep spindles increases after learning and their increased occurrence correlates with memory consolidation[64,73,156]. Upregulation of sleep spindles improves memory[74,76]. We found that LC stimulation without learning reduced the occurrence of sleep spindles more than 60%, while under the pressure of learning, LC stimulation significantly reduced spindles, but to a lesser magnitude, possibly due to a training-induced spindle drive. Long spindles (>0.5 s) increased by almost 50% under learning conditions, but LC stimulation during sleep prevented such increase, instead reducing long spindles by ~20%, making the effective long spindle reduction roughly 70% under learning conditions. We provide here the first evidence that preventing an increase in sleep spindles following learning prevents consolidation of a new memory and reconsolidation of a familiar memory, with error types revealing deficits in the disambiguation of information that distinguishes the two experiences. Further studies will be necessary to investigate the contribution of long spindles to the integration of new information into preexisting memory circuits.

Persistent LC activity reduced REM sleep theta power, which could have REM sleep-dependent memory consolidation implications[52,104]. REM sleep is a time of synaptic downscaling[157]. Norepinephrine blocks depotentiation[114,158] and sleep-dependent synaptic downscaling[159]. Normally place fields maintain stable place coding over week[152], despite backwards expansion occurring during task performance[150], necessitating synaptic downscaling between sessions. We show that when we sustain LC activity across sleep, place fields grow abnormally large across days, providing indirect evidence of unchecked LTP and a failure to depotentiate during REM sleep. These REM sleep

disruption results support Boyce et al., 2016[40] showing the importance of REM sleep theta for memory consolidation. We further provide indirect evidence of a possible depotentiation deficit underlying these consolidation errors.

In addition to decreasing sleep spindle occurrence and power, and REM sleep theta power, 2 Hz LC stimulation also led to a significant decrease in slow wave-delta power--which also correlated with the number of procedural errors on both tasks. Previous work in humans has highlighted the function of NREM slow waves in the consolidation of visual perceptual and implicit paired-associate learning[72,160]. Artificial enhancement or disruption of slow waves has been shown to enhance paired-associate [56,59]or impair motor skill memory consolidation, respectively. In rodents LC neuron activity is shown to synchronize to the rising phase of slow waves[134]. It is possible that our manipulation of LC activity during sleep interferes with the timing of LC activity in relation to slow waves, which may result in decreased delta power or disrupt the effect of memory processing thought to occur during sharp-wave ripples at slow wave peaks. More work is necessary to understand the relationship between NREM slow waves and LC activity in relation to memory consolidation.

While previous work has highlighted the importance of noradrenergic activity in memory formation during waking[119,120,123,128], little has been done to examine what function the presence or, especially, the absence of norepinephrine during sleep may have on learning and memory. Further work is needed to understand if the effects of aberrant LC activity during sleep on hippocampal spatial encoding and memory are due to noradrenergic receptor activation or to dopamine, which is released from the same terminals when norepinephrine is depleted[109,161]. The low stimulation rate used in our study make dopaminergic mechanisms less likely.

An interesting facet of our results is the persistence of rodent behavioral performance deficits despite cessation of LC optogenetic stimulation. Although stimulation ceases after day 2, the ChR2+ rats' performance continues to decline. The initial decrease in performance up to day 3 in both ChR2- and ChR2+ rats on the familiar task may be due to the interference of information from the altered task on familiar task performance. Then ChR2- rats' performance improves due to the use of efficient spatial strategies from healthy hippocampal function. However, the adaptation of ChR2+ rats to

disrupted hippocampal place cell encoding is to adopt a performance strategy that does not require hippocampal spatial mapping. After day 3, this inefficient procedural strategy produces a behavioral deficit relative to the improving ChR2- controls. We postulate that ChR2+ rats do not return to a hippocampal strategy as there is little motivation to attempt a strategy shift; i.e. despite frequent errors, they consume the same number of rewards. Long term hippocampal impairment is not a factor; once the formerly LC stimulated ChR2+ rats were introduced to another hippocampus-dependent task in a different context (the novel task), they were able to learn the task at similar rates to ChR2- rats. Future work is needed to understand why only 2 days of post-learning abnormal LC activity during sleep caused lasting, but context-specific hippocampal deficits.

We propose that LC silences permit sleep spindle generation by preventing noradrenergic depolarization of thalamocortical circuits as depolarization prevents the calcium spikes necessary for spindle generation[24]. Persistent LC activity, as in our study, would decrease spindle occurrence, thereby reducing spindle-ripple related neural activity. Higher frequencies of LC stimulation during sleep used in another study also suppressed ripple-spindle events[96]. LC silences prior to spindles could be key to ripple-spindle coupling and inter-regional communication during memory consolidation[63,81,82,162].

We have shown profound learning and memory reconsolidation behavioral deficits with a mild physiological increase in LC cell activity during the sleep consolidation period. We also show subsequent neural coding instability. Together these results likely explain the animals' inability to use a neural code to solve the spatial memory task. More work is required to study the replay patterns and plasticity effects of inappropriate LC activity during sleep consolidation.

In light of our current data, we conclude that LC silences play an important role in spindle generation and ripple-spindle coupling, as well as in normal NREM delta and REM sleep theta rhythm power—oscillations essential to normal offline processing of memory[40,63,162]. Our research suggests that LC activity, or lack thereof, during sleep may play a role in memory expression and be related to memory issues in conditions of abnormal LC activity during sleep such as post-traumatic stress disorder and Alzheimer's disease[163,164].

# CHAPTER III

# Sex Differences within Sleep in Gonadally Intact rats

## 3.1 Introduction and methods

### Introduction

Hormonal release across the estrous cycle in mammals and the menstrual cycle in women causes systemic changes in physiology and behavior associated with reproduction, metabolism, and cognitive functions[165–169]. One facet that is often overlooked is the relationship between the estrous and menstrual cycles on sleep-wake activity (for review see[165,170,171]). Early work in rats demonstrated that the amount of waking, non-rapid eye movement (NREM) sleep, and rapid eye movement (REM) sleep is altered by the estrous cycle[172,173]; these changes occur specifically in the phases of proestrus and estrus when high hormonal release is present. Additional work in ovariectomized female rodents demonstrated the necessity of the gonadal hormones estradiol and progesterone[174] to produce these changes in sleep-waking behavior. Reintroducing these hormones in ovariectomized rodents demonstrated their sufficiency in producing effects on sleep-waking behavior[173,175].Finally, while there are sex differences in sleep amount between gonadally-intact animals, the removal of the gonads abolishes these differences—supporting the role of sex hormones in sleep[176,177].

In humans, the use of electroencephalographic (EEG) polysomnographic recordings showed the first objective changes in sleep-waking behavior in women across the menstrual cycle[178]. Further work showed that changes in ovarian hormones alter sleep both across the cycle and throughout life[178–181]. Increased prevalence of insomnia in women compared to men appears at puberty onset. Furthermore, sex differences in sleep onset dissipate following menopause [182,183], suggesting that sex differences in sleep are in part due to changes in reproductive hormones[171].

Human studies have shown that both spindle frequency and density change across the menstrual cycle[178,184]. However, it is unknown if the estrous cycle has similar effects in rodents. Sleep in mice appears to be highly strain specific[185] and while studies in mice have shown sex differences in sleep[176] other work demonstrates the opposite: the estrous cycle does not affect mouse sleep-wake behavior[185]. Finally, studies examining the effects of estrous hormones on sleep and sleep rhythms are often conducted in gonadectomized animals[176,186,187] which can complicate comparisons between animal and clinical research. Overall there remains a gap in basic research in gonadally-intact cycling females that must be filled to better understand how the estrous cycle affects sleep. Moreover, such estrous cycle changes should also be compared to similarly treated gonadally intact males to better understand sex differences in sleep relevant to many fields of basic research.

In the present study, we recorded sleep in gonadally intact male and female rats across the estrous cycle. We replicated previous work showing that high hormonal phases, proestrus and estrus, produce changes in sleep amount and sleep architecture. Proestrus and estrus produce marked increases in NREM sleep delta power while proestrus also shows an increase in NREM slow gamma power. Furthermore, there are increases in NREM sleep spindles, NREM interregional coherence, and NREM slow wave activity and NREM slow gamma homeostasis. Finally, we identified sex differences in sleep amount, sleep architecture, slow gamma homeostasis, and sleep spindle characteristics in some phases of the estrous cycle compared with males. This work supports and extends our knowledge on the manner in which the estrous cycle alters many facets of sleep and is responsible for producing differences in sleep quantity and quality between males and females.

## Methods

Seven male and ten female Long-Evans rats (Charles River), age 3-4 months and weighing approximately 300-400 g (male) and 225-300g (female), were used in this study. Food, water, and environmental enrichment were available *ad libitum,* and animals were housed on shaved paper bedding in climate controlled (23 ± 3°C and 35 ± 10% humidity) chambers with a 12:12 hour light/dark cycle. All animal procedures were carried out in

accordance with the National Institutes of Health Guide for the Care and Use of Laboratory Animals and in accordance with the University of California Los Angeles Chancellor's Animal Use Research Committee.

Electrode Implantation and Experimental Procedures

All animals were individually housed and administered 650 mg/kg acetaminophen in water two days prior to and three days following surgery and 5 mg/kg enrofloxacin one day prior to and for five days following surgery. Rats were anesthetized with isoflurane vapor (4% induction, 1-2% maintenance), and placed in a stereotaxic frame. All stereotaxic measurements were from bregma. Stainless steel screw electrodes (Plastics1) and a tungsten depth electrode (Plastics1) were implanted to measure cortical electroencephalographic (EEG) activity, and hippocampal local field potentials (LFP), respectively. Within each animal, all electrodes were placed within either the left or the right hemisphere of the brain with the side picked for implantation selected pseudo-randomly (Fig 1A). EEG screw electrodes were implanted over the medial prefrontal cortex (+2.7 mm AP, ± 0.6 mm ML) and over the secondary visual cortex (-5.0 mm AP, ± 1.5 mm ML). An additional screw electrode was placed over the frontal sinus (+11 mm AP) as a reference. The tungsten electrode targeting the CA1 field of the hippocampus was implanted at-3.5 mm AP, ± 2.1 mm ML, -2.6 mm DV. A nuchal electromyographic (EMG) electrode was implanted into the dorsal neck muscles to measure muscle activity. Inputs from all electrodes were wired into a pedestal connector (Plastics1) which was secured to the skull with stainless steel anchor screws and dental acrylic. Animals were given ten days for post-operative recovery in their home cages.

After recovery, animals were connected to a chronic recording tether that was attached on the opposite end to a commutator that allowed the animals to move freely in their home cage without entanglement. (Fig 1B). Animals were given 48 hours to adapt to the tether prior to any recording of sleep-waking behavior. Recordings took place over five consecutive days to ensure they encompassed an entire estrous cycle (Fig 1C).

Estrous Phase Determination

The estrous cycle has four phases: metestrus, diestrus, proestrus, and estrus, with each phase associated with changes in vaginal histology (for review of phase identification see[188]) (Figure 3.1A). To determine estrous phase, female rats were vaginally swabbed once a day with a cotton-tipped applicator moistened with saline. Swabbing was performed within the first 30 minutes of the light phase each day (Fig 1C). Vaginal smears were applied to microscope slides and left to dry at room temperature at least a day prior to staining. The staining protocol was as follows: slides were fixed in methanol for 3 minutes and air dried for 15 minutes. Slides were then immersed in 1:20 dilution of the Giemsa stain (Sigma-Aldrich) in deionized water for 5 minutes, followed by rinsing in deionized water. Finally, slides were cover-slipped and examined under light microscope for estrous stage identification. To equalize handling time amounts and time of day for male-female comparisons, males were sham-swabbed by taking a similarly moistened cotton swab and applying light pressure between the anus and the scrotum. All rats were swabbed every day for two weeks prior to any recording in order to habituate them to the process. One female rat was removed from the study due to irregularities in the estrous cycle, i.e., three contiguous days of identifiable estrus shown by >80% of cells displaying a flattened, cornified appearance.

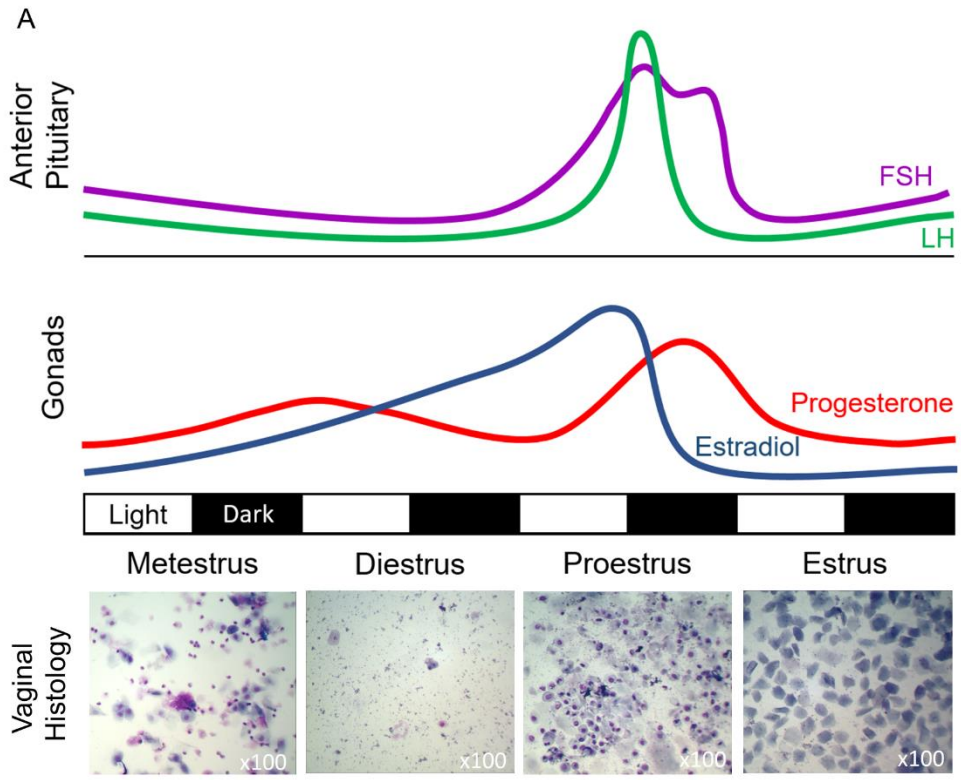


Figure 3.1 Schematic representation of the relative level of reproductive hormones released from the anterior pituitary and gonads across the estrous cycle on a 12:12 lights on-off cycle**.** (A) Proestrus is marked by large fluctuations in hormones: the steady rise in follicle stimulating hormone (FSH) and estradiol triggers a luteinizing hormone (LH) surge leading to ovulation, and a subsequent decrease in estradiol and rise in progesterone. Hormonal changes in each estrous phase are associated with changes in vaginal epithelium histology across the cycle (representative histology from each phase below

## Electrophysiological Data

Electrode data were continuously recorded at a sampling rate of 1 kHz using the Neuralynx Digital Lynx system (Neuralynx, Bozeman, MT). Recordings were halted for ~1 minute each day in order to perform the swabbing.

## Sleep State Analysis

Sleep/waking states were scored manually using cortical EEG, CA1 LFP, and EMG recordings in the same manner as previously published studies from our lab[36,65]. For state identification, EMG data were filtered from 30-250 Hz, and EEG and LFP data were filtered from 1-25 Hz and viewed in ten-second epochs. Epochs were assigned a state of waking, NREM sleep, or REM sleep using a manual scoring program developed in our

lab[189]. Previous work has shown that the cortex and the hippocampus can simultaneously exhibit two different sleep states[36]. In epochs where the interregional sleep states were in conflict, the state of the cortex was selected as the overall sleep state. For females, each day of sleep was scored with the scorer blinded to the identity of the estrous phase. Males were scored unblinded to the order of days, and each day was identified as day 1, day 2, etc. For each day of each animal, the scored sleep was divided into four, six-hour time periods ZT0-6 and ZT6-12 (the lights-on sleep-intensive circadian phases), and ZT12-18 and ZT18-24 (the lights-off waking dominant circadian phase).

Power Spectral Analysis

Power spectra were analyzed using Neuroexplorer 5 software (Nex Technologies, Madison, AL). Raw EEG and LFP data underwent a fast-Fourier transform (FFT) using a 500 msec window with a Hann taper, and a window overlap of 50% to calculate the average power spectra from 0.5 to 100 Hz. A 60Hz notch filter was applied to remove environmental signal noise when calculating power spectral densities.

Spectral Coherence Between Brain Regions

The coherence of raw EEG and LFP at a given frequency (*f*) was analyzed using Neuroexplorer 5 software (Nex Technologies, Madison, AL) utilizing previously published methodology[190]. Field-field coherence corresponds to the similarity of two signals, "*x*" and "y", at each frequency. Coherence value between signals x and y for any given frequency, $C_{xy}(f)$, was calculated as a function of the spectral densities of *x*, $P_{xx}(f)$, and *y*, $P_{yy}(f)$, and of the cross spectral density of x and y, $P_{xy}(f)$ similar to previous work:

$$C_{xy}(f) = \frac{|P_{xy}(f)|^2}{P_{xx}(f)P_{yy}(f)}$$

Coherence was calculated using a 0.5 s Welch's window with a 50% overlap. $C_{xy}(f)$ for a given frequency window is expressed from 0 to 1.0, with 0 indicating no relationship between the two signals at a given frequency, and 1.0 indicating a perfect linear relationship. Band coherence was calculated by averaging the coherence values at each frequency within a frequency band of interest.

Sleep Spindle Identification

Automatic spindle identification was performed similar to previous work[64]. Cortical EEG from the mPFC and V2 were filtered for the sigma frequency (10-15 Hz) and data were down-sampled to 200 Hz. Then the root-means-square (RMS) over a moving 100 msec window was calculated and smoothed with a moving average. Spindles were counted where the RMS exceeded 2.5 times the standard deviation of the RMS mean from all NREM sleep for that time period lasting at least 0.5 s but not exceeding 2.0 s in length. When examining spindle length and peak frequency, spindles were treated as independent measures, rather than finding the average spindle length or peak frequency within an individual subject.

Statistical Analysis

All statistical tests were conducted using Prism 8 analytical software (GraphPad). All data sets were first tested for normality using the Shapiro-Wilk normality test, as recommended[144]. Data set normality was calculated without performing any transform (e.g. log10, or z-score) on the data. Statistical tests used repeated measures two-way ANOVAs or linear mixed effect models, followed by a Tukey's multiple comparisons test to compared repeated measures within males and females. To compare differences between males and females, first, the average value across four days for each measure was calculated within males; this was to maintain the variability between subjects. Then, the male averages were compared to each phase of the estrous cycle using a two-way ANOVA or linear mixed model followed by a Dunnett's multiple comparisons test. The alpha value was set to 0.05 for all analyses and was always calculated in a two-tail manner. Graphical representations of data were created using Graphpad Prism 8 and MATLAB 2018a. Statistical tests used for each comparison within a figure can be found in the figure legend, or within the results section if a figure for a specific analysis is not shown. Significance of females from males is denoted using a pound sign (#), with the color of the pound sign displaying the difference from a specific estrous phase (see Fig 5 for example). Significant differences between different estrous phases are denoted with an asterisk (*). In figures where it was difficult to use bracket lines to denote comparisons

between groups, colored asterisks were used to denote comparisons and significance between groups phases of the estrous cycle.

### 3.2 Proestrus and estrus differ in sleep and waking quantity

Previous work in rodents established that males and females have differing amounts of waking, NREM, and REM sleep. We first sought to replicate these results. Figure 3.2D displays ten-second epochs of representative traces of the three identified behavioral states: waking, NREM sleep, and REM sleep. Males showed no difference in the percent of time spent in waking, NREM sleep, or REM sleep across the four days of recording when compared at circadian matched times (repeated measures two-way ANOVA, Tukey post hoc: Wake $p=0.48$ to $>0.99$, NREM $p=0.58$ to $>0.99$, REM $p=0.46$ to $>0.99$). Female rats showed changes in sleep-wake amounts across the estrous cycle (Fig 3.2 E, F). Females displayed increases in time spent waking and decreases in NREM and REM sleep throughout the day during proestrus as compared other phases of the estrous cycle (Fig 3.2 G-I). These proestrus-affiliated changes peaked at the onset of the dark phase of proestrus. Additionally, during the subsequent estrus phase, there was a rebound increase in the time spent in NREM and REM sleep and a decrease in waking during the light phase (ZT0-6 and ZT6-12) compared to the light phase of proestrus the previous day (Fig 3.2G-I).

Compared to males (Fig 3.2 G-I), females showed increased waking and decreased NREM sleep from ZT0-18 of proestrus and decreased REM sleep during ZT6-18 of proestrus (Fig 3.2 G-I). Additionally, females had decreased waking and increased NREM sleep during ZT18-24 of metestrus, and increased REM sleep during ZT18-24 of estrus.

Looking within sleep, REM sleep expressed as a percent of total sleep did not vary in males across four days of recording (Fig 3.2J). However, in females, REM sleep was selectively suppressed during proestrus ZT12-18 compared to all other phases, and from proestrus ZT18-24 compared to estrus (Fig 3.2K)

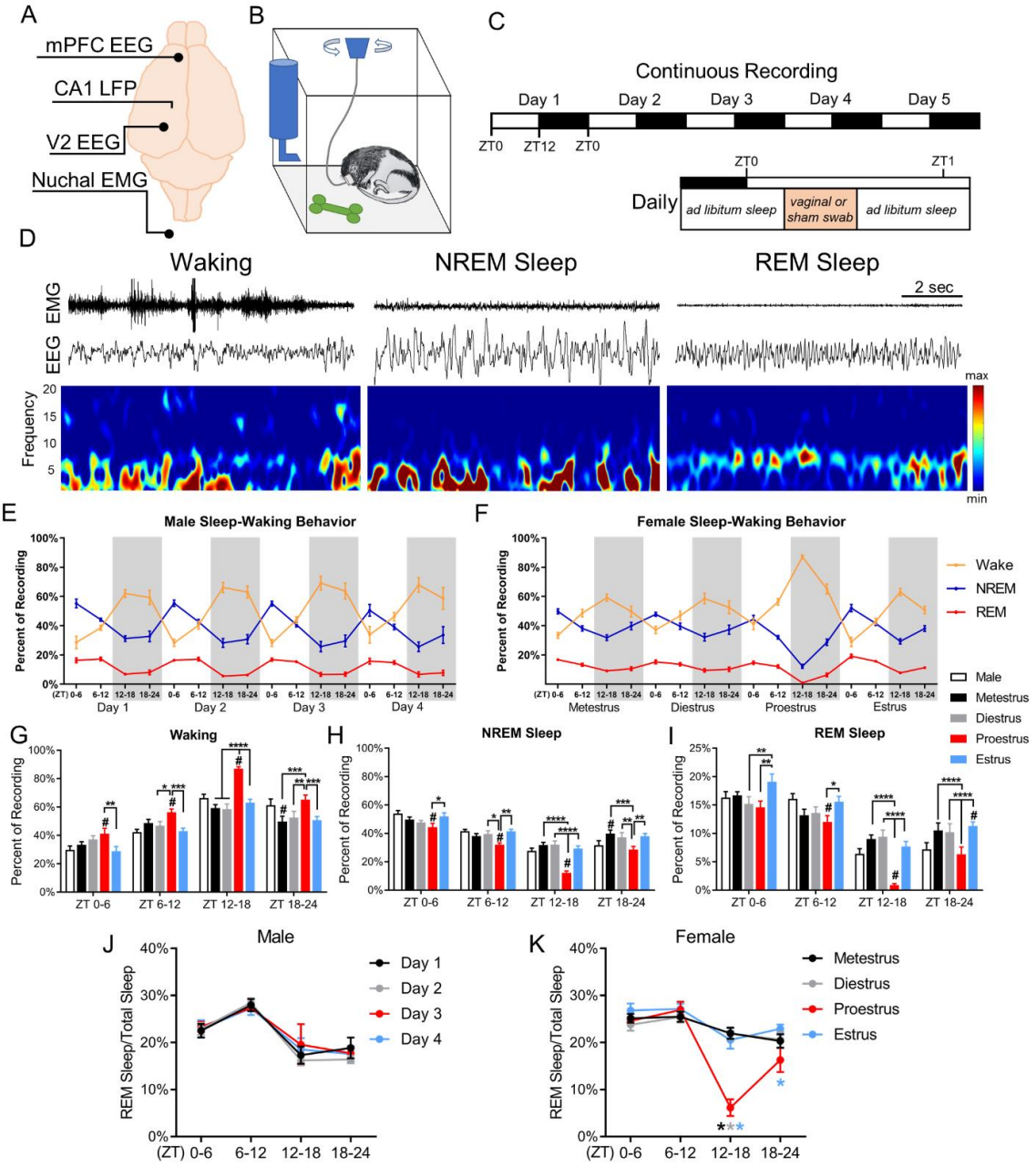


Figure 3.2 Sleep-waking behavior changes across the estrous cycle. (A) Configuration of recording electrodes. (B) Schematic of home cage recording set up allowing movement and sleep postures. (C) Experimental timeline of five days of continuous recording with 12:12 light-dark cycle (top), and the time within the day where swabbing occurred. (D) Representative ten second epochs showing EEG and EMG for waking, NREM sleep, and REM sleep. (E) Male sleep-waking behavior across four days of recording. Each day is broken into quartiles ZT0-6, ZT6-12, ZT12-18, and ZT18-24. The grey shaded areas represent the dark phase. (F) Female sleep-waking behavior across one complete estrous cycle. (G) The percent time spent in waking, NREM sleep (H), and REM sleep (I). (J) REM sleep as a percent of total sleep across four days of recording in males and (K) across the estrous cycle in females. Females were analyzed across phases of the estrous cycle using repeated measures two-way ANOVA, Tukey post hoc. *p<0.05, **p<0.01, ***p<0.005, ****p<0.0005. Females compared to males using two-way ANOVA, Dunnett post hoc. $^{\#}$<0.05. Data displayed as mean±SEM; males n=7, females n=9.

### 3.3 Proestrus and estrus possess a unique sleep architecture

We next examined whether sleep architecture was affected by the estrous cycle. Similar to the time spent in each state, males showed no variation in the number of bouts per hour of waking, NREM or REM sleep across the four days of recording (repeated measures two-way ANOVA, Tukey post hoc: waking p=0.16 to >0.99, NREM p=0.07 to >0.99, REM p=0.32 to >0.99; Fig 3.3A), whereas females showed variation across the estrous cycle (Fig 3.3B-E). During ZT0-6 of estrus there was a significant decrease from proestrus in the number of waking bouts per hour. Further, during ZT6-12 estrus, there were fewer bouts of waking and NREM compared to all other estrous phases (Fig 3.3C, D). The frequency of REM bouts per hour during the dark phase (ZT12-14) of proestrus was significantly reduced from all other phases of the estrous cycle (Fig 3.3E).

Compared to males, females in proestrus had an increase in the number of waking bouts per hour during ZT6-12 and increased the number of NREM bouts per hour during ZT18-24 of metestrus. Also, females had significantly more bouts of REM sleep than males during ZT12-18 of diestrus and during ZT18-24 of metestrus, diestrus, and estrus. In other words, females had more REM sleep in the latter half of the dark phase than males except during proestrus. During ZT12-18 of proestrus, females had less REM sleep than males.

We next examined the length of the bouts of each state. Males again did not show any circadian-matched day-to-day changes in the length of bouts of any state across the four recording days (repeated measures two-way ANOVA, Tukey post hoc: Wake p=0.14 to 0.99, NREM p=0.11 to >0.99, REM p=0.25 to 0.99), whereas females displayed differences across the estrous cycle. During proestrus ZT12-18 females showed increased waking bout lengths and decreased NREM and REM sleep bout lengths compared to all other estrous phases (Fig 3.3H-J). These changes in bout length closely matched changes in the amount of each state shown in Figure 3.2. Proestrus NREM sleep bouts were also shorter than diestrus and estrus at ZT18-24. Additionally, during ZT0-6 and ZT6-12 of estrus, both NREM and REM sleep bouts were longer than any other phase of the estrous cycle, underlying estrus rebound in the amount of NREM and REM seen in Figure 3.2.

Compared to males, females had longer bouts of waking during ZT12-18 of proestrus. Males also had waking bouts during ZT18-24 of metestrus. Additionally, females had shorter bouts of NREM sleep compared to males during ZT0-6, ZT6-12, and ZT12-18 of proestrus. Finally, females had shorter bouts of REM sleep than males during ZT0-6 and ZT6-12 of metestrus, diestrus, and proestrus. The most significant difference in REM sleep between males and females was the drop in REM sleep in females during ZT12-18 of proestrus.

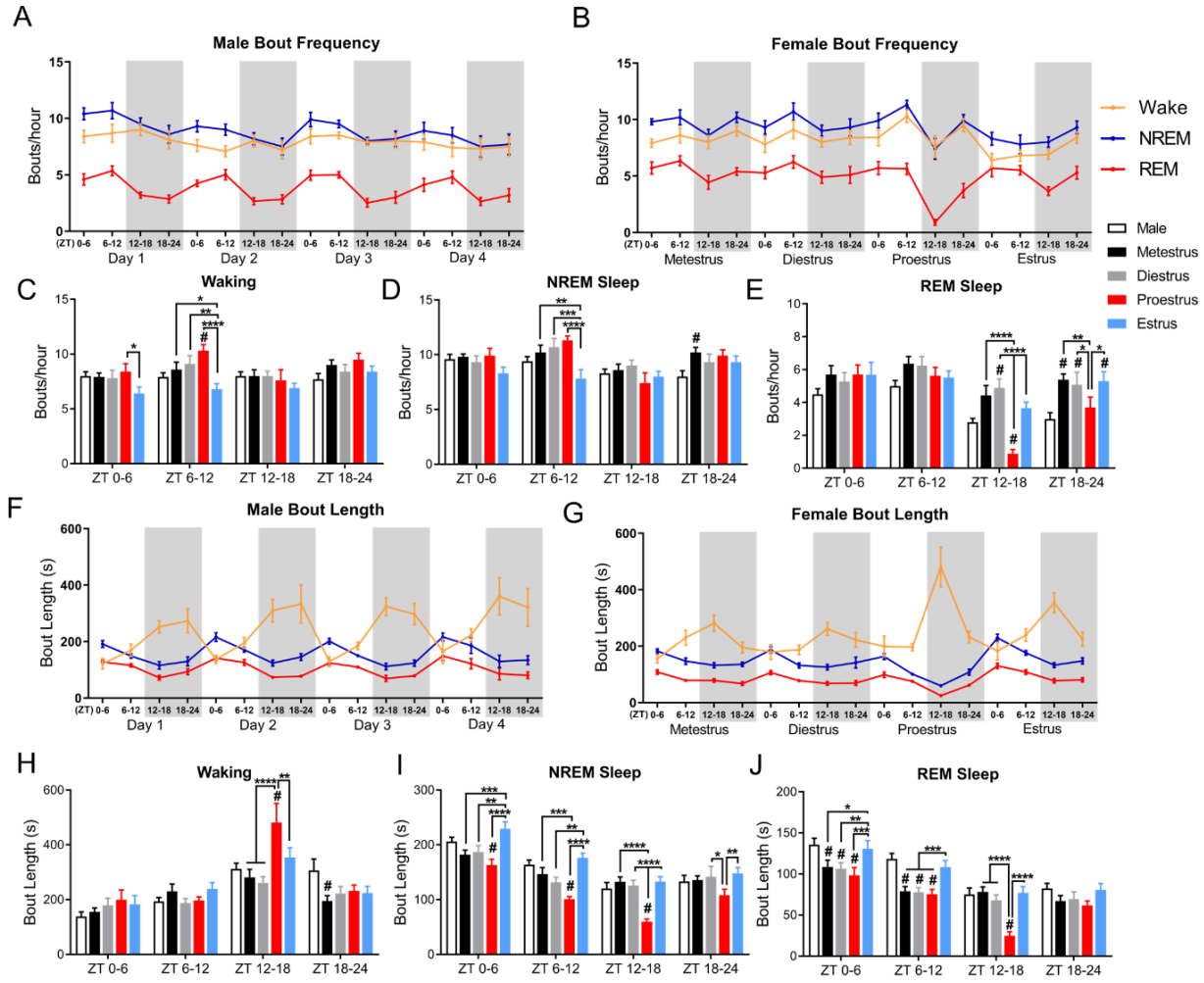


Figure 3.3 Sleep architecture changes across the estrous cycle. (A) Male and female (B) bouts per hour of waking, NREM sleep, and REM sleep across four days of recording and the complete estrous cycle. (C) Comparison of bouts per hour of waking, NREM sleep (D), and REM sleep (E). Male (F) and female (G) average bout length for waking, NREM sleep, and REM sleep across four days or the estrous cycle respectively. (H) Comparison of bout length of waking, NREM sleep (I), and REM sleep (J). For both bouts per hour and bout length, females were analyzed across phases of the estrous cycle using repeated measures two-way ANOVA, Tukey post hoc. *p<0.05, **p<0.01, ***p<0.005, ****p<0.0005. Females compared to males using two-way ANOVA, Dunnett post hoc. #p<0.05. Data displayed as mean±SEM; males n=7, females n=9.

### 3.4 NREM and REM sleep power spectra changes across the estrous cycle

Previous work in women and in female rodents showed changes in the NREM and REM sleep power spectra across the menstrual cycle and estrous cycle, respectively[178,191]. We investigated whether similar changes occurred in multiple brain regions within male rats over time, and female rats across the estrous cycle.

Within the medial prefrontal cortex (mPFC), the secondary visual cortex (V2), and the hippocampus-CA1in males, there were no changes in the circadian-matched power spectrum during NREM sleep over the four days of recording (Figure 3.4A-C). However, in females during ZT12-18 and ZT18-24 of proestrus and the following ZT0-6 of estrus, there were significant increases in delta (0.5-4Hz) power in mPFC, CA1, and V2. Additionally, we saw an increase in frequencies in the beta band (16-30 Hz) and the slow gamma band in the mPFC, CA1, and V2 during ZT12-18 of proestrus, as well as the beta band in the mPFC during ZT18-24 of proestrus (Figure 3.5A-C). Unlike the increases in the delta band, these beta and gamma increases in the late (dark) phase of proestrus did not carry over into the first 6-hour light phase of estrus in any recorded brain area.

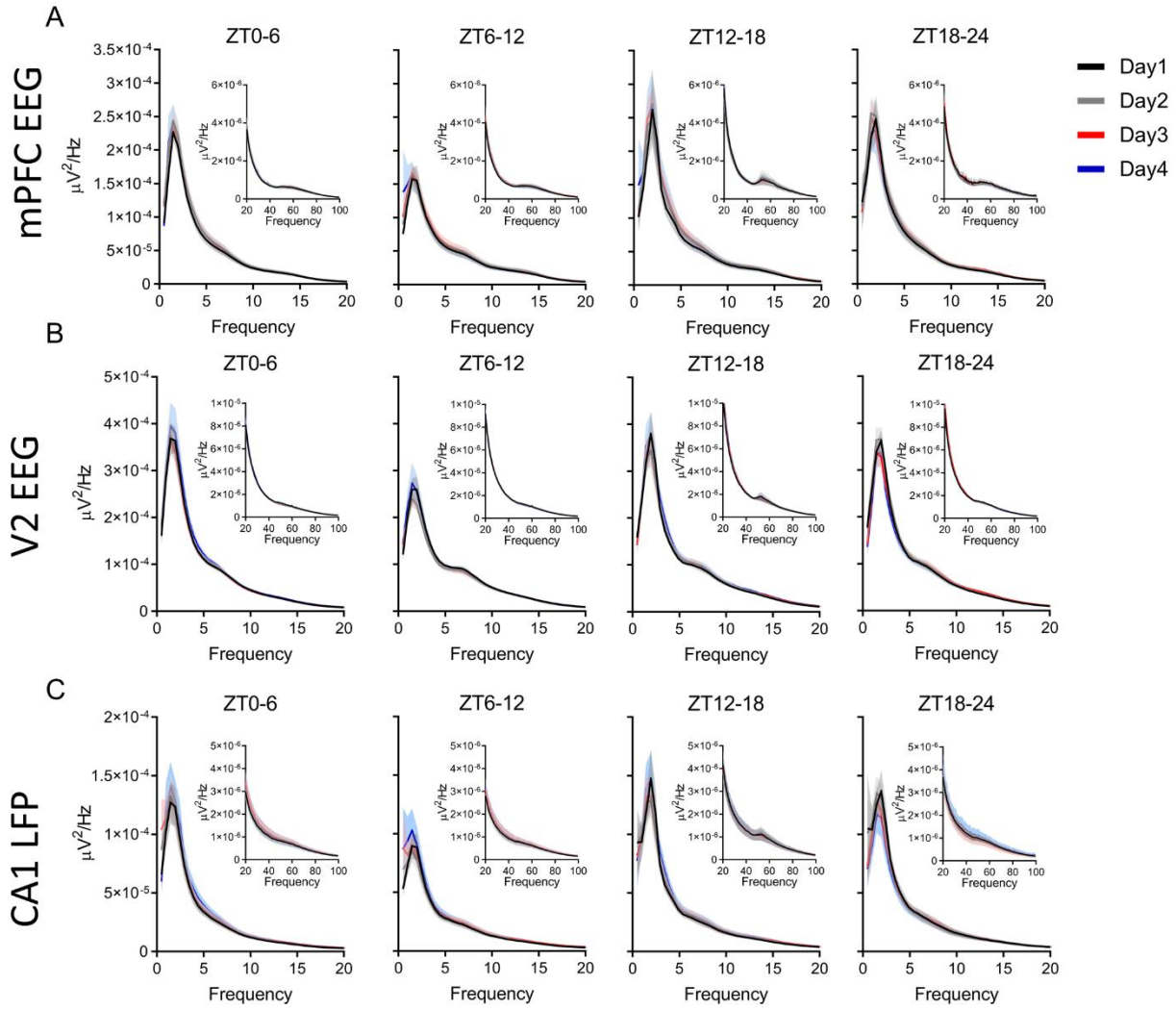


Figure 3.4. Male NREM sleep power spectrum does not change across four days of recording. (A) Distribution of male rat power spectra during NREM sleep in the medial prefrontal cortex (mPFC) EEG, secondary visual cortex (V2) EEG (B), and CA1 LFP (C). Each 0-20 Hz panel contains a sub panel displaying 20-100 Hz to highlight changes that occur at higher frequencies, but lower voltage. The power at each frequency was analyzed using a repeated measures two-way ANOVA, Tukey post hoc. Data displayed as the darker line represents the mean and the lighter shaded region of analogous color represents the SEM for that group. Males n=7 for all figures.

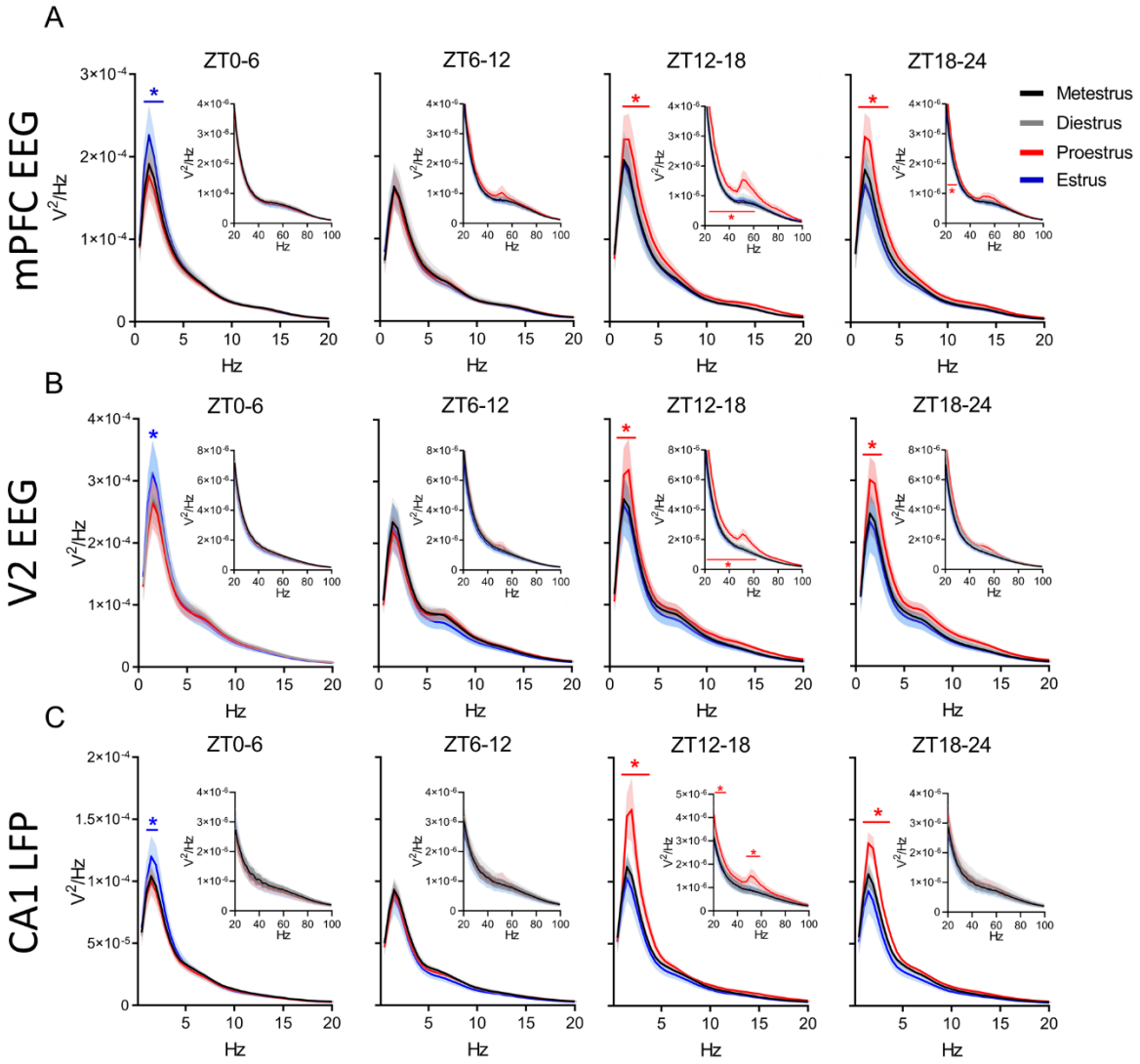


Figure 3.5 NREM sleep delta power and slow gamma power changes during proestrus and estrus. (A) Distribution of female rat power spectra during NREM sleep in the medial prefrontal cortex (mPFC) EEG, secondary visual cortex (V2) EEG (B), and CA1 LFP (C). Each 0-20 Hz panel contains a sub panel displaying 20-100 Hz to highlight changes that occur at a higher frequency, but at a lower voltage. The power at each frequency was analyzed across phases of the estrous cycle using repeated measures two-way ANOVA, Tukey post hoc. *p<0.05 The colored line with similar colored asterisk above it represents frequencies where one phase of the estrous cycle is significantly different from all other phases of the estrous cycle. Data displayed as the darker line represents the mean and the lighter shaded region of analogous color represents the SEM for that group. For both mPFC EEG and V2 EEG n=9 females. For CA1 LFP n=8, as one animal had a broken depth electrode.

Looking at REM sleep in males, there were no differences in mPFC, V2, or CA1 REM sleep theta across four days of recording (Figure 3.6A-C). Female power spectra changed during REM sleep across the estrous cycle, but, unlike NREM sleep, these changes did not occur simultaneously in all regions. We found no changes in REM

sleep theta power throughout the estrous cycle in CA1 (Figure 3.7C). However, in the mPFC, REM sleep peak theta power was significantly lower during ZT0-6 of proestrus in the mPFC (Figure 3.7A) at a time when REM bout length was also reduced (Figure 3.3J). In contrast, REM sleep theta power was higher in the V2 are of the cortex during ZT18-24 of proestrus (Figure 3.7B) when total REM sleep time (Figure 3.2I) and the number of REM sleep bouts per hour (Figure 3.3E) was lower than at other estrous phases. REM sleep theta power fell from that later proestrus high, to another low in V2 during ZT6-12 of estrus (Figure 3.7A, B) when REM bout length increased.

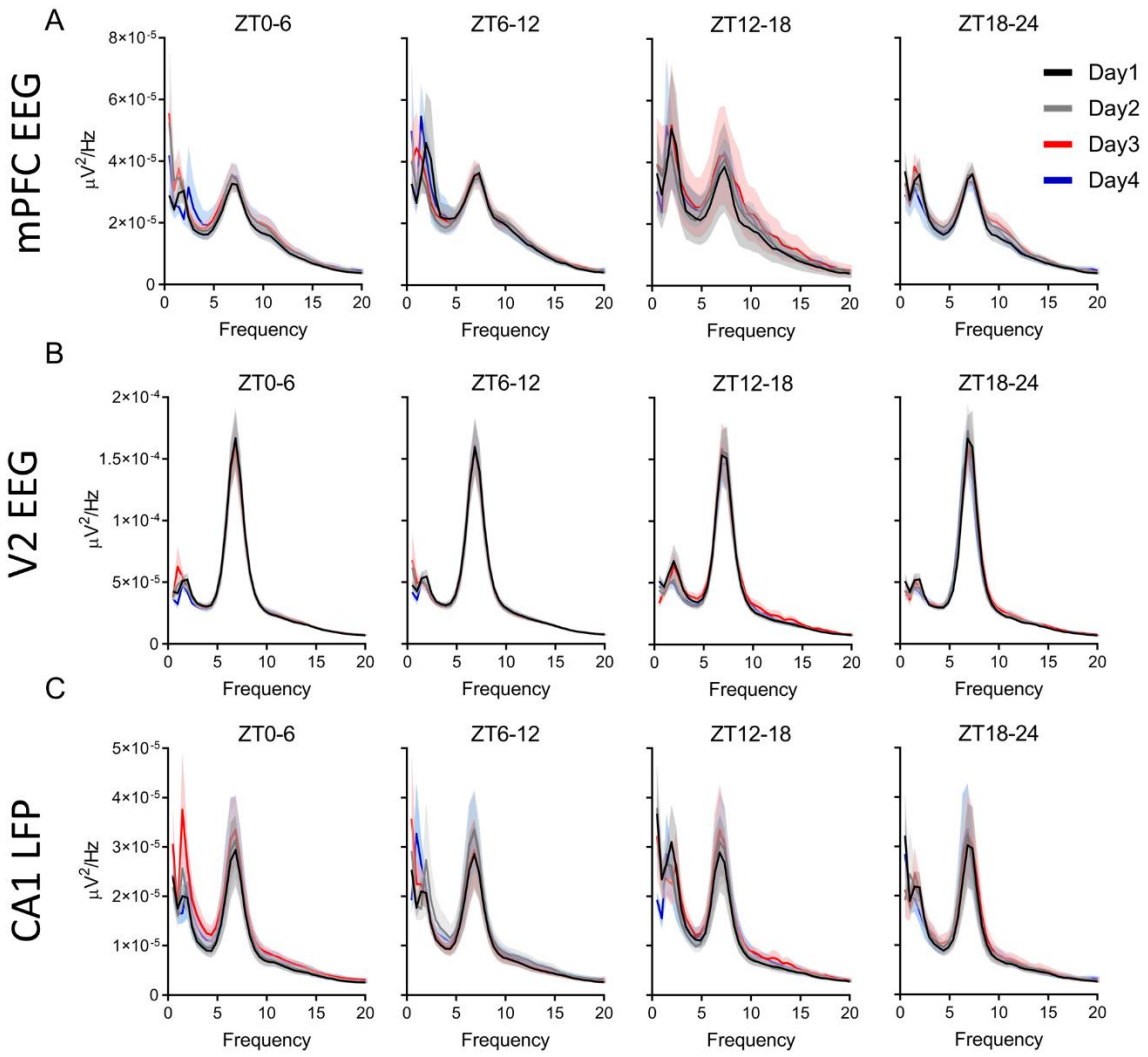


Figure 3.6 Male REM sleep power spectrum does not change across four days of recording**.** (A) Distribution of male rat power spectra during REM sleep in the medial prefrontal cortex (mPFC) EEG, secondary visual cortex (V2) EEG (B), and CA1 LFP (C). Each panel has a range of 0-20 Hz; there were no changes at frequencies >20Hz so that data is not displayed. The power at each frequency was analyzed across each day using repeated measures two-way ANOVA, Tukey post hoc. Data displayed as the darker line is the mean and the lighter shaded region of analogous color represents the SEM for that group. Males n=7 for all figures.

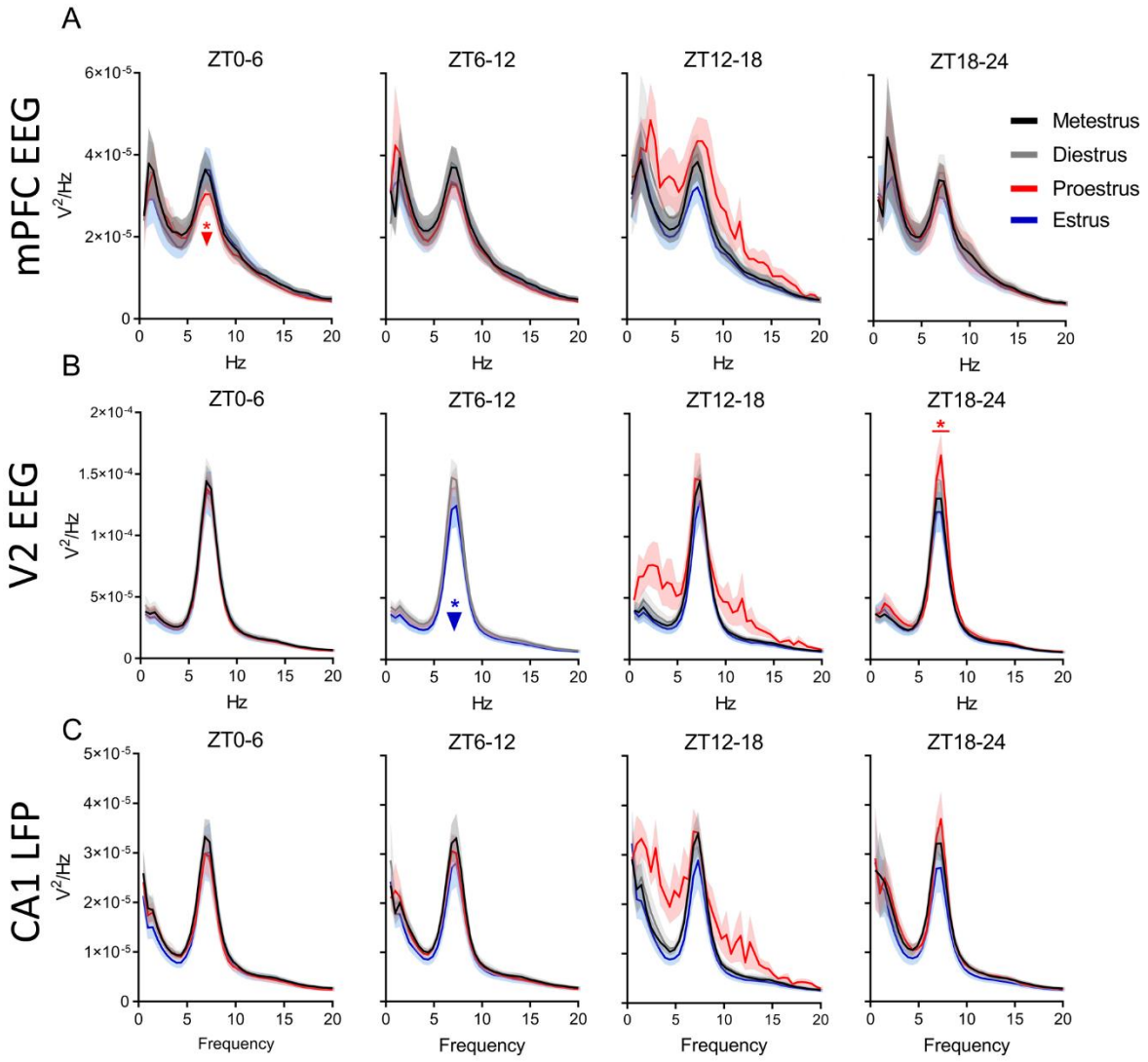


Figure 3.7 REM sleep theta power varies across the estrous cycle. (A) Distribution of female rat power spectra during REM sleep in the medial prefrontal cortex (mPFC) EEG, secondary visual cortex (V2) EEG (B), and CA1 LFP (C). Each panel depicts 0-20 Hz; no changes occurred at frequencies greater than 20 Hz, so higher frequencies are not displayed. The power at each frequency was analyzed across phases of the estrous cycle using repeated measures two-way ANOVA, Tukey post hoc. *p<0.05, the colored line with similar colored asterisk above it represents frequencies where one phase of the estrous cycle is significantly different from all other phases of the estrous cycle. The colored downward arrow with similar colored asterisk represents frequencies where one phase of the cycle is significantly lower power than all other phases. Data displayed as the darker line represents the mean and the lighter shaded region of analogous color represents the SEM for that group. For both mPFC EEG and V2 EEG n=9 females. For CA1 LFP n=8, as one animal had a broken depth electrode.

.

## 3.5 NREM slow wave activity and slow gamma activity are increased during proestrus

Prior studies have indicated that slow wave activity (SWA), or delta power, homeostatically changes throughout the light phase in rodents and that the estrous

cycle can affect SWA homeostasis[191]. We wanted to see if males and female rats had similar SWA changes across the day. Across the four days of recording, males had similar SWA homeostasis in the mPFC, V2 and in CA1 (Fig 3.8A-C). In females, there was a SWA increase in mPFC and CA1, and to a lesser extend in V2 during the dark phase of proestrus compared to all other phases (Fig 3.9A-C). Later in the first two hours of the estrus light phase, mPFC and V2, SWA increased (Fig 3.9A, B). Finally, in the last two hours of the dark phase of estrus, both V2 and CA1 SWA was reduced in females compared to males (Fig 3.9B, C).

Previous work also found that NREM 10-25 Hz activity was homeostatically increased during the dark phase of proestrus[191]. We examined whether 31-60 Hz slow gamma was similarly homeostatically upregulated during proestrus. There were no differences across the four days within the mPFC or CA1 in males (Fig 3.8D, F). We did find a small rise from day 2 to day 4 in V2 slow gamma activity at the very end of the light phase in males (Fig 3.8E). In females, there was an increase in slow gamma activity in all areas recorded during the dark phase of proestrus compared with all other estrous phases. This increased dark phase proestrus slow gamma was also higher than males in the mPFC and V2 cortices (Fig 3.9D-F). In contrast, V2 slow gamma activity during estrus was significantly lower than males during the dark phase.

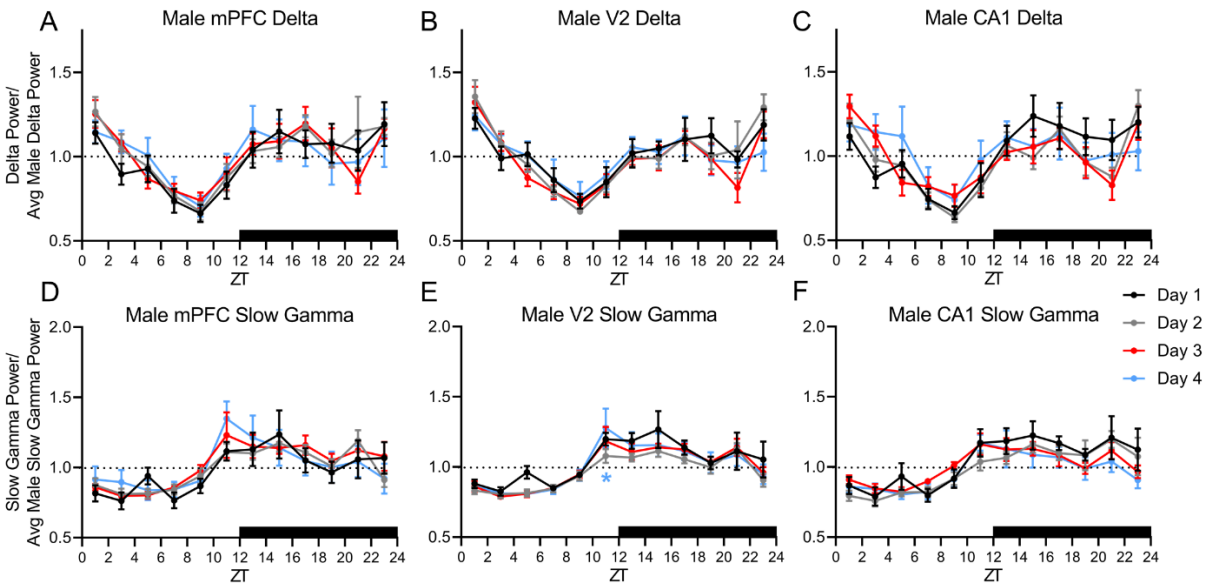


Figure 3.8 NREM slow wave delta power (0.5-4Hz) and slow gamma power (31-60Hz) homeostasis is consistent in males. (A) Male medial prefrontal cortex (mPFC), (B) secondary visual cortex (V2) and (C) CA1 delta power expressed as the average delta power. (D) Male mPFC, (E) V2, and (F) CA1 NREM slow gamma power across expressed as the average slow gamma power. As some two-hour bins did not contain NREM sleep, for repeated measures statistical comparisons were calculated via a mixed-effects model followed by Tukey post hoc. *$p<0.05$, asterisk color denotes which day the adjacent data is significantly different from. Data displayed as the mean±SEM for that group. Males n=7 for all figures.

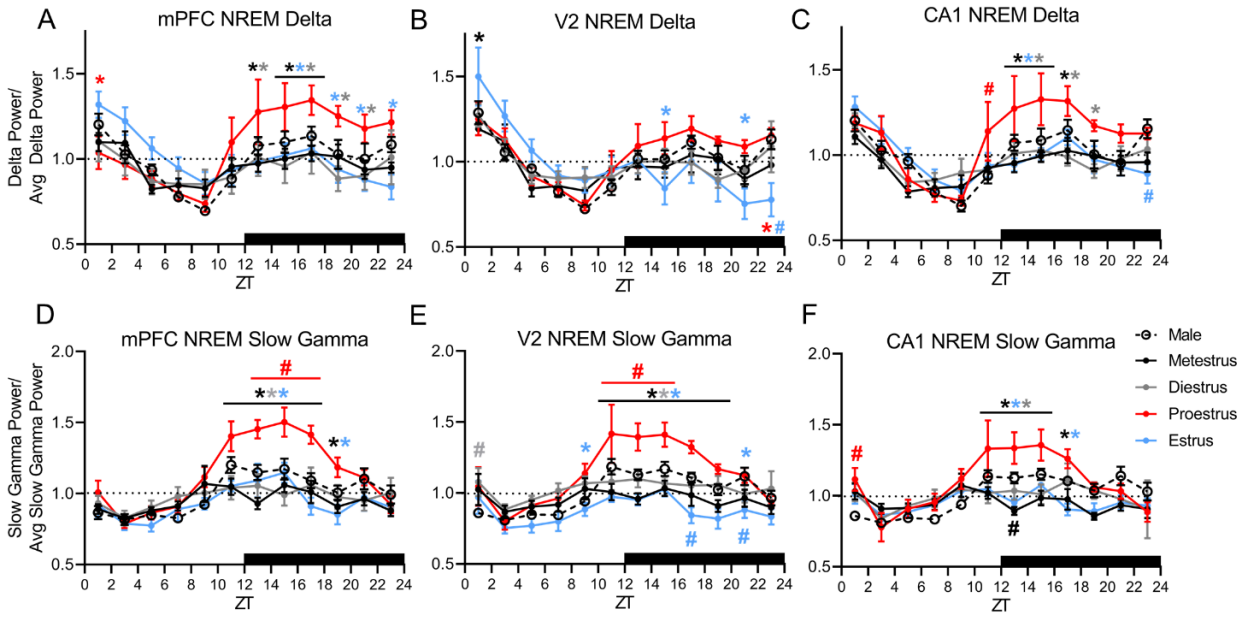


Figure 3.9 NREM slow wave activity (0.5-4Hz) and slow gamma activity (31-60Hz) homeostasis is altered across the estrous cycle. (A) Female medial prefrontal cortex (mPFC), (B) secondary visual cortex (V2) and (C) CA1 delta power across the estrous cycle expressed as the average delta power across the whole estrous cycle (D) Female mPFC, (E) V2, and (F) CA1 NREM slow gamma power across the estrous cycle expressed as the average slow gamma power across the whole estrous cycle. Male data in A-F represents average male values from similar figures (see supplemental figure 4). As some two-hour bins do not contain NREM sleep, for repeated measures, statistical comparisons within females were calculated via a mixed-effects model followed by Tukey post hoc. *p<0.05, asterisk color denotes which day or estrous phase which the adjacent data is significantly different from. Comparisons between male average and females are done via mixed-effects model, Dunnett post hoc. #p<0.05, the color of the pound sign corresponds to phase of the estrous cycle that males are significantly different from. Data displayed as the mean±SEM for that group. Females n=9, males n=7 for all figures.

### 3.6 Interregional spectral coherence during sleep changes across the estrous cycle

We next examined whether there were any spectral coherence changes between recorded areas throughout the estrous cycle. Figure 3.10 displays the average spectral coherence during NREM sleep from 0.5-100 Hz in males and females. In males there were no differences in the coherence at any frequency band between brain areas during NREM sleep. (Fig 3.10A, B). In females, delta and sigma band coherence was increased during early dark phase ZT12-18 of proestrus in the mPFC-V2. Delta coherence also increased mPFC-CA1 coherence (Figure 3.10C, D). Additionally, sigma band coherence also increased between the mPFC and CA1. (Fig 3.10D). There were no significant differences between males and females in any band coherence in either

mPFC-V2 or mPFC-CA1 during NREM sleep (mixed-effects model, Dunnett post hoc: p=0.31 to >0.99 mPFC-V2, p=0.17 to >0.99 mPFC- CA1)

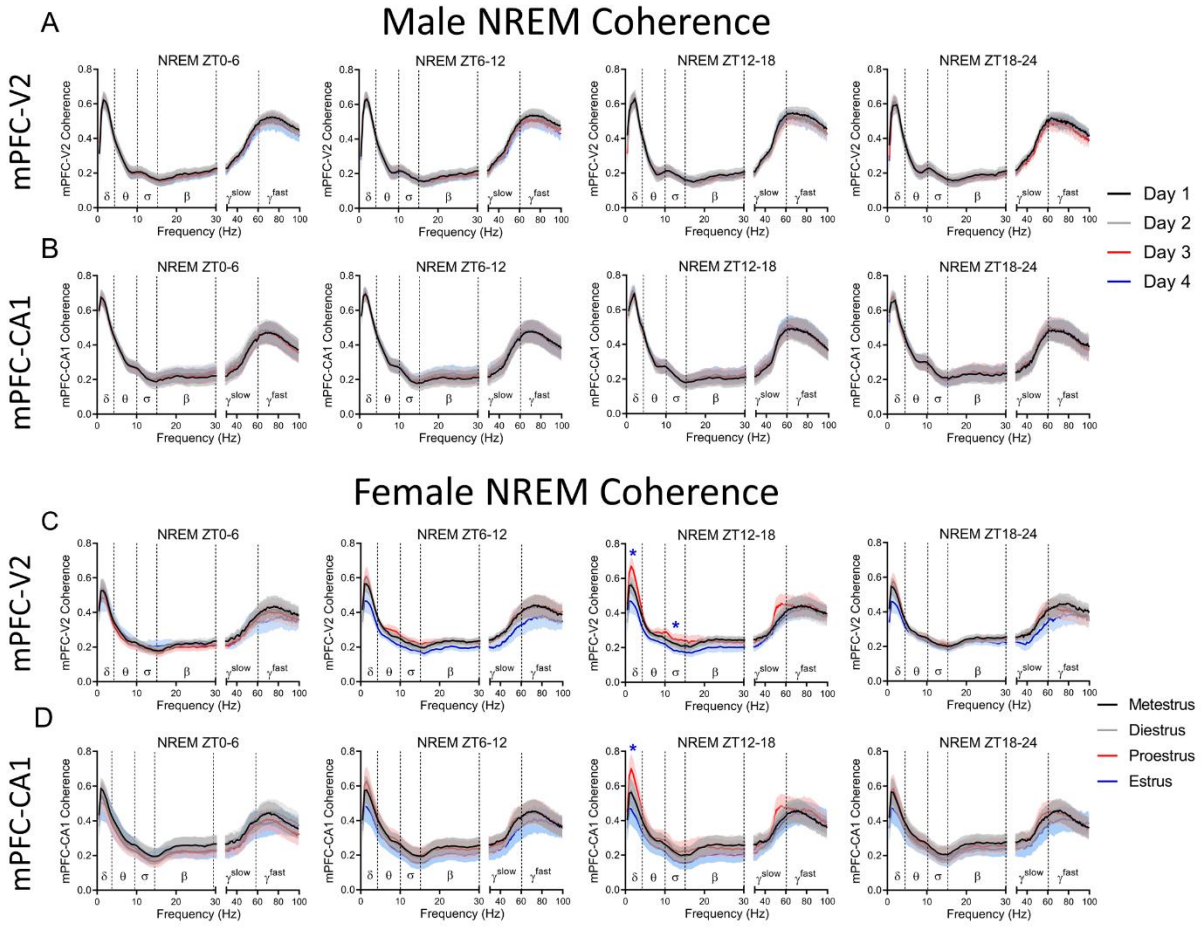


Figure 3.10 Interregional field coherence during NREM sleep changes throughout the estrous cycle. Each panel displays coherence values for 0.5-100Hz, throughout the phases of the estrous cycle in females and across days in males. Different frequency bands are denoted with their symbol and divided by dotted lines: δ=0.5-4Hz, θ=5-9Hz, σ=10-15Hz, β=16-30Hz, $\gamma^{slow}$=30-60Hz, $\gamma^{fast}$=61-100Hz. (A) medial prefrontal cortex (mPFC)-secondary visual cortex (V2) NREM spectral coherence across the estrous cycle. (B) mPFC-CA1 NREM spectral coherence across the estrous cycle. (C) mPFC-V2 and (D) mPFC-CA1 NREM spectral coherence across four days of recording in males. Statistical comparisons within males and females were calculated on the average coherence in each band via a mixed-effects model, Tukey post hoc; proestrus vs estrus *p<0.05. Comparisons between male and females was done via mixed-effects model, Dunnett post hoc. No different between the sexes were found across any band. Data displayed as the darker line in the mean and the lighter shaded region of analogous color represents the SEM for that group. Females n=9 for mPFC-V2, and n=8 for mPFC-CA1 as one animal had a broken CA1 electrode; males n=7 for all figures.

Looking next at REM sleep coherence, there were no coherence changes in males in any frequency band in either mPFC-V2 or mPFC-CA1 (Fig 3.11A, B). In females, slow gamma and fast gamma coherence was increased during ZT12-18 of

proestrus in both mPFC-V2 and mPFC-CA1 (Fig 3.11 C, D). Fast gamma coherence in mPFC-CA1 was also increased during ZT12-18 of proestrus. There were no differences between males and females in any coherence band during REM sleep (mixed-effects model, Dunnett post hoc: p=0.31 to >0.99 mPFC-V2, p=0.27 to >0.99 mPFC-CA1).

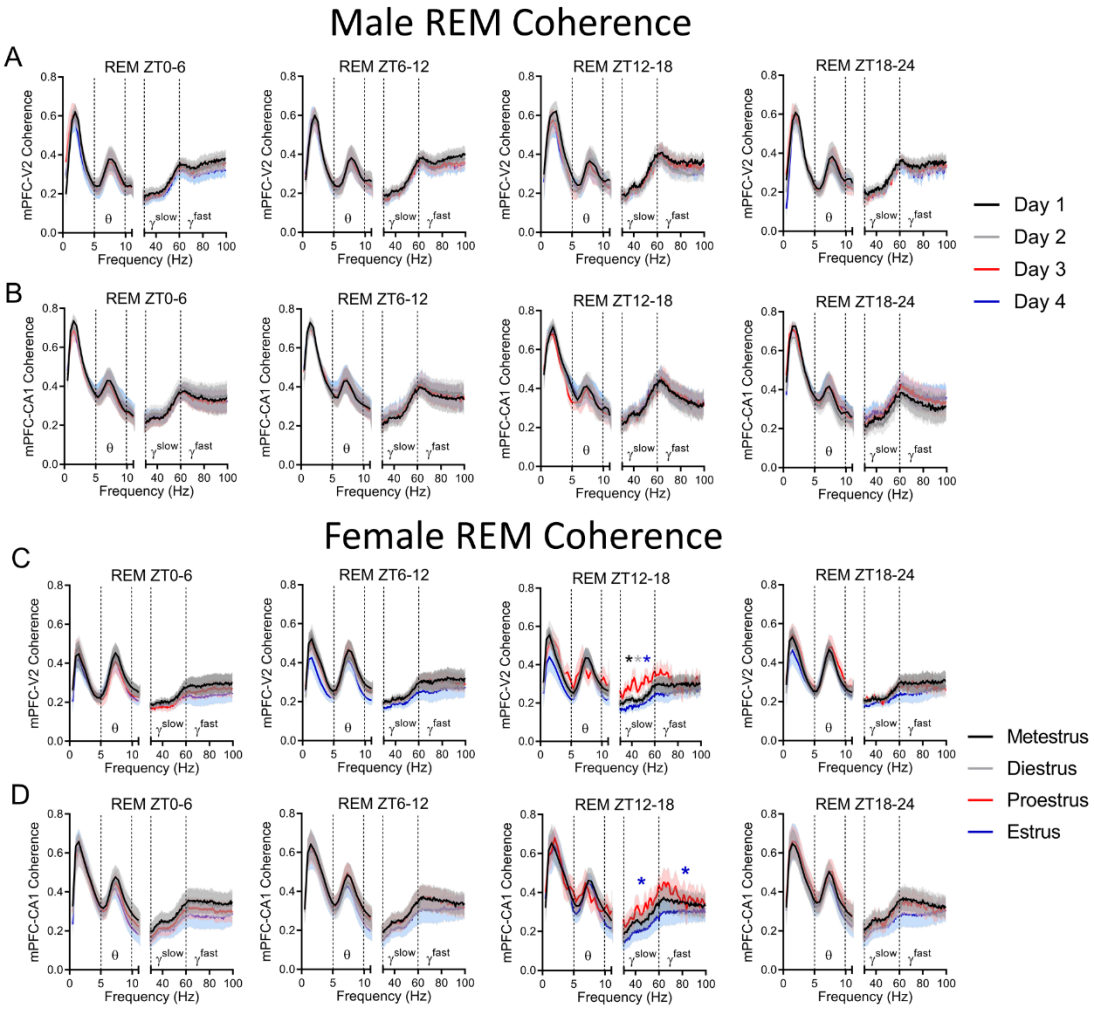


Figure 3.11 Interregional field coherence during REM sleep changes throughout the estrous cycle. Each panel displays coherence values for 0.5-100Hz, throughout the phases of the estrous cycle in females and across days in males. Different frequency bands are denoted with their symbol and divided by dotted lines: δ=0.5-4Hz, θ=5-9Hz, σ=10-15Hz, β=16-30Hz, $\gamma^{slow}$=30-60Hz, $\gamma^{fast}$=61-100Hz. (A) medial prefrontal cortex (mPFC)-secondary visual cortex (V2) NREM spectral coherence across the estrous cycle. (B) mPFC-CA1 NREM spectral coherence across the estrous cycle. (C) mPFC-V2 and (D) mPFC-CA1 NREM spectral coherence across four days of recording in males. Statistical comparisons within males and females were calculated on the average coherence of each band via a mixed-effects model followed by Tukey post hoc; *p<0.05, asterisk color denotes which day or estrous phase which the adjacent data is significantly different from. Comparisons between male average coherence and females were done via mixed-effects model, Dunnett post hoc. Data displayed as the darker line in the mean and the lighter shaded region of analogous color represents the SEM for that group. Females n=9 for mPFC-V2, and n=8 for mPFC-CA1 as one animal had a broken CA1 electrode; males n=7 for all figures.

### 3.7 Sleep spindle density, length, and peak frequency differ across the estrous cycle

Previous work in humans has shown that females have more spindles than males[192], and that spindle density changes across the menstrual cycle[178,184]. Thus, we wanted to know whether similar changes occurred across the estrous cycle in female rats and whether spindle density differed from males. We only analyzed spindle characteristics recorded from cortical area (e.g. Fig 3.12A), as spindles have been little described in the hippocampus[65,193–195]. There were no differences between males and females in spindle density in either cortical area. There were also no changes in male mPFC or V2 sleep spindle density across the four days (Fig 3.12B). However, there were spindle density changes across the estrous cycle. Female mPFC sleep spindle density increased during ZT0-6 and ZT6-12 of proestrus compared to estrus and was also higher at ZT6-12 in proestrus than diestrus (Fig 3.12C). However, female V2 spindle density was reduced during ZT18-24 of proestrus compared to estrus. Male mPFC spindle density positively correlated with V2 spindle density across four days of recording (Fig 3.12D). Although females showed no correlation in spindle density between regions when the four days of the estrous cycle were combined, there was a positive correlation during proestrus and a trend in estrus (Fig 3.12E).

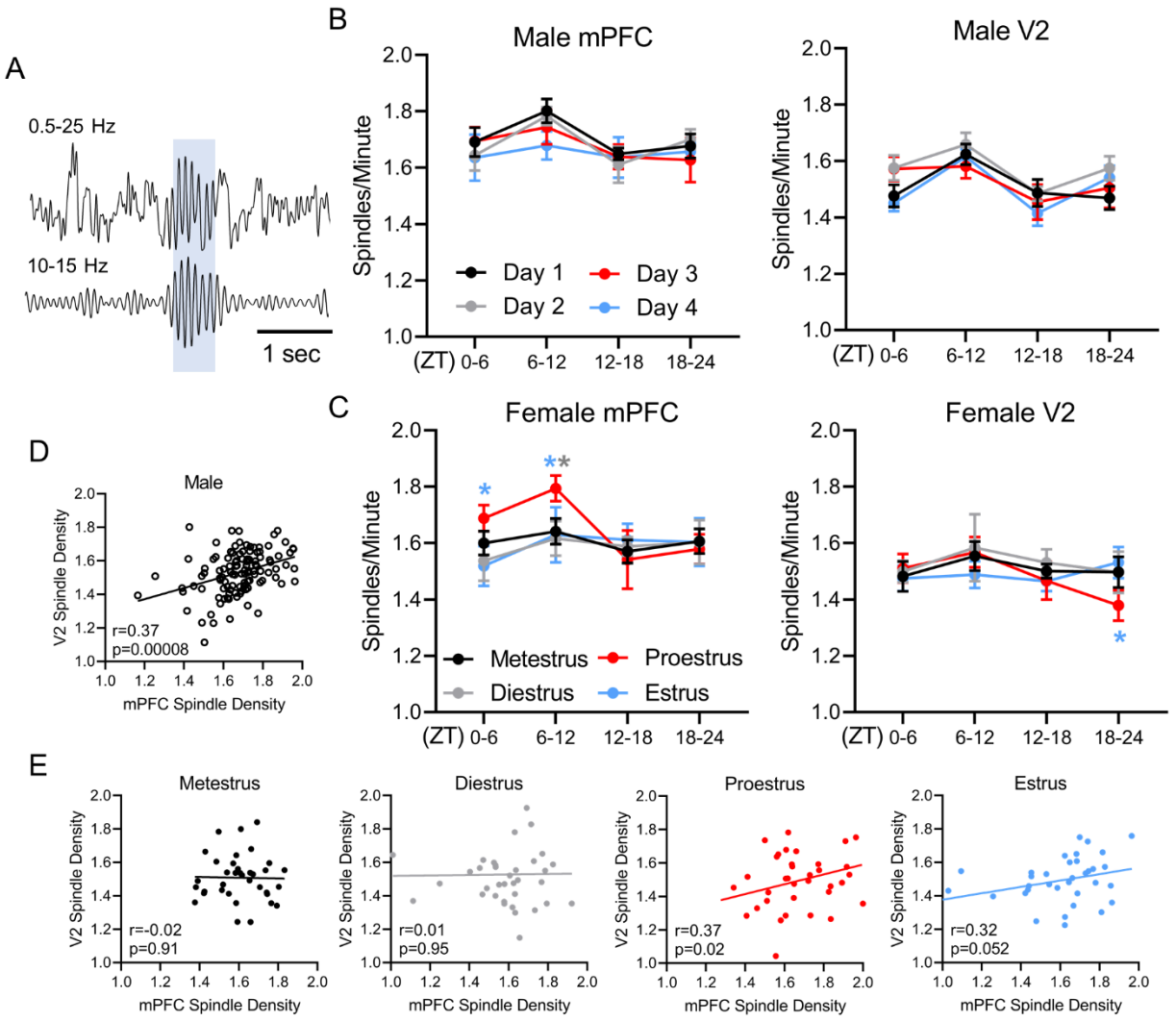


Figure 3.12 Sleep spindles density changes across the estrous cycle**.** (A) Example sleep spindle identified from medial prefrontal cortex (mPFC) EEG with 0.5-25 Hz filter on top and 10-15 Hz spindle frequency on the bottom panel. Blue shaded region represents an identified spindle. (B) Male mPFC and secondary visual cortex (V2) sleep spindle density (spindles per minute) across four days of recording. (C) Female mPFC and V2 sleep spindle density across the estrous cycle. (D) Pearson correlation of male mPFC spindle density vs male V2 spindle density. (E) Pearson correlation of female mPFC spindle density vs male V2 spindle density across each phase of the estrous cycle. Analysis within males and females was done via repeated measure two-way ANOVA, Tukey post hoc *p<0.05, asterisk color denotes which day or estrous phase which the adjacent data is significantly different from. Analysis comparing male average to females done via two-way ANOVA Dunnett post hoc; no differences found. All plots in B and C display mean ± SEM. Males n=7, females n=9. For correlations in D and E each point represents sleep spindle density during a single quartile of the day for each animal. Male correlations include all four days of recording, whereas female correlations are divided by estrous cycle phase. Males n=112 (7 males * 4 days * 4 quartiles/day). Females n=36/phase (9 females * 4 quartiles/phase).

Spindle characteristics such as frequency are also altered by the menstrual cycle[184]. We found no differences in sleep spindle peak frequency in male cortical areas across the four days of recording (data not shown, two-way ANOVA, Tukey post hoc: mPFC p=0.12 to >0.99, V2 p=0.07 to >0.99). In female mPFC, ZT0-6 of metestrus had a significantly higher spindle peak frequency than all other phases and V2 had a higher peak frequency compared to diestrus and estrus (Fig 3.13A-B). Also, ZT6-12 of both metestrus and proestrus had a higher mPFC peak spindle frequency compared to diestrus and estrus (Fig 3.13A). Female mPFC peak spindle frequency rose higher than males at the end of the estrus phase and continued higher than males through the light phase of metestrus, then dipped below that of males in the light phase of diestrus. Peak spindle frequency did not differ between males and females during proestrus or the first 6 hours of the dark phase (ZT12-18) of any estrous cycle phase. In V2, females had higher spindle peak frequency during ZT0-6 of metestrus, and during ZT12-18 of proestrus compared to males. Finally, we examined spindle length. There was no difference in male cortical spindle length across the four days of recording at either cortical site (data not shown, two-way ANOVA, Tukey post hoc: mPFC p=0.20 to >0.99, V2 p=0.26 to >0.99). Female mPFC spindles also showed no changes in length across the estrous cycle but were shorter than males at diestrus and proestrus ZT18-24 (Fig 3.13C). Female V2 spindles were shorter than males at proestrus ZT18-24 and diestrus ZT0-6. Conversely, female V2 spindles were longer than males during metestrus ZT0-6 when they were also longer than spindles at all other estrous phases. V2 spindles were also long at proestrus ZT12-18– significantly longer than spindles during estrus (Fig 3.13D).

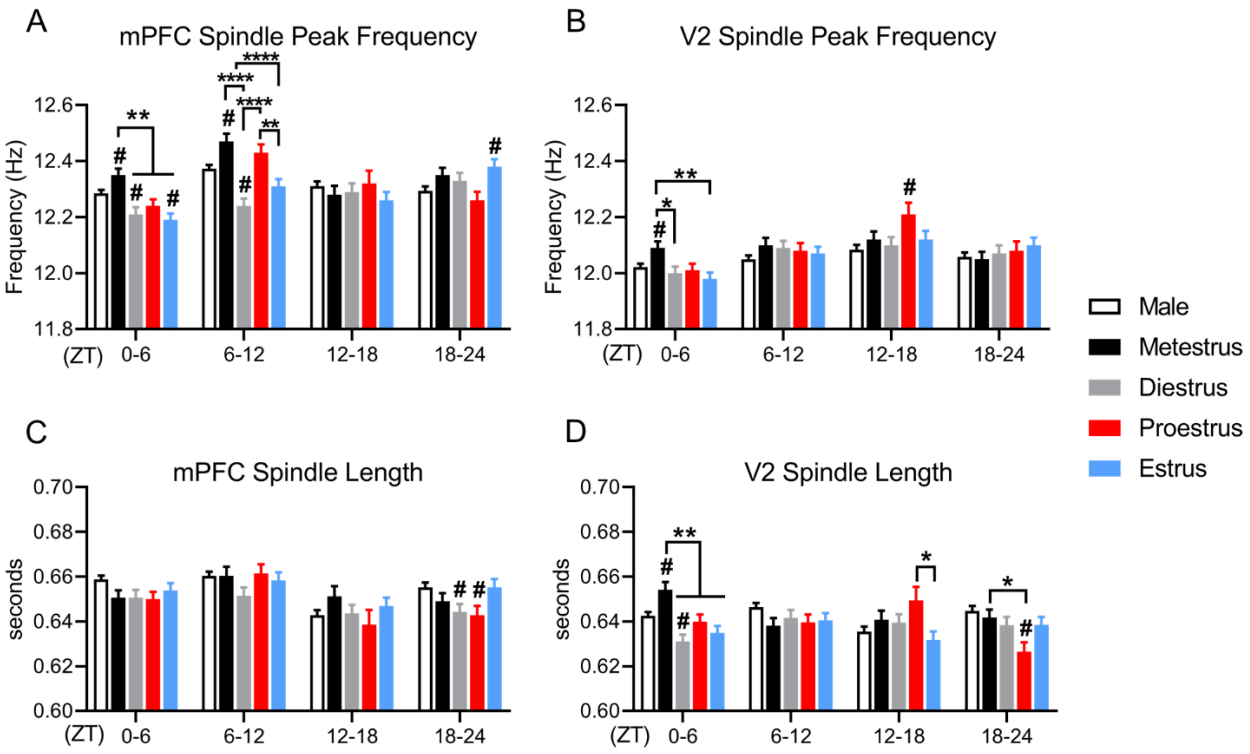


Figure 3.13 Sleep spindle peak frequency and spindle length changes across the estrous cycle. (A) Medial prefrontal cortex (mPFC) spindle peak frequency in males (average) and females across the estrous cycle. (B) Secondary visual cortex (V2) spindle peak frequency in males (average) and females across the estrous cycle. (C) mPFC spindle length in males (average) and females across the estrous cycle. (D) mPFC spindle length in males (average) and females across the estrous cycle. Analysis within females was done via two-way ANOVA, Tukey post hoc. *p<0.05, **p<0.01, ****p<0.0005. Analysis comparing male average to females was done via two-way ANOVA, Dunnett post hoc. #p<0.05 vs males. All plots display mean±SEM. Females n=9, males n=7.

### 3.8 Discussion

Hormonal fluctuations accompanying the estrous cycle in rats have marked effects on sleep and sleep architecture. While original studies utilized Sprague Dawley rats, we found similar effects of the estrous cycle on sleep-waking behavior in Long Evans rats[172,191,196,197]. Thus, sleep in female rats remains consistent across at least two strains.

During proestrus, the rise in estradiol and progesterone promotes waking and suppresses NREM and REM sleep[175,186,187,198]. Similarly, we found that during proestrus there was significantly more waking all through the night, with the most prominent spike in waking during ZT12-18 of proestrus when hormonal levels are at their peak (Fig 3.1A). We show this spike was chiefly due to an increase in the length of each waking bout. The subsequent decrease in NREM was due to a decrease in the NREM bout

length rather than the bouts/per hours, whereas the most dramatic decreases in REM sleep were due to a decrease in both bout length and frequency. However, during the morning of estrus there was a significant rebound from the prior deprivation of NREM and REM, with the increase in NREM and REM sleep due to an increase in bout length in both states.

Between males and females, the most prominent differences in total sleep time and sleep architecture occurred during the dark phase of proestrus and the subsequent light phase of estrus. While males remained consistent in total sleep amount and sleep architecture over the four days of recording, the changes within females in waking, NREM, and REM during proestrus resulted in prominent differences between sexes. While sex differences also manifested during metestrus and diestrus, namely, an increase in dark phase REM bouts per hour and contrasting decrease in light phase REM bout lengths as well as changes in sleep spindles, these phases showed sleep that more closely resembled sleep in males.

Within NREM sleep, changes in delta power (0.5-4 Hz) the morning of estrus have been reported[191]. However, we show for the first time that these effects are not isolated to the cortex or a specific region within it. Interestingly, NREM delta power was also increased during the prior night of proestrus, which was not found in other work[191]. Both of these increases are likely due to delta rebound following earlier sleep deprivation, which is a normal compensatory response to sleep deprivation[191,199].

The increase in the slow gamma power (31-60 Hz) during ZT12-18 of proestrus is a novel finding. Previous work has reported an increase in the beta (15-30 Hz) band during the night of proestrus[191]; however, there are no reports of changes in slow gamma. One potential reason this change has not been identified previously is that during NREM sleep, frequencies greater than 18Hz (excluding hippocampal ripples of 100-200 Hz) are often ignored; or when higher frequencies are analyzed, they are investigated for disease conditions such as insomnia[200]. The presence of increased gamma, a frequency range that has been associated with consciousness[201], during NREM sleep in proestrus and in the company of increased delta activity is unique. We posit that these changes may be due to competing mechanisms. On one hand, increased estradiol and progesterone levels promote wakefulness to maximize mate-

seeking behavior necessary for reproduction. As estradiol and progesterone receptors are expressed throughout arousal pathways such as the cholinergic basal forebrain, orexinergic neurons in the hypothalamus, and noradrenergic neurons of the locus coeruleus[202–204], and as these arousal pathways are implicated in reproduction[205–207], it is likely the increased wakefulness is due to their activation. Further, as activation of these arousal centers promotes gamma power during waking it is possible that increased gamma during NREM is related[208–210]. Meanwhile, the resulting sleep deprivation increases NREM delta pressure. Thus, when animals are able to sleep there is an increase in both delta and slow gamma.

Unlike the more global NREM sleep delta power changes across the estrous cycle which seemed to reflect homeostatic pressure, changes in REM sleep theta power were localized to specific brain regions. Further, changes in REM theta were independent of the prior amount of time spent in REM sleep. Previous work did not identify specific changes in REM sleep theta power across the estrous or menstrual cycle and treating ovariectomized female rodents with gonadal sex hormones has provided mixed theta power results [178,191,211,212]. However, as REM sleep theta has been linked to memory consolidation[40,65,102], even isolated theta power reductions may have detrimental effects on cognition. Also, REM theta is reduced in post-traumatic stress disorder (PTSD), which is considered by many to be a memory consolidation disorder[103]. PTSD affects a higher percentage of trauma exposed women than men[213]. Our study suggests that windows of decreased theta power across the hormonal cycle could present vulnerable periods where maladaptive responses to traumatic stress are more likely to result. Conversely, higher theta power in the late proestrus phase could present a window of resilient sleep

Schwierin et al., established that both NREM 0.75-4 Hz SWA and 10-25 Hz activity were regulated differently during the dark phase of proestrus: SWA decreased and 10-25 Hz frequency activity increased. In contrast, we found both 0.5-4 Hz SWA and 31-60 Hz slow gamma activity increased during the dark phase of proestrus. This increase in slow gamma homeostasis during proestrus was also different from males in both the mPFC and V2. The prominent cortical homeostatic increase in slow gamma is likely due to the aforementioned effects of estradiol and progesterone and is further

supported by the complete absence of slow gamma changes (whether in raw spectral power or homeostasis) in males. Further work is necessary to replicate and to better understand these homeostatic changes in SWA and slow gamma activity.

We show novel changes in intracortical sleep coherence and cortical-hippocampal coherence across the estrous cycle. While there were no differences between male and female coherence, within females, NREM sleep delta (SWA) and sigma band (sleep spindle frequency) coherence increased during ZT12-18 of proestrus. In REM sleep, although there was not a change in the theta coherence across the estrous cycle, there was enhanced slow and fast gamma band coherence between cortical areas and between the mPFC and hippocampus in the same early dark phase of proestrus. Despite the decrease in sleep during the dark phase of proestrus the increase in coherence may be indicative of enhanced offline processing[214]. Specifically, memory processing, which requires sleep, may be preserved by enhanced coherence despite a decrease in overall sleep.

To the best of our knowledge, no previous work exists examining sleep spindles within female rodents across the estrous cycle. We show that spindle density increases during the light phase of proestrus in the mPFC and decreases at the end of the dark phase of proestrus in V2. While the mechanism for the increase in spindle density during proestrus remains unknown, we can speculate about the function. As spindles have been linked to memory consolidation[65,73,88], an increase in spindles, specifically in the mPFC, a region necessary for decision making and higher cognitive function (for review see[215]), may be indicative of enhanced memory processing. Strengthening memory processing just prior to fertility could enhance, among other things, consolidation of the mating context in order to maximize future reproductive success. Interestingly, the increased spindle density in rats did not occur at a similar point within the cycle as in women. In women, spindle density increases during the luteal phase following ovulation[178], whereas we report in rats that the increase occurred during the light phase of proestrus just prior to ovulation.

While there was no difference in spindle density between males and females within either cortical region, there were differences in spindle length and peak frequency between the sexes, and across the estrous cycle. Previous work found an ~0.5 Hz

increase in spindles frequency across the menstrual cycle[184]. We found a mild but significant increase of ~0.2 Hz in spindle frequency during metestrus and proestrus compared to other phases. The increase in V2 spindle length during the early dark phase of proestrus and the early dark phase of metestrus is more interesting, as we have found that foreshortening longer spindles was associated with learning deficits[26]. Thus, modulations in spindle density and spindle length in different cortical areas at different estrous phases could alter memory consolidation Further work in learning and memory and estrous cycle phases is necessary to determine whether these changes in sleep spindle characteristics have any physiological relevance.

# CHAPTER IV
# Conclusions and Future Directions

## 4.1 Noradrenergic control of memories: sleep as the new frontier

Both noradrenergic activity and sleep support the consolidation of memories, but previous work enhancing or suppressing the effect of norepinephrine to alter memory consolidation has been conducted exclusively during waking[118–120,123]. The design of studies that manipulate norepinephrine during waking produces two critical unanswered questions: first, whether these manipulations alter sleep, and if so, are the changes in memory affiliated with sleep changes; second, whether manipulating noradrenergic activity outside of waking affects memory. The study presented in chapter two partially addressed these issues.

Addressing the first issue, it is well established that increasing or decreasing LC activity suppresses or promotes sleep, respectively[137]. Yet, studies manipulating LC activity or NE to alter memory do not consider the confounding effects of potential sleep deprivation. Despite failing to consider sleep deprivation, enhancing NE levels during waking following learning generally improves memory, whereas decreased level impairs it—likely by increasing or decreasing the synaptic strength within a memory trace[114]. Thus, even if sleep is disrupted by enhanced noradrenergic activity at the time of encoding, the loss of the beneficial effects of sleep may be outweighed by enhanced synaptic strength. In certain circumstances, such as one-trial learning tasks, (e.g., fear conditioning or object placement/novelty recognition) that show improved performance with either noradrenergic enhancement or sleep, simply enhancing synaptic strength may be sufficient to improve memory without sleep, or even at the expense of sleep[123,216–218]. However, in more complex learning that requires either multiple learning trials or updating of a previous memory circuit to integrate new information, simple enhancement of synaptic strength is not enough to improve memory. Rather, the weakening of memory circuits via depotentiation, which occurs chiefly during sleep and

is important for learning and memory, may be necessary for proper consolidation[219,220]. The need for sleep and synaptic depotentiation in learning is further supported by previous studies suggesting that more complex learning tasks benefit particularly from sleep[16]. Our study utilized a complex learning task involving consolidation of new information and reconsolidation of familiar information. Moreover, we were able to manipulate LC activity within a physiological range without altering sleep architecture, albeit we did alter the neural rhythms within sleep[65]. As noradrenergic activity clearly affects both learning and sleep, future work must consider whether noradrenergic manipulations alter sleep, and if so, if these changes in sleep affect memory.

The second issue concerns whether noradrenergic activity during sleep affects memory consolidation. Previous work has established endogenous LC activity within sleep has specific activity patterns in relation to neural oscillations associated with memory consolidation: LC activity phase locks to up-states of cortical slow waves, ceases and then resumes activity during spindles, and completely ceases for the duration of REM sleep[134,139]. Interfering with the temporal relationship between LC activity and these oscillations by maintaining 2 Hz LC activity during sleep deleteriously affected both the oscillations and memory consolidation. Our study provides the first evidence that LC activity during sleep plays a role in memory consolidation.

However, our study has several caveats which future work could address to improve the accuracy of our interpretations and further our understanding of the function of noradrenergic activity during sleep. First, while our 2Hz LC stimulation was specific to sleep, it was not specific to either NREM or REM sleep; therefore, the resulting memory deficits could be due to increased LC activity in NREM or REM sleep alone. Future studies should perform the same experiment, but isolate the stimulation to a specific state, to determine if enhanced LC activity during NREM or REM is enough to produce similar memory deficits. Similarly, while LC stimulation prevented learning-induced increases in spindle density, the stimulation did not target spindles specifically. By using closed-loop feedback stimulation to generate an LC spike during spindle onset, it would be possible to specifically target spindles, and determine if the decrease in spindles alone is enough to produce memory deficits. In the same manner, closed loop

optogenetic inhibition of LC activity during spindles would indicate whether which activity is necessary for spindle termination.

Another future direction would be to examine whether increased LC activity during sleep, whether artificial or as previously observed following learning, could improve memory rather than interfere with it, if timed correctly[138]. We demonstrate that within a complex learning task, LC stimulation during sleep prevents both memory consolidation and reconsolidation. However, in a simple one-trial learning task that involves only consolidation of novel information, LC stimulation may enhance performance—likely by enhancing the synaptic strength of the memory circuit. Thus, the nature of the memory task itself may determine whether LC stimulation during sleep is beneficial or maladaptive.

Moreover, the combination of both the state in which the LC stimulation occurs, i.e. NREM or REM, and the nature of the behavioral task could both determine the effect of LC stimulation during sleep on memory consolidation. By isolating LC stimulation to either NREM or REM sleep we may be able to differentially effect learning in our own (8-box) learning paradigm.

The effect of LC stimulation on neural oscillations also requires further investigation. As our stimulation targeted the LC projections throughout the whole brain, and across both NREM and REM sleep, the differential effects of LC stimulation on specific oscillations is impossible to parse. Future studies targeting LC terminals in specific regions which generate different oscillations during sleep would further our understanding of the results. For example, by utilizing retro-tracing canine-adenovirus vectors[147], it would be possible to specifically target and optogenetically stimulate LC projections to the medial septum whose inhibitory projections generate the theta rhythm within REM sleep[40]. Similar methods could be used to target LC terminals in the thalamic reticular nucleus which is responsible for generating sleep spindles[22]. Similarly, by stimulating LC projections to a single hemisphere of the cortex, and measuring EEG activity from both hemispheres, it would be possible to determine whether LC activity can alter slow waves within a single hemisphere.

We demonstrate that abnormal LC activity alters consolidation and reconsolidation at the cellular (place fields), tissue (oscillations), and the behavioral-

organismal (task performance) level. These finding are relevant to the treatment of post-traumatic stress disorder (PTSD). In PTSD, patients experience an array of symptoms including, but not limited to, intrusive memories, sleep disturbances, and hyper arousa[221]. PTSD patients display increased NE levels in cerebral spinal fluid during waking and increased plasma NE (an indirect measure of central NE levels and sympathetic nervous activity) during sleep[163,222,223]. This increased NE likely plays a role in both sleep disturbances and intrusive memories[224]. As sleep broadly downscales synaptic strength, sleep and particularly REM sleep is essential for the processing of emotional memories that are strongly consolidated[221,225]. However, if NE levels remain high during sleep, synapses cannot weaken, leading inability to properly contextualize consolidated fear circuits. Further, if NE levels are too high during sleep it can cause fragmented sleep more prone to arousal[226]. The combination of these factors may contribute to the presence of intrusive memories and blunted emotional processing displayed in PTSD patients[221]; thus, pharmacologically manipulating the effect of NE on adrenergic receptors during sleep has been proposed as a potential therapy for treating PTSD patients[221,226,227]. That being said, a recent seminal study demonstrated that prazosin, an $\alpha^1$-AR antagonist commonly prescribed to PTSD patients to treat sleep disturbances, was ineffective at treating PTSD associated sleep issues (arousals, nightmares, etc.)[228]. Additionally, the β-AR antagonists have been shown to cause nightmares and insomnia[227,229]. More work is necessary to better understand what role existing noradrenergic drugs, receptors, and sites of action can play in treating both sleeping and waking PTSD symptoms.

### 4.2 On the basis of sex and sleep

Chapter 2's study utilizing optogenetic stimulation of the LC, like much of basic research, has the limitation that all the studies were performed in males. According to the National Institute of Health, while clinical studies have achieved near equal participation of males and females, basic research overwhelmingly utilizes only males. Studies examining sleep are no exception. Despite early evidence from the 1960's that the estrous cycle affect sleep[172], there is astoundingly little known about how

reproductive cycles affect neural processes during sleep in either humans or other animals.

Chapter 3 replicates previous work showing that the estrous cycle affects sleep and provides further evidence that the estrous cycle alters broadly affects sleep-wake architecture and neural rhythms during sleep; the most prominent of which, is the suppression of sleep during the dark phase of proestrus[186,187]. This suppression co-occurs with and is caused by estradiol and progesterone[211,230]. Moreover, while the suppression of sleep during proestrus is conserved across rodent strains the exact mechanism for increased wakefulness is not known[231,232]. Current hypotheses point to several potential mechanisms presented here and discussed further below: first, increased levels of ovarian hormones suppress activity in sleep promoting neurons; second, ovarian hormones activate arousal pathways; three, a combination of the prior two mechanisms could be at work.

Evidence for hormonal suppression of sleep promoting centers comes primarily from examination of neural markers of activity following hormonal administration in gonadectomized animals. Administration of estradiol into the ventral lateral preoptic area (VLPO), a region known to promote sleep, suppresses synthesis of prostaglandin D2, which signals downstream to promote sleep[233]. Estradiol administration also decreased c-fos expression, a marker of neural activity, in the VLPO in ovariectomized females[187,234].

In addition, estradiol and progesterone are implicated in activation of arousal centers. Receptors for both progesterone and estradiol are widely present throughout neuromodulatory arousal centers including the cholinergic basal forebrain, dopaminergic ventral tegmental area, noradrenergic locus coeruleus, serotonergic dorsal raphe, and the orexinergic hypothalamus[202–204]. Administration of estradiol increases c-fos expression within additional arousal promoting regions such the medial amygdala, bed nucleus of the stria terminalis, anteroventral periventricular nucleus[234]. Despite estradiol alone affecting arousal centers, estradiol and progesterone together produce the most prominent decreases in NREM and REM sleep[230]. This effect is most prominent during the dark phase when rodents are awake—as if estradiol and progesterone further enhance arousal states. Despite this, even less is known about the

role of solely progesterone in arousal in rodents. Studies of sleep and progesterone in ovariectomized rodents fail to consider that progesterone receptor expression is dependent on estrogen receptor gene expression[235]; i.e., progesterone may not be able to act at its receptor in the absence of estradiol. In humans, progesterone has been reported to induce sleep in contrast to promoting arousal in animals models[236]. Further work is necessary to examine the effects of progesterone on sleep-wake activity.

While suppression of sleep promoting neurons and enhanced activity in arousal promoting centers both promote wakefulness, these mechanisms likely work in together rather than in isolation. One study highlighted that administration of estradiol simultaneously decreased c-fos expression in sleep-promoting VLPO neurons while increasing c-fos expression in tuberomammillary nucleus (TMN), another key arousal center in the rodent brain[187]. Reciprocal connections between the VLPO and the TMN have been linked and are associated with control of wake and arousal[237]. Thus, estradiol increases activity in TMN neurons which then likely inhibit VLPO neurons, suggesting estradiol promotes arousal by both mechanisms[187]. However, without recordings from VLPO and TMN neurons it is difficult to conclude the exact effect of estradiol on the circuit. Future work recording from sleep- and arousal-promoting centers is necessary to better understand the role sex hormones play in modulating sleep-wake behavior across the estrous cycle.

REM sleep is disproportionately inhibited by estradiol and progesterone—particularly within the first 6 hours of dark phase of proestrus. During with first 6 hours of the dark phase of proestrus we found a ~70% reduction of REM sleep from circadian-matched times during other estrous cycle phases, and an ~90% reduction from the first 6 hours of the light phase. Interestingly, this suppression is dark phase dependent as administration of estradiol and progesterone in OVX-rats in the light phase does not replicate the same magnitude of suppression[230]. Maximal REM sleep suppression occurs at the transition of light to dark implicating a potential diurnal influence in estradiol-progesterone induced suppression. Additionally, it remains unknown whether estradiol and progesterone inhibit REM-on cells of the subcoeruleus, which promote REM sleep generation[238]. Future studies examining the suppression of REM sleep

during proestrus should examine the effects estradiol and progesterone on circuits controlling REM sleep.

### 4.3 Potential effects of estrous induced changes in sleep-wake behavior on memory

Despite the well-studied links between sleep and memory, and the links between the estrous cycle and sleep, the link between sleep changes within the cycle and memory consolidation remain poorly understood. This relationship is difficult to parse as estrous cycle hormones, both endogenously occurring and exogenous hormones administered to OVX animals, alter memory formation. Generally, higher levels of hormones promote memory consolidation[239]. Normally cycling females undergoing learning in proestrus generally have increased performance in spatial learning tasks, fear extinction, and object learning tasks[240–243]. However, this proestrus effect on learning is inconsistent as other studies have reported no advantage in the radial arm maze or the T-maze[242]. Independent of the estrous cycle, ovarian hormones themselves are important for learning and memory.  OVX rats show decreased performance on the Morris water maze, radial maze, and object recognition tasks[244–246]. Reintroduction of estradiol ameliorates performance loss, particularly in spatial tasks[242,244,247]; this is likely due to estradiol's well documented effect of promoting synaptic plasticity and long-term potentiation within hippocampal circuits[242].

The suppression of sleep by elevated sex hormones in the presence of enhanced memory consolidation is an antithetical relationship—or at least an unexpected one. Despite this, there are two probable explanations for improved memory in the presence of suppressed sleep: one, that sleep itself is more efficient at consolidation, or two, compensatory mechanisms, whether hormonal or neuromodulatory, facilitate consolidation in the absence of sleep. Chapter 3 suggests improved sleep efficiency as evident by the increased density of sleep spindles and interregional coherence. Under this premise, it is the quantity of sleep itself, but rather, the processes contained within sleep that drive the consolidation process. A useful future experiment would be to determine whether the time of day affects learning in estrus and proestrus. As the subjective morning of estrus displays increased NREM and

REM sleep, but proestrus has increased spindles during the light phase and enhanced coherence during the dark phase, it would be interesting to see if these specific times benefit different facets of memory consolidation; i.e., whether the sleep changes within specific cycle phases benefit different memory consolidation tasks.

The alternative hypothesis of compensatory support from hormones and neuromodulators enhancing memory consolidation at the expense of sleep is less supported, but equally as likely. This is chiefly because we know little about how sleep-wake behavior across the estrous cycle affects neuromodulatory systems activity. Estrogen and progesterone receptors on the LC and the VTA that alter noradrenergic or dopaminergic activity respectively could increase synaptic strength at the expense of sleep[248,249]. Further effects from hormones like estradiol could increase synaptic strength as previously mentioned. If enhanced synaptic strength alone is what preserves memory in the absence of sleep, learning paradigms that require depotentiation or circuit manipulation may conversely be hampered by higher hormonal states, rather than benefited. If this were the case, it would suggest that different phases of the estrous cycle may benefit different forms of memory consolidation.

### 4.4 In sum

This work provides the first evidence that neuromodulator activity during sleep can manipulate neural processes key to normal memory processing. Further, this work supports and expands upon previous studies which demonstrate that sleep is a dynamic state that is influenced by endogenous physiological processes such as the estrous cycle. Changes within proestrus and estrus produced marked sex differences in sleep between male and female rats.

## Bibliography


1. Nickel M. Kinetics and rhythm of body contractions in the sponge Tethya wilhelma (Porifera: Demospongiae). *J Exp Biol*. 2004;207(26):4515-4524. doi:10.1242/jeb.01289
2. Nath R, Bedbrook C, Abrams M, et al. The Jellyfish Cassiopea Exhibits a Sleep-Like State. *Curr Biol*. 2017;27:2984-2990. doi:10.1016/j.cub.2017.08.014
3. Allada R, Siegel JM. Unearthing the Phylogenetic Roots of Sleep. *Curr Biol*. 2008;18(15):14-20. doi:10.1016/j.cub.2008.06.033
4. Van Someren EJW. Mechanisms and functions of coupling between sleep and temperature rhythms. *Prog Brain Res*. 2006;153:309-324. doi:10.1016/S0079-6123(06)53018-3
5. Sharma S, Kavuru M. Sleep and metabolism: An overview. *Int J Endocrinol*. 2010;2010. doi:10.1155/2010/270832
6. Karasov W. Daily Energy Expenditure and the Cost of Activity in Mammals. *Am Zool*. 1992;32(2):238-248.
7. Mignot E. Why We Sleep: The Temporal Organization of Recovery. *PLoS Biol*. 2008;6(4):e106. doi:10.1371/journal.pbio.0060106
8. Bentivoglio M, Grassi-Zucconi G. The History of Sleep Advances: The Pioneering Experimental Studies on Sleep Deprivation. *Sleep*. 1997;20(7):570-576.
9. Everson CA, Bergmann BM, Rechtschaffen A. Sleep deprivation in the rat: III. Total sleep deprivation. *Sleep*. 1989;12(1):13-21. doi:10.1093/sleep/12.1.13
10. Rechtschaffen A, Bergmann BM, Everson CA, Kushida CA, Gilliland MA. Sleep-Deprivation in the Rat .10. Integration and Discussion of the Findings. *Sleep*. 1989;12(1):68-87. doi:10.1016/j.yhbeh.2006.06.003
11. Lu T, Pan Y, Peng L, et al. Fatal familial insomnia with abnormal signals on routine MRI: A case report and literature review. *BMC Neurol*. 2017;17(1):1-6. doi:10.1186/s12883-017-0886-2
12. Yaffe K, Falvey CM, Hoang T. Connections between sleep and cognition in older adults. *Lancet Neurol*. 2014;13(10):1017-1028. doi:10.1016/S1474-4422(14)70172-3
13. Gelber RP, Redline S, Ross GW, et al. Associations of brain lesions at autopsy with polysomnography features before death. *Neurology*. 2015;84(3):296-303. doi:10.1212/WNL.0000000000001163
14. Chen PL, Lee WJ, Sun WZ, Oyang YJ, Fuh JL. Risk of Dementia in Patients with Insomnia and Long-term Use of Hypnotics: A Population-based Retrospective Cohort Study. *PLoS One*. 2012;7(11). doi:10.1371/journal.pone.0049113
15. Malhotra RK. Neurodegenerative Disorders and Sleep. *Sleep Med Clin*. 2018;13(1):63-70. doi:10.1016/j.jsmc.2017.09.006
16. Rasch B, Born J. About Sleep's Role in Memory. *Physiol Rev*. 2013;93:681-766. doi:10.1152/Physrev.00032.2012

17. Caton R. The Electric Currents of the Brain. *Br Med J*. 1875:257-279.
18. Aserinsky E, Kleitman N. Regularly Occurring Periods of Eye Motility, and Concomitant Phenomena, during Sleep. *Science (80- )*. 1953;118(3062):273-274.
19. Iber C, Ancoli-Israel S, Quan S. *The AASM Manual for the Scoring of Sleep and Associated Events*. 1st ed. Westchester, IL; 2007. doi:10.1161/01.STR.0000195177.61184.49
20. Gottesmann C. Detection of seven sleep-waking stages in the rat. *Neurosci Biobehav Rev*. 1992;16(1):31-38. doi:10.1016/S0149-7634(05)80048-X
21. Bryant PA, Trinder J, Curtis N. Sick and tired: Does sleep have a vital role in the immune system? *Nat Rev Immunol*. 2004;4(6):457-467. doi:10.1038/nri1369
22. Steriade M, McCormick D, Sejnowski T. Thalamocortical oscillations in the sleeping and aroused brain. *Science (80- )*. 1993;262(5134):679-685. doi:10.1126/science.8235588
23. Clawson BC, Durkin J, Aton SJ. Form and Function of Sleep Spindles across the Lifespan. *Neural Plast*. 2016;(1):1-16. doi:10.1155/2016/6936381
24. Lee KH, McCormick DA. Abolition of Spindle Oscillations by Serotonin and Norepinephrine in the Ferret Lateral Geniculate and Perigeniculate Nuclei In Vitro. *Neuron*. 1996;77(2):335-350. doi:10.1016/S0306-4522(96)00481-2
25. Gardner RJ, Hughes SW, Jones MW. Differential spike timing and phase dynamics of reticular thalamic and prefrontal cortical neuronal populations during sleep spindles. *J Neurosci*. 2013;33(47):18469-18480. doi:10.1523/JNEUROSCI.2197-13.2013
26. Bonjean M, Baker T, Lemieux M, Timofeev I, Sejnowski T, Bazhenov M. Corticothalamic Feedback Controls Sleep Spindle Duration In Vivo. *J Neurosci*. 2011;31(25):9124-9134. doi:10.1523/JNEUROSCI.0077-11.2011
27. Cash SS, Halgren E, Dehghani N, et al. The Human K-Complex Represents an Isolated Cortical Down-State. *Science (80- )*. 2009;(May):1084-1087.
28. Halász P. K-complex, a reactive EEG graphoelement of NREM sleep: An old chap in a new garment. *Sleep Med Rev*. 2005;9(5):391-412. doi:10.1016/j.smrv.2005.04.003
29. Halász P. K-complex, a reactive EEG graphoelement of NREM sleep: An old chap in a new garment. *Sleep Med Rev*. 2005;9(5):391-412. doi:10.1016/j.smrv.2005.04.003
30. Amzica F, Steriade M. Cellular substrates and laminar profile of sleep K-complex. *Neuroscience*. 1997;82(3):671-686. doi:10.1016/S0306-4522(97)00319-9
31. Numminen J, Mäkelä JP, Hari R. Distributions and sources of magnetoencephalographic K-complexes. *Electroencephalogr Clin Neurophysiol*. 1996;99(6):544-555. doi:10.1016/S0013-4694(96)95712-0
32. Arnaud C, Gauthier E, Gottesmann C, et al. Atropine effects on the intermediate stage and paradoxical sleep in rats. *Psychopharmacology (Berl)*. 1994;(116):304-308. doi:10.1007/BF02245333
33. Gottesmann C, Trefouret S, Depoortere H. Influence of zolpidem, a novel hypnotic, on the intermediate-stage and paradoxical sleep in the rat. *Pharmacol Biochem Behav*. 1994;47(2):359-362. doi:10.1016/0091-3057(94)90023-X
34. Gandolfo G, Scherschlicht R, Gottesmann C. Benzodiazepines promote the intermediate stage at the expense of paradoxical sleep in the rat. *Pharmacol*

*Biochem Behav*. 1994;49(4):921-927. doi:10.1016/0091-3057(94)90244-5
35. Diekelmann S, Born J. The memory function of sleep. *Nat Rev Neurosci*. 2010;11(2):114-126. doi:nrn2762 [pii]\r10.1038/nrn2762
36. Emrick JJ, Gross BA, Riley BT, Poe GR. Different Simultaneous Sleep States in the Hippocampus and Neocortex. *Sleep*. 2016;39(12):2201-2209. doi:10.5665/sleep.6326
37. Muller L, Chavane F, Reynolds J, Sejnowski TJ. Cortical travelling waves: Mechanisms and computational principles. *Nat Rev Neurosci*. 2018;19(5):255-268. doi:10.1038/nrn.2018.20
38. Brooks PL, Peever JH. Unraveling the mechanisms of REM sleep atonia. *Sleep*. 2008;31(11):1492-1497.
39. Mitchell J, Rawlins JNP, Steward O, Olton DS. Medial Area Lesions 8 Rhythm and Staining in Medial Cortex and Produce Impaired Radial Arm Maze Behavior in Rats. *J Neurosci*. 1982;2(3):292-302.
40. Boyce R, Glasgow SD, Williams S. Casual evidence for the role of REM sleep theta rhythm in contexual memory consolidaiton. *Science (80- )*. 2016;23(352):812-816.
41. Hutchison IC, Rathore S. The role of REM sleep theta activity in emotional memory. *Front Psychol*. 2015;6(10):1-15. doi:10.3389/fpsyg.2015.01439
42. Ng M, Pavlova M. Why Are Seizures Rare in Rapid Eye Movement Sleep? Review of the Frequency of Seizures in Different Sleep Stages. *Epilepsy Res Treat*. 2013:1-10. doi:10.1155/2013/932790
43. Minecan D, Natarajan A, Marzec M, Malow B. Relationship of epileptic seizures to sleep stage and sleep depth. *Sleep*. 2002;25(8):899-904. doi:10.1093/sleep/25.8.56
44. Frankland PW, Bontempi B. The organization of recent and remote memories. *Nat Rev Neurosci*. 2005;6(2):119-130. doi:10.1038/nrn1607
45. Lechner HA, Squire LR, Byrne JH, Mu G. 100 Years of Consolidation-Remembering Muller and Pilzecker. *Learn Mem*. 1999;6:77-88.
46. Jenkins JG, Dallenbach KM. Obliviscence during Sleep and Waking. *Am J Psychol*. 1924;35(4):605-612.
47. Ekstrand BR. Effect of Sleep on Memory. *J Exp Psychol*. 1967;75(1):64-72. doi:10.1037/h0024907
48. Fowler MJ, Sullivan MJ, Ekstrand BR. Sleep and Memory. *Science (80- )*. 1973;179(4070):302-304.
49. Benson K, Feinberg I. Sleep and memory: retention 8 and 24 hours after intial learning. *Psychophsiology*. 1975;12(2):192-195.
50. Abel T, Havekes R, Saletin JM, Walker MP. Sleep, plasticity and memory from molecules to whole-brain networks. *Curr Biol*. 2013;23(17):R774-R788. doi:10.1016/j.cub.2013.07.025
51. Mednick S, Nakayama K, Stickgold R. Sleep-dependent learning: a nap is as good as a night. *Nat Neurosci*. 2003;6(7):697-698. doi:10.1038/nn1078
52. Poe GR. Sleep Is for Forgetting. *J Neurosci*. 2017;37(3):464-473. doi:10.1523/JNEUROSCI.0820-16.2017
53. Chen Z, Wilson MA. Deciphering Neural Codes of Memory during Sleep. *Trends Neurosci*. 2017;40(5):260-275. doi:10.1016/j.tins.2017.03.005

54. Sara SJ. Sleep to remember. *J Neurosci*. 2017;37(3):457-463. doi:10.1177/1073858406292647
55. Huber R, Ghilardi MF, Massimini M, Tononi G. Local sleep and learning. *Nature*. 2004;430(6995):78-81. doi:10.1038/nature02663
56. Marshall L, Helgadóttir H, Mölle M, Born J. Boosting slow oscillations during sleep potentiates memory. *Nature*. 2006;444(7119):610-613. doi:10.1038/nature05278
57. Ngo HV V., Martinetz T, Born J, Mölle M. Auditory closed-loop stimulation of the sleep slow oscillation enhances memory. *Neuron*. 2013;78(3):545-553. doi:10.1016/j.neuron.2013.03.006
58. Papalambros NA, Santostasi G, Malkani RG, et al. Acoustic Enhancement of Sleep Slow Oscillations and Concomitant Memory Improvement in Older Adults. *Front Hum Neurosci*. 2017;11(109). doi:10.3389/fnhum.2017.00109
59. Fattinger S, De Beukelaar TT, Ruddy KL, et al. Deep sleep maintains learning efficiency of the human brain. *Nat Commun*. 2017;8(May 2017):1-13. doi:10.1038/ncomms15405
60. Miyamoto D, Hirai, Fung C, et al. Top-down cortical input during NREM sleep consolidates perceptual memory. *Science (80- )*. 2016;352(6291):1315-1318. doi:http://dx.doi.org/10.1126/science.aaf0902
61. Binder S, Rawohl J, Born J, Marshall L. Transcranial slow oscillation stimulation during NREM sleep enhances acquisition of the radial maze task and modulates cortical network activity in rats. *Front Behav Neurosci*. 2014;7(January):1-10. doi:10.3389/fnbeh.2013.00220
62. Rembado I, Zanos S, Fetz EE. Cycle-Triggered Cortical Stimulation during Slow Wave Sleep Facilitates Learning a BMI Task: A Case Report in a Non-Human Primate. *Front Behav Neurosci*. 2017;11(4):1-13. doi:10.3389/fnbeh.2017.00059
63. Maingret N, Girardeau G, Todorova R, Goutierre M, Zugaro M. Hippocampo-cortical coupling mediates memory consolidation during sleep. *Nat Neurosci*. 2016;19(7):959. doi:10.1038/nn.4304
64. Eschenko O, Molle M, Born J, Sara SJ. Elevated Sleep Spindle Density after Learning or after Retrieval in Rats. *J Neurosci*. 2006;26(50):12914-12920. doi:10.1523/JNEUROSCI.3175-06.2006
65. Swift KM, Gross BA, Frazer MA, et al. Abnormal Locus Coeruleus Sleep Activity Alters Sleep Signatures of Memory Consolidation and Impairs Place Cell Stability and Spatial Memory. *Curr Biol*. 2018:1-11. doi:10.1016/J.CUB.2018.09.054
66. Nader RS, Murkar AL, Smith CT. Sleep changes in adolescents following procedural task training. *Front Psychol*. 2016;7(10):1-7. doi:10.3389/fpsyg.2016.01555
67. Peters KR, Ray L, Smith V, Smith C. Sleep and performance Changes in the density of stage 2 sleep spindles following motor learning in young and older adults. *J Sleep Res*. 2008;17:23-33. doi:10.1111/j.1365-2869.2008.00634.x
68. Fogel SM, Smith CT, Beninger RJ. Evidence for 2-stage models of sleep and memory: Learning-dependent changes in spindles and theta in rats. *Brain Res Bull*. 2009;79(6):445-451. doi:10.1016/j.brainresbull.2009.03.002
69. Fogel SM, Smith CT. Learning-dependent changes in sleep spindles and stage 2 sleep. *J Sleep Res*. 2006;15:250-255. doi:10.1111/j.1365-2869.2006.00522.x
70. Fogel SM, Smith CT, Cote KA. Dissociable learning-dependent changes in REM

and non-REM sleep in declarative and procedural memory systems. 2007;180:48-61. doi:10.1016/j.bbr.2007.02.037
71. Binder S, Baier PC, Mölle M, Inostroza M, Born J, Marshall L. Sleep enhances memory consolidation in the hippocampus-dependent object-place recognition task in rats. *Neurobiol Learn Mem*. 2012;97(2):213-219. doi:10.1016/j.nlm.2011.12.004
72. Gais S, Mölle M, Helms K, Born J. Learning-dependent increases in sleep spindle density. *J Neurosci*. 2002;22(15):6830-6834. doi:20026697
73. Nishida M, Walker MP. Daytime naps, motor memory consolidation and regionally specific sleep spindles. *PLoS One*. 2007;2(4):e341. doi:10.1371/journal.pone.0000341
74. Mednick SC, Mcdevitt EA, Walsh JK, et al. The Critical Role of Sleep Spindles in Hippocampal-Dependent Memory : A Pharmacology Study. *J Neurosci*. 2013;13(10):4494-4504. doi:10.1523/JNEUROSCI.3127-12.2013
75. Tamaki M, Matsuoka T, Nittono H, Hori T. Fast sleep spindle (13-15 Hz) activity correlates with sleep-dependent improvement in visuomotor performance. *Sleep*. 2008;31(2):204-211. doi:10.1093/sleep/31.2.204
76. Kaestner E, Wixted J, Mednick S. Pharmacologically increasing sleep spindles enhances recognition for negative and high arousal memories. *J Cogn Neurosci*. 2013;26(3):194-198. doi:10.1162/jocn
77. Demaneuele C, BArtsch U, Baran B, et al. Coordination of Slow Waves with Sleep Spindles Predicts Sleep Dependent Memory Consolidation in Schizophrenia. *Sleep*. 2016;40(September):5030. doi:10.1007/s11548-012-0737-y
78. Iotchev IB, Kis A, Bódizs R, Van Luijtelaar G, Kubinyi E. EEG Transients in the Sigma Range during non-REM Sleep Predict Learning in Dogs. *Sci Rep*. 2017;7(1):1-11. doi:10.1038/s41598-017-13278-3
79. Ujma PP, Konrad BN, Genzel L, et al. Sleep Spindles and Intelligence: Evidence for a Sexual Dimorphism. *J Neurosci*. 2014;34(49):16358-16368. doi:10.1523/JNEUROSCI.1857-14.2014
80. Ujma PP, Bódizs R, Gombos F, et al. Nap sleep spindle correlates of intelligence. *Sci Rep*. 2015;5:1-8. doi:10.1038/srep17159
81. Siapas AG, Wilson MA. Coordinated Interactions between Hippocampal Ripples and Cortical Spindles during Slow-Wave Sleep. *Neuron*. 1998;21:1123-1128.
82. Wierzynski CM, Lubenov E V., Gu M, Siapas AG. State-Dependent Spike-Timing Relationships between Hippocampal and Prefrontal Circuits during Sleep. *Neuron*. 2009;61(4):587-596. doi:10.1016/j.neuron.2009.01.011
83. Clemens Z, Mölle M, Eross L, et al. Fine-tuned coupling between human parahippocampal ripples and sleep spindles. *Eur J Neurosci*. 2011;33(3):511-520. doi:10.1111/j.1460-9568.2010.07505.x
84. Staresina BP, Bergmann TO, Bonnefond M, et al. Hierarchical nesting of slow oscillations, spindles and ripples in the human hippocampus during sleep. *Nat Neurosci*. 2015;18(11):1679-1686. doi:10.1038/nn.4119
85. Tamminen J, Payne JD, Stickgold R, Wamsley EJ, Gaskell MG. Sleep spindle activity is associated with the integration of new memories and existing knowledge. *J Neurosci*. 2010;30(43):14356-14360.

doi:10.1523/JNEUROSCI.3028-10.2010
86. Hennies N, Lambon Ralph MA, Kempkes M, Cousins JN, Lewis PA. Sleep Spindle Density Predicts the Effect of Prior Knowledge on Memory Consolidation. *J Neurosci*. 2016;36(13):3799-3810. doi:10.1523/JNEUROSCI.3162-15.2016
87. Saletin JM, Goldstein AN, Walker MP. The role of sleep in directed forgetting and remembering of human memories. *Cereb Cortex*. 2011;21(11):2534-2541. doi:10.1093/cercor/bhr034
88. Latchoumane C, Ngo HV V., Born J, Shin H-S. Thalamic Spindles Promote Memory Formation during Sleep through Triple Phase-Locking of Article Thalamic Spindles Promote Memory Formation during Sleep through Triple Phase-Locking of Cortical, Thalamic, and Hippocampal Rhythms. *Neuron*. 2017;95:1-12. doi:10.1016/j.neuron.2017.06.025
89. Lustenberger C, Boyle MR, Alagapan S, Mellin JM, Vaughn B V., Fröhlich F. Feedback-Controlled Transcranial Alternating Current Stimulation Reveals a Functional Role of Sleep Spindles in Motor Memory Consolidation. *Curr Biol*. 2016;26(16):2127-2136. doi:10.1016/j.cub.2016.06.044
90. Manoach DS, Pan JQ, Purcell SM, Stickgold R. Reduced Sleep Spindles in Schizophrenia: A Treatable Endophenotype That Links Risk Genes to Impaired Cognition? *Biol Psychiatry*. 2016;80(8):599-608. doi:10.1016/j.biopsych.2015.10.003
91. Manoach DS, Stickgold R. Sleep, Memory and Schizophrenia. *Sleep Med*. 2015;16(5):553-554. doi:0.1016/j.sleep.2015.01.009.
92. Wilson M a, Mcnaughton BL. Reactivation of Hippocampal Ensemble Memories During Sleep. *Science (80- )*. 1994;265:676-679.
93. Roux L, Hu B, Eichler R, Stark E, Buzsáki G. Sharp wave ripples during learning stabilize the hippocampal spatial map. *Nat Neurosci*. 2017;20(6):845-853. doi:10.1038/nn.4543
94. Foster DJ. Replay Comes of Age. *Annu Rev Neurosci*. 2017;40(1):581-602. doi:10.1146/annurev-neuro-072116-031538
95. Girardeau G, Benchenane K, Wiener SI, Buzsáki G, Zugaro MB. Selective suppression of hippocampal ripples impairs spatial memory. *Nat Neurosci*. 2009;12(10):1222-1223. doi:10.1038/nn.2384
96. Novitskaya Y, Sara SJ, Logothetis NK, Eschenko O. Ripple-triggered stimulation of the locus coeruleus during post-learning sleep disrupts ripple/spindle coupling and impairs memory consolidation. *Learn Mem*. 2016;23(5):238-248. doi:10.1101/lm.040923.115
97. Goutagny R, Jackson J, Williams S. Self-generated theta oscillations in the hippocampus. *Nat Neurosci*. 2009;12(12):1491-1493. doi:10.1038/nn.2440
98. Ognjanovski N, Maruyama D, Lashner N, Zochowski M, Aton SJ. CA1 hippocampal network activity changes during sleep-dependent memory consolidation. *Front Syst Neurosci*. 2014;8(April):1-11. doi:10.3389/fnsys.2014.00061
99. Ognjanovski N, Schaeffer S, Wu J, et al. Parvalbumin-expressing interneurons coordinate hippocampal network dynamics required for memory consolidation. *Nat Commun*. 2017;8(15039):1-13. doi:10.1038/ncomms15039
100. Hellman K, Abel T. Fear Conditioning increases NREM sleep. *Behav Neurosci*.

2007;121(2):310-323. doi:10.1037/0735-7044.121.2.310.Fear
101. Popa D, Duvarci S, Popescu AT, Lena C, Pare D. Coherent amygdalocortical theta promotes fear memory consolidation during paradoxical sleep. *Proc Natl Acad Sci*. 2010;107(14):6516-6519. doi:10.1073/pnas.0913016107
102. Nishida M, Pearsall J, Buckner RL, Walker MP. REM sleep, prefrontal theta, and the consolidation of human emotional memory. *Cereb Cortex*. 2009;19(5):1158-1166. doi:10.1093/cercor/bhn155
103. Cowdin N, Kobayashi I, Mellman TA. Theta frequency activity during rapid eye movement (REM) sleep is greater in people with resilience versus PTSD. *Exp Brain Res*. 2014;232(5):1479-1485. doi:10.1007/s00221-014-3857-5
104. Poe GR, Nitz DA, Mcnaughton BL, Barnes CA. Experience-dependent phase-reversal of hippocampal neuron firing during REM sleep. *Brain Res*. 2000;855:176-180. doi:10.1016/S0006-8993(99)02310-0
105. Louie K, Wilson MA. Temporally Structured Replay of Awake Hippocampal Ensemble Activity during Rapid Eye Movement Sleep. *Neuron*. 2001;29:145-156. doi:10.1016/S0896-6273(01)00186-6
106. Schwarz LA, Luo L. Organization of the locus coeruleus-norepinephrine system. *Curr Biol*. 2015;25(21). doi:10.1016/j.cub.2015.09.039
107. Sara SJ. The locus coeruleus and noradrenergic modulation of cognition. *Nat Rev Neurosci*. 2009;10:211-223. doi:10.1038/nrn2573
108. Vankov A, Herve-Minvielle A, Sara SJ. Response to Novelty and its Rapid Habituation in Locus Coeruleus Neurons of the Freely Exploring Rat. *Eur J Neurosci*. 1995;7(6):1180-1187. doi:10.1111/j.1460-9568.1995.tb01108.x
109. Wagatsuma A, Okuyama T, Sun C, Smith LM, Abe K, Tonegawa S. Locus coeruleus input to hippocampal CA3 drives single-trial learning of a novel context. *Proc Natl Acad Sci*. 2017. doi:10.1073/pnas.1714082115
110. Sara SJ, Dyon-Laurent C, Hervé A. Novelty seeking behavior in the rat is dependent upon the integrity of the noradrenergic system. *Cogn Brain Res*. 1995;2(3):181-187. doi:10.1016/0926-6410(95)90007-1
111. Delgado PL, Moreno FA. Role of norepinephrine in depression. *J Clin Psychiatry*. 2000;61(SUPPL. 1):5-12.
112. Goddard AW, Ball SG, Martinez J, et al. Current perspectives of the roles of the central norepinephrine system in anxiety and depression. *Depress Anxiety*. 2010;27(4):339-350. doi:10.1002/da.20642
113. Thomas MJ, Moody TD, Makhinson M, Dell TJO. Activity-Dependent B-Adrenergic Modulation of Low Frequency Stimulation Induced LTP in the Hippocampal CA1 Region. *Neuron*. 1996;17:475-482. doi:10.1016/S0896-6273(00)80179-8
114. O'Dell TJ, Connor SA, Guglietta R, Nguyen P V. β-Adrenergic receptor signaling and modulation of long-term potentiation in the mammalian hippocampus. *Learn Mem*. 2015;22(9):461-471. doi:10.1101/lm.031088.113
115. Blitzer R, Connor J, Brown G, et al. Gating of CaMKII by cAMP-regulated protein phosphatase activity during LTP. *Science (80- )*. 1998;280(5371):1940-1943. doi:10.1126/science.280.5371.1940
116. Krupp JJ, Vissel B, Thomas CG, Heinemann SF, Westbrook GL. Calcineurin acts via the C-terminus of NR2A to modulate desensitization of NMDA receptors.

*Neuropharmacology*. 2002;42(5):593-602. doi:10.1016/S0028-3908(02)00031-X
117. Skeberdis VA, Chevaleyre V, Lau CG, et al. Protein kinase A regulates calcium permeability of NMDA receptors. *Nat Neurosci*. 2006;9(4):501-510. doi:10.1038/nn1664
118. McGaugh JL. Memory - a Century of Consolidation. *Science (80- )*. 2000;287(5451):248-251. doi:10.1126/science.287.5451.248
119. Cahill L, Prins B, Weber M, McGaugh JL. Beta-adrenergic activation and memory for emotional events. *Nature*. 1994;371(6499):702-704. doi:10.1038/371702a0
120. Roozendaal B, Nguyen BT, Power AE, McGaugh JL. Basolateral amygdala noradrenergic influence enables enhancement of memory consolidation induced by hippocampal glucocorticoid receptor activation. *Proc Natl Acad Sci*. 1999;96(20):11642-11647. doi:10.1073/pnas.96.20.11642
121. O'Carroll RE, Drysdale E, Cahill L, Shajahan P, Ebmeier KP. Stimulation of the noradrenergic system enhances and blockade reduces memory for emotional material in man. *Psychol Med*. 1999;29(5):1083-1088. doi:10.1017/S0033291799008703
122. Van Stegeren AH, Everaerd W, Cahill L, McGaugh JL, Gooren LJG. Memory for emotional events: Differential effects of centrally versus peripherally acting B-blocking agents. *Psychopharmacology (Berl)*. 1998;138(3-4):305-310. doi:10.1007/s002130050675
123. Gazarini L, Stern CAJ, Carobrez AP, Bertoglio LJ. Enhanced noradrenergic activity potentiates fear memory consolidation and reconsolidation by differentially recruiting α1- and β-adrenergic receptors. *Learn Mem*. 2013;20(4):210-219. doi:10.1101/lm.030007.112
124. Sara SJ, Roullet P, Przybyslawski J. Consolidation of Memory for Odor–Reward Association: β-Adrenergic Receptor Involvement in the Late Phase. *Learn Mem*. 1999;6(2):88-96. doi:10.1101/lm.6.2.88
125. Roozendaal B, Hermans EJ. Norepinephrine effects on the encoding and consolidation of emotional memory: improving synergy between animal and human studies. *Curr Opin Behav Sci*. 2017;14:115-122. doi:10.1016/j.cobeha.2017.02.001
126. McGaugh JL, Roozendaal B. Drug enhancement of memory consolidation: historical perspective and neurobiological implications. *Psychopharmacology (Berl)*. 2009;202(1-3):3-14. doi:10.1007/s00213-008-1285-6
127. Milton AL, Lee JLC, Everitt BJ. Reconsolidation of appetitive memories for both natural and drug reinforcement is dependent on {beta}-adrenergic receptors. *Learn Mem*. 2008;15(2):88-92. doi:10.1101/lm.825008
128. Przybyslawski J, Roullet P, Sara SJ. Attenuation of emotional and nonemotional memories after their reactivation: Role of beta adrenergic receptors. *J Neurosci*. 1999;19(15):6623-6628. doi:10.1523/JNEUROSCI.19-15-06623.
129. Kindt M, Soeter M, Vervliet B. Beyond extinction: Erasing human fear responses and preventing the return of fear. *Nat Neurosci*. 2009;12(3):256-258. doi:10.1038/nn.2271
130. Dębiec J, Ledoux JE. Disruption of reconsolidation but not consolidation of auditory fear conditioning by noradrenergic blockade in the amygdala. *Neuroscience*. 2004;129(2):267-272. doi:10.1016/j.neuroscience.2004.08.018

131. Dębiec J, Bush DEA, LeDoux JE. Noradrenergic enhancement of reconsolidation in the amygdala impairs extinction of conditioned fear in rats - A possible mechanism for the persistence of traumatic memories in PTSD. *Depress Anxiety*. 2011;28(3):186-193. doi:10.1002/da.20803
132. Do-Monte FHM, Allensworth M, Carobrez AP. Impairment of contextual conditioned fear extinction after microinjection of alpha-1-adrenergic blocker prazosin into the medial prefrontal cortex. *Behav Brain Res*. 2010;211(1):89-95. doi:10.1016/j.bbr.2010.03.014
133. Aston-Jones G, Bloom F. Activity of norepinephrine-containing locus coeruleus neurons in behaving rats anticipates fluctuations in the sleep-waking cycle. *J Neurosci*. 1981;1(8). doi:0.1523/JNEUROSCI.01-08-00876.1981
134. Eschenko O, Magri C, Panzeri S, Sara SJ. Noradrenergic Neurons of the Locus Coeruleus Are Phase Locked to Cortical Up-Down States during Sleep. 2012;22(2). doi:10.1093/cercor/bhr121
135. Sirota A, Csicsvari J, Buhl D, Buzsáki G. Communication between neocortex and hippocampus during sleep in rodents. *Proc Natl Acad Sci*. 2003;100(4):2065-2069. doi:10.1073/pnas.0437938100
136. Ji D, Wilson MA. Coordinated memory replay in the visual cortex and hippocampus during sleep. *Nat Neurosci*. 2007;10(1):100-107. doi:10.1038/nn1825
137. Carter ME, Yizhar O, Chikahisa S, et al. Tuning arousal with optogenetic modulation of locus coeruleus neurons. *Nat Neurosci*. 2010;13(12):1526-1533. doi:10.1038/nn.2682
138. Eschenko O, Sara SJ. Learning-Dependent , Transient Increase of Activity in Noradrenergic Neurons of Locus Coeruleus during Slow Wave Sleep in the Rat : Brain Stem--Cortex Interplay for Memory Consolidation ? 2008;18(11). doi:10.1093/cercor/bhn020
139. Aston-Jones G, Bloom FE. Activity of norepinephrine-containing locus coeruleus neurons in behaving rats anticipates fluctuations in the sleep-waking cycle. *J Neurosci*. 1981;1(8):876-886. doi:doi.org/10.1523/JNEUROSCI.01-08-00876.1981
140. Braunewell KH, Manahan-Vaughan D. Long-term depression: a cellular basis for learning? *Rev Neurosci*. 2001;12(2):121-140. doi:10.1515/REVNEURO.2001.12.2.121
141. Manahan-Vaughan D, Braunewell K-H. Novelty acquisition is associated with induction of hippocampal long-term depression. *Proc Natl Acad Sci*. 1999;96(15):8739-8744. doi:10.1073/pnas.96.15.8739
142. Watts A, Gritton HJ, Sweigart J, Poe GR. Antidepressant Suppression of Non-REM Sleep Spindles and REM Sleep Impairs Hippocampus-Dependent Learning While Augmenting Striatum-Dependent Learning. *J Neurosci*. 2012;32(39):13411-13420. doi:10.1523/JNEUROSCI.0170-12.2012
143. Poe GR, Thompson CM, Riley BT, et al. A spatial memory task appropriate for electrophysiological recordings. *J Neurosci Methods*. 2002;121(1):65-74. doi:10.1016/S0165-0270(02)00233-9
144. Ghasemi A, Zahediasl S. Normality tests for statistical analysis: A guide for non-statisticians. *Int J Endocrinol Metab*. 2012;10(2):486-489. doi:10.5812/ijem.3505

145. William E. Skaggs and Bruce L. McNaughton and Katalin M. Gothard and Etan J. Markus. An Information-Theoretic Approach to Deciphering the Hippocampal Code. *Proc IEEE*. 1993;(1990):1030--1037. doi:10.1109/PROC.1977.10559
146. Fuhs C, Vanrhoads SR, Casale AE, et al. Influence of path integration versus environment orientation on place cell remapping between visually identical environments. *J Neurophysiol*. 2005;(94):2603-2616. doi:10.1152/jn.00132.2005.
147. Li Y, Hickey L, Perrins R, et al. Retrograde optogenetic characterization of the pontospinal module of the locus coeruleus with a canine adenoviral vector. *Brain Res*. 2016;1641:274-290. doi:10.1016/j.brainres.2016.02.023
148. Booth V, Poe GR. Input Source and Strength Influences Overall Firing Phase of Model Hippocampal CA1 Pyramidal Cells During Theta : Relevance to REM Sleep Reactivation and Memory Consolidation. 2006;173:161-173. doi:10.1002/hipo.20143
149. Mehta MR, Barnes CA, McNaughton BL. Experience-dependent, asymmetric expansion of hippocampal place fields. *Proc Natl Acad Sci*. 1997;94(16):8918-8921. doi:10.1073/pnas.94.16.8918
150. Mehta MR, Quirk MC, Wilson MA. Experience-Dependent Asymmetric Shape of Hippocampal Receptive Fields. *Neuron*. 2000;25(3):707-715. doi:10.1016/S0896-6273(00)81072-7
151. Ekstrom AD, Meltzer J, McNaughton B, Barnes C. NMDA Receptor Antagonism Blocks Experience-Dependent Expansion of Hippocampal Place Fields. *Neuron*. 2001;31(4):631-638. doi:10.1016/S0896-6273(01)00401-9
152. Thompson LT, Best PJ. Long-term stability of the place-field activity of single units recorded from the dorsal hippocampus of freely behaving rats. *Brain Res*. 1990;509(2):299-308. doi:10.1016/0006-8993(90)90555-P
153. Bjorness TE, Riley BT, Tysor MK, Poe GR. REM restriction persistently alters strategy used to solve a spatial task. *Learn Mem*. 2005;12(3):352-359. doi:10.1101/lm.84805
154. Aston-Jones G, Segal M, Bloom F. Brain aminergic axons exhibit marked variablility in conduction velocity. *Brain Res*. 1980;195(96):215-222. doi:10.1016/0006-8993(80)90880-X
155. Aston-Jones G, Foote SL, Segal M. Impulse conduction properties of noradrenergic locus coerlueus axons pojecting to monkey cerebrocortex. *Neuroscience*. 1985;15(3):765-777. doi:10.1016/0306-4522(85)90077-6
156. Tamminen J, Payne JD, Stickgold R, Wamsley EJ, Gareth M. Sleep spindle activity is associated with the integration of new memories into existing knowledge. *J Neurosci*. 2010;30(43):14356-14360. doi:10.1523/JNEUROSCI.3028-10.2010.
157. Li W, Ma L, Yang G, Gan W. REM sleep selectively prunes and maintains new synapses in development and learning. 2017;20(3). doi:10.1038/nn.4479
158. Katsuki H, Izumi Y, Zorumski CF. Noradrenergic regulation of synaptic plasticity in the hippocampal CA1 region. *Neurophysiol*. 1997;77:3013-3020. doi:10.1152/jn.1997.77.6.3013
159. Diering GH, Nirujogi RS, Roth RH, Worley PF, Pandey A, Huganir RL. Homer1z drives homeostatic scaling-down of excitatory synapses during sleep. *Science (80- )*. 2017;355(6324):511-515. doi:10.1126/science.aai8355

160. Stickgold R, Whidbee D, Schirmer B, Patel V, Hobson JA. Visual discrimination task improvement: A multi-step process occurring during sleep. *J Cogn Neurosci*. 2000;12(2):246-254. doi:10.1162/089892900562075
161. Kempadoo KA, Mosharov E V, Choi SJ, Sulzer D, Kandel ER. Dopamine release from the locus coeruleus to the dorsal hippocampus promotes spatial learning and memory. *Proc Natl Acad Sci*. 2016;113(51):201616515. doi:10.1073/pnas.1616515114
162. Walker MP. The role of slow wave sleep in memory processing. *J Clin Sleep Med*. 2009;5(2 Suppl):S20-S26. doi:10.1016/j.neurobiolaging.2015.05.014
163. Mellman TA, Kumar A, Kulick-Bell R, Kumar M, Nolan B. Nocturnal/daytime urine noradrenergic measures and sleep in combat-related PTSD. *Biol Psychiatry*. 1995;38(3):174-179. doi:10.1016/0006-3223(94)00238-X
164. Berridge CW, Waterhouse BD. The locus coeruleus – noradrenergic system : modulation of behavioral state and state-dependent cognitive processes. 2003;42(1):33-84. doi:10.1016/S0165-0173(03)00143-7
165. Baker FC, Lee KA. Menstrual Cycle Effects on Sleep. *Sleep Med Clin*. 2018;13(3):283-294. doi:10.1016/j.jsmc.2018.04.002
166. Symonds CS, Gallagher P, Thompson JM, Young AH. Effects of the menstrual cycle on mood, neurocognitive and neuroendocrine function in healthy premenopausal women. *Psychol Med*. 2004;34(1):93-102. doi:10.1017/S0033291703008535
167. Cahill L. Why sex matters for neuroscience. *Nat Rev Neurosci*. 2006;7(6):477-484. doi:10.1038/nrn1909
168. Clegg DJ, Brown LM, Woods SC, Benoit SC. Gonadal hormones determine sensitivity to central leptin and insulin. *Diabetes*. 2006;22(4):978-987. doi:10.2337/diabetes.55.04.06.db05-1339
169. Hirschberg AL. Sex hormones, appetite and eating behaviour in women. *Maturitas*. 2012;71(3):248-256. doi:10.1016/j.maturitas.2011.12.016
170. Baker FC, Driver HS. Circadian rhythms, sleep, and the menstrual cycle. *Sleep Med*. 2007;8(6):613-622. doi:10.1016/j.sleep.2006.09.011
171. Mong JA, Baker FC, Mahoney MM, et al. Sleep, Rhythms, and the Endocrine Brain: Influence of Sex and Gonadal Hormones. *J Neurosci*. 2011;31(45):16107-16116. doi:10.1523/JNEUROSCI.4175-11.2011
172. Colvin G, Whitmoyer D, Lisk R, Walter D, Sawyer C. Changes in sleep-wakefulness in female rates during circadian and estrous cycles. *Brain Res*. 1968;7(1):173-181. doi:10.1080/02697459008722788
173. Malven P, Sawyer C. Sleeping patterns in female guinea pigs; effects of sex hormones. *Exp Neurol*. 1966;15(2):229-239.
174. Colvin GB, Whitmoyer DI, Sawyer CH. Circadian sleep-wakefulness patterns in rats after ovariectomy and treatment with estrogen. *Exp Neurol*. 1969;25(4):616-625. doi:10.1016/0014-4886(69)90104-6
175. Branchey M, Branchey L, Nadler RD. Effects of estrogen and progesterone on sleep patterns of female rats. *Physiol Behav*. 1971;6(6):743-746. doi:10.1016/0031-9384(71)90267-8
176. Paul KN, Dugovic C, Turek FW, Laposky AD. Diurnal sex differences in the sleep-wake cycle of mice are dependent on gonadal function. *Sleep*. 2006;29(9):1211-

1223. doi:10.1093/sleep/29.9.1211
177. Fang J, Fishbein W. Sex differences in paradoxical sleep: Influences of estrus cycle and ovariectomy. *Brain Res*. 1996;734(1-2):275-285. doi:10.1016/0006-8993(96)00652-X
178. Driver HS, Dijk DJ, Werth E, Biedermann K, Borbély AA. Sleep and the sleep electroencephalogram across the menstrual cycle in young healthy women. *J Clin Endocrinol Metab*. 1996;81(2):728-735. doi:10.1210/jcem.81.2.8636295
179. Esearch R, Dzaja A, Arber S, et al. Women's sleep in health and disease. *J Psychiatr Res*. 2005;39:55-76. doi:10.1016/j.jpsychires.2004.05.008
180. Moline ML, Broch L, Zak R. Sleep in women across the life cycle from adulthood through menopause. *Med Clin North Am*. 2004;88:705-736. doi:10.1016/j.mcna.2004.01.009
181. Manber R, Armitage R. Sex, Steroids, and Sleep : A Review. *Sleep*. 1999;22(5):540-555.
182. Johnson EO, Roth T, Schultz L, Breslau N. Epidemiology of DSM-IV Insomnia in Adolescence : Lifetime Prevalence, Chronicity, and an Emergent. *Pediatrics*. 2006;117(2):e247-e256. doi:10.1542/peds.2004-2629
183. Roenneberg T, Kuehnle T, Juda M, et al. Epidemiology of the human circadian clock. *Sleep Med*. 2007;11:429-438. doi:10.1016/j.smrv.2007.07.005
184. Ishizuka, Y., Pollak, C.P., Shirakawa, S., Kakuma, T., Azumi, K., Usui, A., Shiraishi, K., Fukuzawa, H., Kariya T. Sleep spindle frequency changes during the menstrual cycle. *J Sleep Res*. 1994;3(1):26-29. doi:10.1111/j.1365-2869.1994.tb00100.x
185. Koehl M, Battle SE, Turek FW. Sleep in female mice: A strain comparison across the estrous cycle. *Sleep*. 2003;26(3):267-272. doi:10.1093/sleep/26.3.267
186. Cusmano DM, Hadjimarkou MM, Mong JA. Gonadal steroid modulation of sleep and wakefulness in male and female rats is sexually differentiated and neonatally organized by steroid exposure. *Endocrinology*. 2014;155(1):204-214. doi:10.1210/en.2013-1624
187. Hadjimarkou MM, Benham R, Schwarz JM, Holder MK, Mong JA. Estradiol suppresses rapid eye movement sleep and activation of sleep-active neurons in the ventrolateral preoptic area. *Eur J Neurosci*. 2008;27(7):1780-1792. doi:10.1111/j.1460-9568.2008.06142.x
188. Westwood FR. The Female Rat Reproductive Cycle: A Practical Histological Guide to Staging. *Toxicol Pathol*. 2008;36(3):375-384. doi:10.1177/0192623308315665
189. Gross BA, Walsh CM, Turakhia AA, Booth V, Mashour GA, Poe GR. Open-source logic-based automated sleep scoring software using electrophysiological recordings in rats. *J Neurosci Methods*. 2009;184(1):10-18. doi:10.1016/j.jneumeth.2009.07.009
190. Kattla S, Lowery MM. Fatigue related changes in electromyographic coherence between synergistic hand muscles. *Exp Brain Res*. 2010;202(1):89-99. doi:10.1007/s00221-009-2110-0
191. Schwierin B, Borbély AA, Tobler I. Sleep homeostasis in the female rat during the estrous cycle. *Brain Res*. 1998;811(1-2):96-104. doi:10.1016/S0006-8993(98)00991-3

192. Gaillard JM, Blois R. Spindle density in sleep of normal subjects. *Sleep*. 1981;4(4):385-391. doi:10.1093/sleep/4.4.385
193. Malow BA, Carney PR, Kushwaha R, Bowes RJ. Hippocampal sleep spindles revisited: Physiologic or epileptic activity? *Clin Neurophysiol*. 1999;110(4):687-693. doi:10.1016/S1388-2457(99)00008-5
194. Sullivan D, Mizuseki K, Sorgi A, Buzsaki G. Comparison of Sleep Spindles and Theta Oscillations in the Hippocampus. *J Neurosci*. 2014;34(2):662-674. doi:10.1523/jneurosci.0552-13.2014
195. Ferrara M, Moroni F, Lo Russo G, et al. Hippocampal sleep spindles preceding neocortical sleep onset in humans. *Neuroimage*. 2013;86:425-432. doi:10.1016/j.neuroimage.2013.10.031
196. Kleinlogel H. The female rat's sleep during oestrous cycle. *Neuropsychobiology*. 1983;10(4):228-237. doi:10.1159/000118016
197. Zhang SQ, Kimura M, Inoué S. Sleep patterns in cyclic and pseudopregnant rats. *Neurosci Lett*. 1995;193(2):125-128. doi:10.1016/0304-3940(95)11685-P
198. Mongrain V, Carrier J, Dumont M. Chronotype and sex effects on sleep architecture and quantitative sleep EEG in healthy young adults. *Sleep*. 2005;28(7):819-827. doi:10.1093/sleep/28.7.819
199. Borbély AA, Baumann F, Brandeis D, Strauch I, Lehmann D. Sleep deprivation: effect on sleep stages and EEG power density in man. *Electroencephalogr Clin Neurophysiol*. 1981;51:483-493. doi:10.1016/0013-4694(92)90069-T
200. Perlis ML, Smith MT, Andrews PJ, Orff H, Giles DE. Beta/Gamma EEG Activity in Patients with Primary and Secondary Insomnia and Good Sleeper Controls. *Sleep*. 2001;24(1):110-117.
201. Başar-Eroglu C, Strüber D, Schürmann M, Stadler M, Başar E. Gamma-band responses in the brain: A short review of psychophysiological correlates and functional significance. *Int J Psychophysiol*. 1996;24(1-2):101-112. doi:10.1016/S0167-8760(96)00051-7
202. Shughrue PJ, Lane M V, Merchenthaler I. Comparative distribution of estrogen receptor-alpha and -beta mRNA in the rat central nervous system. *J Comp Neurol*. 1997;388(4):507-525. doi:10.1002/(SICI)1096-9861(19971201)388:4<507::AID-CNE1>3.0.CO;2-6 [pii]
203. Curran-Rauhut MA, Petersen SL. The distribution of progestin receptor mRNA in rat brainstem. *Brain Res Gene Expr Patterns*. 2002;1(3-4):151-157. doi:10.3390/molecules20023290
204. Mong JA, Cusmano DM. Sex differences in sleep: Impact of biological sex and sex steroids. *Philos Trans R Soc B Biol Sci*. 2016;371(1688). doi:10.1098/rstb.2015.0110
205. Earnest DJ, Turek FW. Role for acetylcholine in mediating effects of light on reproduction. *Science (80- )*. 1983;219(4580):77-79. doi:10.1126/science.6849121
206. Kohsaka A, Watanobe H, Kakizaki Y, Suda T, Schiöth HB. A significant participation of orexin-A, a potent orexigenic peptide, in the preovulatory luteinizing hormone and prolactin surges in the rat. *Brain Res*. 2001;898(1):166-170. doi:10.1016/S0006-8993(01)02157-6
207. Deaver DR, Dailey RA. Effects of dopamine, norepinephrine and serotonin on

plasma concentrations of luteinizing hormone and prolactin in ovariectomized and anestrous ewes. *Biol Reprod*. 1982;27(3):624-632. doi:10.1095/biolreprod27.3.624
208. Betterton RT, Broad LM, Tsaneva-Atanasova K, Mellor JR. Acetylcholine modulates gamma frequency oscillations in the hippocampus by activation of muscarinic M1 receptors. *Eur J Neurosci*. 2017;45(12):1570-1585. doi:10.1111/ejn.13582
209. Hajos M, Hoffmann WE, Robinson DD, Yu JH, Hajós-Korcsok É. Norepinephrine but not serotonin reuptake inhibitors enhance theta and gamma activity of the septo-hippocampal system. *Neuropsychopharmacology*. 2003;28(5):857-864. doi:10.1038/sj.npp.1300116
210. Vassalli A, Franken P. Hypocretin (orexin) is critical in sustaining theta/gamma-rich waking behaviors that drive sleep need. *Proc Natl Acad Sci*. 2017;114(27):E5464-E5473. doi:10.1073/pnas.1700983114
211. Deurveilher S, Rusak B, Semba K. Female reproductive hormones alter sleep architecture in ovariectomized rats. *Sleep*. 2011;34(4):519-530. doi:10.1016/j.photonics.2013.10.001
212. Pawlyk AC, Alfinito PD, Deecher DC. Effect of 17α-ethinyl estradiol on active phase rapid eye movement sleep microarchitecture. *Eur J Pharmacol*. 2008;591(1-3):315-318. doi:10.1016/j.ejphar.2008.06.084
213. Shalev A, Liberzon I, Marmar C. Post-traumatic stress disorder. *N Engl J Med*. 2017;376(25):2459-2469. doi:10.1016/B978-0-12-803457-6.00013-1
214. Montgomery S, Sirota A, Buzsáki G. Theta and gamma coordination of hippocampal networks during waking and REM sleep. *J Neurosci*. 2008;28(26):6731-6741. doi:10.1523/JNEUROSCI.1227-08.2008
215. Euston DR, Gruber AJ, McNaughton BL. The Role of Medial Prefrontal Cortex in Memory and Decision Making. *Neuron*. 2012;76(6):1057-1070. doi:10.1016/j.neuron.2012.12.002
216. Hagewoud R, Whitcomb SN, Heeringa AN, Havekes R, Koolhaas JM, Meerlo P. A time for learning and a time for sleep: the effect of sleep deprivation on contextual fear conditioning at different times of the day. *Sleep*. 2010;33(10):1315-1322. http://www.pubmedcentral.nih.gov/articlerender.fcgi?artid=2941417&tool=pmcentrez&rendertype=abstract.
217. Barsegyan A, McGaugh JL, Roozendaal B. Noradrenergic activation of the basolateral amygdala modulates consolidation of object recognition memory. *Front Behav Neurosci*. 2014;8:1-8. doi:10.1016/j.nlm.2008.06.010
218. Palchykova S, Winsky-Sommerer R, Meerlo P, Dürr R, Tobler I. Sleep deprivation impairs object recognition in mice. *Neurobiol Learn Mem*. 2006;85(3):263-271. doi:10.1016/j.nlm.2005.11.005
219. Kemp A, Manahan-vaughan D. Hippocampal long-term depression and long-term potentiation encode different aspects of novelty acquisition. 2004.
220. Vivo L De, Bellesi M, Marshall W, et al. Ultrastructural evidence for synaptic scaling across the wake/sleep cycle. *Science (80- )*. 2017;355(February):507-510.
221. Goldstein AN, Walker MP. The Role of Sleep in Emotional Brain Function. *Annu Rev Clin Psychol Vol 10*. 2014;10:679-708. doi:10.1146/annurev-clinpsy-032813-153716.

222. Baker DG, Ekhator NN, West S a, et al. CSF Norepinephrine Concentrations in Posttraumatic Stress Disorder Thomas. *Am J Psychiatry*. 2001;158(8):1227-1230.
223. Goldstein DS, McCarty R, Polinsky RJ, Kopin IJ. Relationship between plasma norepinephrine and sympathetic neural activity. *Hypertension*. 1983;5(4):552-559. doi:10.1161/01.HYP.5.4.552
224. Mellman TA, Hipolito MMS. Sleep disturbances in the aftermath of trauma and posttraumatic stress disorder. *CNS Spectr*. 2006;11(8):611-615. doi:10.1017/S1092852900013663
225. Niethard N, Born J. Back to baseline: sleep recalibrates synapses. *Nat Neurosci*. 2019:1. doi:10.1038/s41593-018-0327-6
226. Raskind MA, Peskind ER, Kanter ED, et al. Reduction of nightmares and other PTSD symptoms in combat veterans by prazosin: A placebo-controlled study. *Am J Psychiatry*. 2003;160(2):371-373. doi:10.1176/appi.ajp.160.2.371
227. R.N. A, R.S. Z, R.K. M, et al. Best practice guide for the treatment of nightmare disorder in adults. *J Clin Sleep Med*. 2010;6(1):85-95. http://ovidsp.ovid.com/ovidweb.cgi?T=JS&PAGE=reference&D=emed12&NEWS=N&AN=358410077.
228. Raskind MA, Peskind ER, Chow B, et al. Trial of Prazosin for Post-Traumatic Stress Disorder in Military Veterans. *N Engl J Med*. 2018;378(6):507-517. doi:10.1056/NEJMoa1507598
229. Betts TA, Alford C. β-Blockers and sleep: A controlled trial. *Eur J Clin Pharmacol*. 1985;28:65-68. doi:10.1007/BF00543712
230. Deurveilher S, Rusak B, Semba K. Estradiol and progesterone modulate spontaneous sleep patterns and recovery from sleep deprivation in ovariectomized rats. *Sleep*. 2009;32(7):865-877.
231. Paul KN, Laposky AD, Turek FW. Reproductive hormone replacement alters sleep in mice. *Neurosci Lett*. 2009;463(3):239-243. doi:10.1016/j.neulet.2009.07.081
232. Deurveilher S, Rusak B, Semba K. Estradiol and progesterone modulate spontaneous sleep patterns and recovery from sleep deprivation in ovariectomized rats. *Sleep*. 2009;32(7):865-877.
233. Mong JA, Devidze N, Goodwillie A, Pfaff DW. Reduction of lipocalin-type prostaglandin D synthase in the preoptic area of female mice mimics estradiol effects on arousal and sex behavior. *Proc Natl Acad Sci*. 2003;100(25):15206-15211. doi:10.1073/pnas.2436540100
234. Deurveilher S, Cumyn EM, Rusak B, Semba K, Peers T. Estradiol replacement enhances sleep deprivation-induced c-Fos immunoreactivity in forebrain arousal regions of ovariectomized rats. *Am J Physiol Integr Comp Physiol*. 2008;295(4):R1328-R1340. doi:10.1152/ajpregu.90576.2008
235. Quadros PS, Wagner CK. Regulation of progesterone receptor expression by estradiol is dependent on age, sex and region in the rat brain. *Endocrinology*. 2008;149(6):3054-3061. doi:10.1210/en.2007-1133
236. Trachsel L, Rupprecht R, Holsboer F, Friess E, Tagaya H. Progesterone-induced changes in sleep in male subjects. *Am J Physiol Metab*. 2017;272(5):E885-E891. doi:10.1152/ajpendo.1997.272.5.e885
237. Saper CB, Fuller PM, Pedersen NP, Lu J, Scammell TE. Sleep State Switching.

*Neuron*. 2011;68(6):1023-1042. doi:10.1016/j.neuron.2010.11.032.Sleep
238. Fraigne JJ, Torontali ZA, Snow MB, Peever JH. REM sleep at its core - Circuits, neurotransmitters, and pathophysiology. *Front Neurol*. 2015;6(MAY):1-9. doi:10.3389/fneur.2015.00123
239. Luine VN. Estradiol and cognitive function: Past, present and future. *Horm Behav*. 2014;66(4):602-618. doi:10.1016/j.yhbeh.2014.08.011
240. Paris JJ, Frye CA. Estrous cycle, pregnancy, and parity enhance performance of rats in object recognition or object placement tasks. *Reproduction*. 2008;136(1):105-115. doi:10.1530/rep-07-0512
241. Frick KM, Berger-Sweeney J. Spatial reference memory and neocortical neurochemistry vary with the estrous cycle in C57BL/6 mice. *Behav Neurosci*. 2001;115(1):229-237. doi:10.1037/0735-7044.115.1.229
242. Frick KM, Kim J, Tuscher JJ, Fortress AM. Sex steroid hormones matter for learning and memory: Estrogenic regulation of hippocampal function in male and female rodents. *Learn Mem*. 2015;22(9):472-493. doi:10.1101/lm.037267.114
243. Milad MR, Igoe SA, Lebron-Milad K, Novales JE. Estrous cycle phase and gonadal hormones influence conditioned fear extinction. *Neuroscience*. 2009;164(3):887-895. doi:10.1016/j.neuroscience.2009.09.011
244. Singh M, Meyer EM, Millard WJ, Simpkins JW. Ovarian steroid deprivation results in a reversible learning impairment and compromised cholinergic function in female Sprague-Dawley rats. *Brain Res*. 1994;644(2):305-312. doi:10.1016/0006-8993(94)91694-2
245. Wallace M, Luine V, Arellanos A, Frankfurt M. Ovariectomized rats show decreased recognition memory and spine density in the hippocampus and prefrontal cortex. *Brain Res*. 2006;1126(1):176-182. doi:10.1016/j.brainres.2006.07.064
246. Daniel JM, Roberts SL, Dohanich GP. Effects of ovarian hormones and environment on radial maze and water maze performance of female rats. *Physiol Behav*. 1999;66(1):11-20. doi:10.1016/S0031-9384(98)00272-8
247. Daniel JM, Fader AJ, Spencer AL, Dohanich GP. Estrogen enhances performance of female rats during acquisition of a radial arm maze. *Horm Behav*. 1997;32(3):217-225. doi:10.1006/hbeh.1997.1433
248. Park JW, Bhimani R V., Park J. Noradrenergic Modulation of Dopamine Transmission Evoked by Electrical Stimulation of the Locus Coeruleus in the Rat Brain. *ACS Chem Neurosci*. 2017:acschemneuro.7b00078. doi:10.1021/acschemneuro.7b00078
249. Vega Helena CV, de Oliveira Poletini M, Sanvitto GL, Hayashi S, Franci CR, Anselmo-Franci JA. Changes in α-estradiol receptor and progesterone receptor expression in the locus coeruleus and preoptic area throughout the rat estrous cycle. *J Endocrinol*. 2006;188(2):155-165. doi:10.1677/joe.1.06268